PERFORMANCE ANALYSIS AND DESIGN OF SPACE-TIME CODES

by

CHEN LIAO

Presented to the Faculty of the Graduate School of

The University of Texas at Arlington in Partial Fulfillment

of the Requirements

for the Degree of

DOCTOR OF PHILOSOPHY

THE UNIVERSITY OF TEXAS AT ARLINGTON

December 2006

To my parents, Kejin Chen and Shu Liao, for their unconditional support and encouragement throughout my doctoral program

ACKNOWLEDGEMENTS

This dissertation is the result of four and half years of work at University of Texas at Arlington (UTA), whereby I have been helped and supported by many very enjoyable and fascinating individuals. The completion of this study would not have been possible without their contributions. Now it is a pleasure to use this opportunity to express my gratitude for all of them.

The first person I would like to thank is my supervisor Dr. Vasant K. Prabhu. His kindness and faith in me provided encouragement, invaluable support and inspiration in the journey of my Ph.D education. I am especially thankful for his listening, his willingness to embrace, and patience to endure. Thank you for being such a wonderful advisor.

I would like to thank my wonderful colleagues in telecommunication research group, Dongdong Li, Feng Liu, Iyad Abdelrazzaqe Al-Falujah, Mahmoud Smadi and Kiran Kuchi, who have become dear and treasured friends. They are so generous and kind to share with me their views and experience, and gave me the feeling of being at home at work. It is my luck to meet all of you here.

I am very grateful to my wife, Hongyu Ye, for her love and patience during the Ph.D period. One of the best experiences in this period was the birth of our daughter, Deya Liao, who has added another dimension to our life. I am truly grateful to our daughter for bringing much joy into our lives.

November 15, 2006

ABSTRACT

PERFORMANCE ANALYSIS AND DESIGN OF SPACE-TIME CODES

Publication No. _____

Chen Liao, Ph.D.

The University of Texas at Arlington, 2006

Supervising Professor: Vasant K. Prabhu

Wireless communication technologies have evolved from the original analog networks to IP-based network. Today's wireless communications have been affected by increasing customer expectations on wireless wideband internet services and continuously evolving improvements on technologies. Wireless communication systems must increase their ability to respond to the challenges. The new generation wireless systems (3G/4G) are designed for this purpose. The notable characteristic of 3G/4G is that it provides high data rate transmission at data rate up to 348kbps/2Mbps for 3G and 100Mbps/1Gbps for 4G.

Designing the system for such high data rate transmission has become very challenging for wireless systems where the multipath fading is an important factor. In recent years, researches are ongoing in the industry and academic to increase capacity performance of wireless systems through antenna diversity. Multiple Input Multiple Output (MIMO) is one of the major recent developments in the study of high data rate transmission. There has been considerable attention paid to remarkable performance improvements in MIMO in terms of capacity. Another technology that has been traditionally

adopted for wireless communications is the channel coding. Combining MIMO with channel coding has received increasing interest to support a variety of high data rate applications. These schemes have been termed as "space-time codes". Space-time codes are currently an area of exciting activity and have been studied as promising candidates for future 3G/4G systems. The most important characteristic of space-time codes is that it can provide full diversity gain as well as coding gain.

In this dissertation, both performance analysis of upper bound of Pair-Wise Error Probability (PEP) and exact PEP are performed. In the derivation of exact PEP, a new method is presented. The method is straightforward and comprehensible. The upper bound provides the insight to understand the performance behavior for high Signal-to-Noise Ratio (SNR), while the exact PEP provides a better understanding of the performance behavior to other range of SNR.

Design criteria for space-time codes had been first developed by Tarokh, which utilize the analysis of the upper bound on PEP to maximize diversity gain and coding gain from the property of the codeword distance matrix. These criteria are the most widely accepted, which form the basis for space-time codes. The criteria assume that the performance of space-time codes is dominated by the dominant error events. However, there are no dominant error events in fading channel for space-time codes. Therefore, Tarokh's criteria do not provide design guideline for the coding gain. Union bound analysis offers a alternative solution to this problem. The union bound technique is a more attractive method that allows us to analyze the contribution of all error events to the performance. In this thesis, the performance of space-time codes are analyzed using union bound analysis. Based on the union bound on Frame Error Rate (FER), new design criteria are proposed. This is achieved by applying more accurate upper bound of PEP in the union bound analysis. With the proposed criteria, new coding gain performance

metrics had been defined. New codes based on the new performance metrics are designed and their coding gain performance superiority are demonstrated.

Space-time block codes have been initially designed to provide full diversity order with low decoding complexity, but without coding gain. By integrating space-time trellis codes with space-time block codes, super-orthogonal space-time trellis codes can significantly enhance the coding gain performance. However, the super-orthogonal space-time trellis codes improve performance only in slow fading channel, but do not perform well in fast fading channel. In fast fading channel, the orthogonal design of space-time block codes has little effect on the coding gain and does not lead to noticeable improvement. Furthermore, super-orthogonal space-time trellis codes introduce the diversity gain loss in fast fading channel. It is well known that the performances of space-time codes are dominated by diversity gain and any diversity gain loss may cause substantial loss in performance. We therefore develop orthogonal space-time trellis codes, which improve performance in diversity gain in fast fading channel. The improvement is achieved by transferring the vector output of space-time trellis codes into an orthogonal matrix of space-time block codes, and meanwhile maintaining the symbol Hamming distance of space-time trellis codes. Theoretical analysis and simulation results had demonstrated that the proposed codes can improve diversity gain linearly with an increase in the number of transmit antennas.

Performance saturation and decoding complexity increase with the increased number of trellis states are the major problems that trellis-based codes have to face in practice. Turbo codes that allow for reaching near Shannon limit performance are a significant advance in digital communications. Space-time turbo codes have been developed to achieve high performance. In a perfect world, system designers would like to achieve high performance while maintaining a full code rate. Therefore, puncture operation is always used in space-time turbo codes. The problem with the puncture operation in space-time

turbo codes is that codeword distance matrix is rank deficient for small diversity gain in slow fading channel, which constitutes a major problem with space-time turbo codes. Space-time turbo codes that concern the rank deficiency have been developed. The codes improve performance by reducing the effect of rank deficiency on performance, but exist high complexity in both code structure and design criteria. This limitation makes the codes not suitable for the design of complex codes with large trellis state and/or large numbers of transmit antennas. A new space-time turbo codes have been proposed in this research. In previous works, it has been demonstrated the systematic structure with the rotation of the output of the low constitute encoder can effectively reduce the rank deficient effect on performance. Our new codes utilize the systematic characteristic to construct a simple code structure. Further, a simple but very effective trace criterion has been proposed. With the simple codes structure and design criteria, the design of complex codes can be achieved with significant improvement in coding gain performance for the systems with small diversity gain in slow fading channel.

Overall, this dissertation presents new design criteria and new codes that contribute to improving performances of space-time codes.

TABLE OF CONTENTS

LIST OF FIGURES

LIST OF TABLES

CHAPTER 1

INTRODUCTION

1.1 Motivations and Background

Wireless communications have undergone rapid development in the last ten years with remarkable improvements in performance. However, the development has not been able to meet the demand for high data rate applications. The internet and broadband services have been the major driving force for increase in the capacity growth for wireless communication systems. The increasing demand on broadband services for wireless systems is expected to continue, which has led to the move towards next generation wireless communication systems (3G/4G). In some extent, the history of wireless communications is the history of seeking for high data rate transmission.

Now, wireless communications have become a part of our lives. However, when the first generation of wireless communication system began to emerge to provide voice service in the early 1980s, it was considered as a luxury. The 1G, called Analog Mobile Phone Service (AMPS), first introduced the concept of cellular service with Frequency Division Multiple Access (FDMA) technology. It exists and has low spectral efficiency and low power efficiency.

In the early 1990's, the second generation (2G) technology was developed using digital techniques. 2G provides basic voice service and Short Messaging Service (SMS). The majority of 2G deployed around world are Global System for Mobile communication (GSM) network. GSM is based on Time Division Multiple Access (TDMA) technologies and supports a data rate of 9.6 kbps. Since 1990's, 2G has evolved to meet the needs of rapidly increased demand for data service, such as wireless internet access. Enhanced 2G

(2.5G), for example the General Packet Radio Service (GPRS), has already conceived most of the basic ideas of what future network might be. GPRS is based on packet switching technology and offers wireless internet access with data rate up to 144 kbps.

As the nineties progressed, 2G/2.5G, coupled with the maturity and proven performance, have been widely deployed throughout the world, and the market of 2G/2.5G continues to develop. Currently, wireless systems are developing continuously, but several factors significantly affect the wireless market. The major one is that customer expectations have risen to demand high data rate multimedia applications, such as real-time video applications. The second factor is the rapid development of internet and multimedia technology. 3G is a new standard that tries to challenge these factors. Services in 3G were broadened from regular telephone service to include high-speed internet access and video communications. The response of industry to meeting these services has led to significant increase in data rate. 3G applies code division multiple access technology (WCDMA, CDMA2000, TD-SCDMA) to offer data rate of 384 kbps for mobile and 2 Mbps for indoor.

4G is an extension of 3G, and offers a more wide range of multimedia applications. The distinguishing feature of 4G is that it is a complete IP-based network and the significant increase in data rate at which we're able to access Wireless Local Area Networks (WLAN) at data rate of up to 100 Mbps for mobile with guaranteed Quality of Service (QoS) and a rate of 1Gbps for indoor application.

As the industry migrates to 3G/4G, wireless system designers are facing two significant technical challenges, namely bandwidth limitations and effect of multipath fading. Multipath fading is an inherent phenomenon in wireless communications that occurs while the transmitted signal experiences reflection and scattering. The characteristic of multipath fading signals is the rapid fluctuation of the amplitude of a radio signal over a short period of time or travel distance [1]. As a consequence, performance of wire-

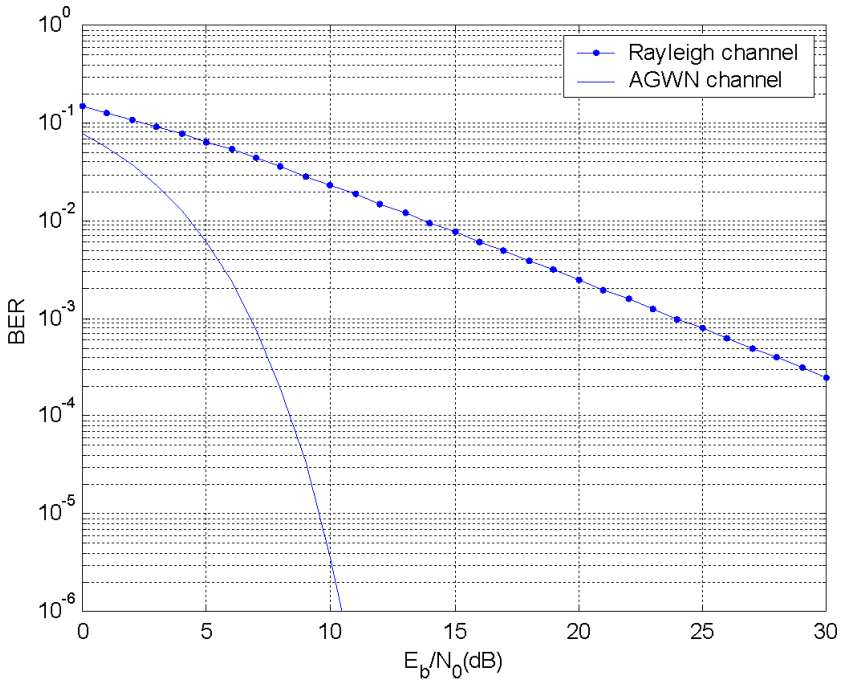

Figure 1.1. BER performance of BPSK in Rayleigh and AWGN channel.

less communication system is significantly degraded in multipath fading environment as shown in Fig. 1.1. Fig. 1.1 displays the Bit Error Rate (BER) performance of BPSK in both Additive White Gaussian Noise (AWGN) and Rayleigh channel. The degradation is up to 15 dB for voice communication (at the BER of 10^{-3}) and up to more than 40 dB for data communication (at the BER of 10^{-6}) in Rayleigh fading channel. Since the frequency resources are sparse, multipath fading appears to be the most limiting characteristics and is becoming a major bottleneck as the data rate increase in wireless communication systems.

Great efforts have been undertaken to combat multipath fading. Attempts made to overcome this problem are equalization, diversity, and channel coding, which can be used independently or in tandem to improve received signal quality [1]. In flat fading channel, diversity technique is of particular concern, given the simple but very effective

means of alleviating multipath fading. The diversity technique is a method of making the replicas of transmitted signal. This technique was developed based on the principle that the replicas will experience different fading condition and the probability that all replicas are in deep fading is low. The replicas can be created in temporal domain, frequency domain, and spatial domain. Among these methods, spatial diversity is technically simpler, improves performance without bandwidth expansion and thus is preferred in most high data rate applications.

Traditionally, spatial diversity denotes transmit diversity or receive diversity. In transmit diversity and receive diversity, multiple antennas are equipped either at transmitter side or receiver side. Historically, the popular means of spatial diversity is to use only a receive diversity. Receive diversity is a simple and practical method for improving performance in fading channels, and has been adopted in IEEE 802.11b for 3G system. On May 04, 2005, QUALCOMM announced sampling of the industry's first single-chip receive diversity device for increased CDMA2000 network capacity. The QUALCOMM's solution gives CDMA2000 operator partners a significant improvement in network performance with increased network data and voice capacity and fewer dropped calls [2]. However, capacity improvement of receive diversity is still limited to the high data rate services.

This situation has stimulated research in a variety of areas, including MIMO system. MIMO is a recent research field, but the history of MIMO can be traced back to 1984 when MIMO was initially developed by Jack Winters of Bell laboratories. MIMO has attracted attention from industry only since 1998, which primarily was due to the development in fundamental theory [3][4][5], where MIMO was showed significant improvements in capacity performance on fading channel. Since then, MIMO has been widely studied. The application of MIMO has broken new ground in implementing high data rate transmission in wireless environment.

MIMO is combined transmit-receive diversity. This technology establishes radio links with multiple antennas at both transmitter and receiver side. The MIMO channel is equivalent to independent parallel sub-channel. The capacity of MIMO is the sum of the capacity of sun-channel. Therefore there is linear increase in MIMO capacity with the minimum of number of transmit and receive antennas. In contrast to the linear logarithmic increase in receive diversity, MIMO results in remarkable capacity improvements.

To date, MIMO has been recognized as a key innovation in 3G/4G and has already been incorporated into the IEEE 802.11n standard to attain a data rate of 100 Mbits/s for WLAN. Channel features when designing wireless network for such high data rate transmission are of the frequency selective. An equalizer or a Rake receiver is commonly used to alleviate the Inter-Symbol Interference (ISI), which results from delay spread in frequency selective channel, with increased complexity of receiver. However, these technologies are impractical to use in MIMO channel because the complexity of receiver is too high. The severe frequency-selective fading environment can be mitigated by combining MIMO with Orthogonal Frequency Division Multiplexing (OFDM). In OFDM, wideband is divided into a set of orthogonal narrow band channels. A very attractive feature of OFDM is that the mild channel conditions are encountered since we have a large number of subcarrier. This feature eliminates the need for equalizer or reduces to a simple a one-tap equalizer, thereby significantly simplifying wireless system. As a practical consequence of the advantage, MIMO-OFDM has been a planning technique used to strengthen 4G. Therefore, the research on MIMO systems has only considered flat fading MIMO channels in this thesis, without Channel State Information (CSI) at transmitter.

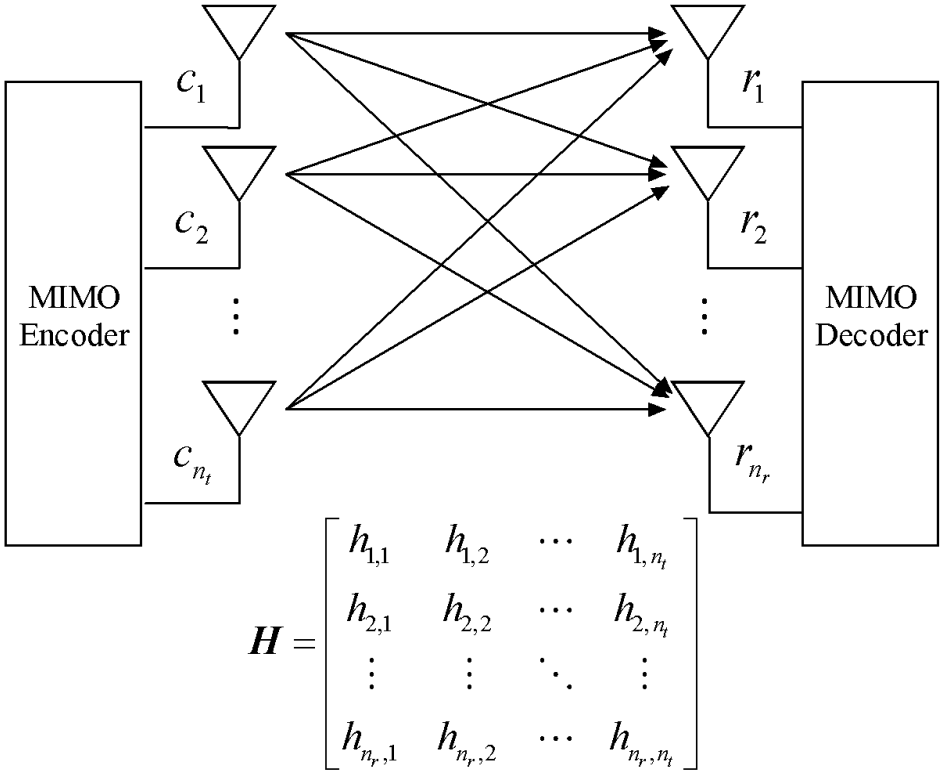

Figure 1.2. Illustrates the basic concept of MIMO.

1.2 MIMO system model

A MIMO system consists of multiple antennas on both side of a communication link. Fig. 1.2 illustrates the basic concept of MIMO, which consists of n_t transmit antennas and n_r receive antennas. We consider that the channel is a Rayleigh channel, which is certainly a worst case situation. The channel coefficient from transmit antenna i to receive antenna j, $h_{j,i}(t)$, is modeled by using independent samples of complex Gaussian random variables with a mean of zero and a variance of 0.5 per dimension. Flat fading channel like above is to be expected in MIMO-OFDM system. Therefore, we will limit our analysis of performance to flat fading channel.

At each time slot t, the encoder of space-time codes output n_t encoded M-PSK symbols, denoted by $\boldsymbol{c}_t = [c_1(t), \cdots, c_{n_t}(t)]^T$ where $c_i(t)$ is the transmitted M-PSK sym-

bol in the i-th transmit antenna at time t. These multiple symbols are transmitted simultaneously out of n_t antennas over frequency nonselective fading channel, and are corrupted by AWGN at receiver. Thus the system model can then be described by the following equation

$$r_j(t) = \sum_{i=1}^{n_t} h_{j,i}(t)c_i(t) + n_j(t),\ j = 1, \cdots, n_r \tag{1.1}$$

where, $r_j(t)$ is the received signal in the j-th receive antenna at time t, and $n_j(t)$ is the complex AWGN with a mean of zero and a variance of $N_0/2$ per dimension in the j-th receive antenna at time t.

The total transmitted power is given by

$$P = E\{\boldsymbol{c}(t)^H \boldsymbol{c}(t)\} \tag{1.2}$$

where, $E\{\cdot\}$ denote the expectation operation and $(\cdot)^H$ denote the Hermitian conjugate.

The channel coefficients are assumed to be perfectly known at receiver only and there is no channel knowledge known at transmitter. The transmitted power is equally distributed to each antenna. Thus, the transmitted symbol energy is

$$E_s = P/n_t \tag{1.3}$$

The channel coefficients of flat fading channel can be further classified into two types: slow fading and fast fading. In slow fading channel, the channel coefficients are constant over the time of a frame and independently vary from frame to frame. In fast fading channel, the channel coefficients remain constant over one symbol duration and independently vary from symbol to symbol.

The model of MIMO system may be described in form of matrix. Let us introduce the channel matrix

$$\boldsymbol{H}_t = \begin{bmatrix} h_{1,1}(t) & h_{1,2}(t) & \cdots & h_{1,n_t}(t) \\ h_{2,1}(t) & h_{2,2}(t) & \cdots & h_{2,n_t}(t) \\ \vdots & \vdots & \ddots & \vdots \\ h_{n_r,1}(t) & h_{n_r,2}(t) & \cdots & h_{n_r,n_t}(t) \end{bmatrix} \tag{1.4}$$

Thus, we can write the system of (1.1) as a matrix equation

$$\boldsymbol{r}_t = \boldsymbol{H}_t \boldsymbol{c}_t + \boldsymbol{n}_t \tag{1.5}$$

where

$$\boldsymbol{r}_t = \begin{bmatrix} r_1(t) & r_2(t) & \cdots & r_{n_r}(t) \end{bmatrix}^T \tag{1.6}$$

$$\boldsymbol{n}_t = \begin{bmatrix} n_1(t) & n_2(t) & \cdots & n_{n_r}(t) \end{bmatrix}^T \tag{1.7}$$

1.3 MIMO System Capacity

In this section MIMO system capacity was analyzed. In a communication system, the capacity of a channel is measured by well-known Shannon capacity, which is defined as the maximum bit rate at which information data can be communicated through this channel without error. In AWGN channel, the Shannon capacity can be expressed as the spectrum efficiency [6]

$$C = \log_2(1 + \rho) \tag{1.8}$$

where, C is channel capacity in bps/Hz, and ρ is the signal-to-noise ratio expressed as a pure ratio.

Obviously, observing from (1.8), the capacity is controlled by the value of SNR. In a wireless fading channel, SNR is modified by multiplying SNR by time-variant channel

coefficients. Thus, the effect of fading on capacity in a wireless fading channel without antenna diversity is modeled by the formula

$$C = \log_2(1 + \rho|h|^2) \tag{1.9}$$

where h is complex channel coefficient.

In the following analysis for the capacity of MIMO system, we consider that Maximum Ratio Combining (MRC) receive diversity processing is used, no channel information know at transmitter (open loop MIMO), the total transmit power is limited to P regardless of the number of transmit antennas, and the power is equally distributed to all transmit antennas. Thus the transmit power at each transmit antenna is given by

$$p = P/n_t \tag{1.10}$$

For receive diversity with MRC, the total SNR is obtained simply by summing the SNR at individual receive antenna, resulting in

$$C = \log_2\left(1 + \rho \sum_{i=1}^{n_r} |h_i|^2\right) \tag{1.11}$$

The capacity for transmit diversity is formulated in the same way as for receive diversity. However, the situation on the SNR is somewhat different for transmit diversity, where transmit power is distributed equally to the antenna elements. From (1.10), this behavior is characterized by replacing ρ with ρ/n_t

$$C = \log_2\left(1 + \frac{\rho}{n_t} \sum_{i=1}^{n_t} |h_i|^2\right) \tag{1.12}$$

A comparison between equation (1.11) with (1.12) shows, that the capacity of receive diversity is superior to that of transmit diversity because of the inclusion of divisor n_t in (1.12), as reflected in figure 1.3 and 1.4. Fig. 1.3 depicts the capacity of transmit

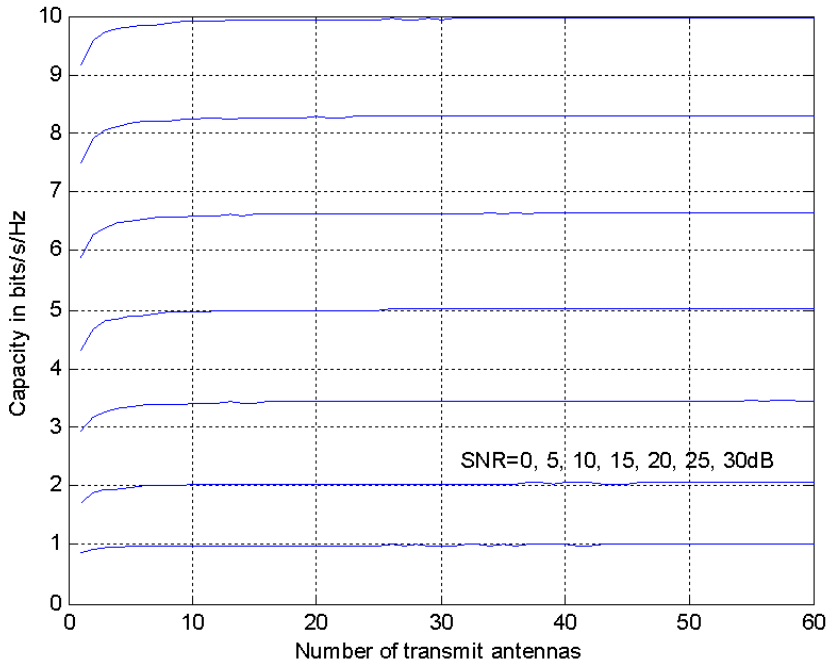

Figure 1.3. Capacity of transmit diversity.

diversity given by (1.12) as a function of number of transmit antennas. The figure shows that the capacity curve is almost flat over the range of more than two transmit antennas. Over the range of less than two transmit antenna, the capacity increases are limited. This result indicates that it is difficult to obtain a noticeable improvement in capacity by means of transmit diversity. This can be explained by the asymptotic behavior of capacity as n_t goes to infinity

$$\lim_{n_t \to \infty} C = \log_2(1 + \rho) \tag{1.13}$$

Fig. 1.4 plots the capacity of receive diversity given by (1.11) as a function of the number of receive antennas. The figure shows that receive diversity have a more noticeable capacity gain, which appears to be a linear increase of capacity with the logarithm of number of receive antennas. This result shows that receive diversity seems

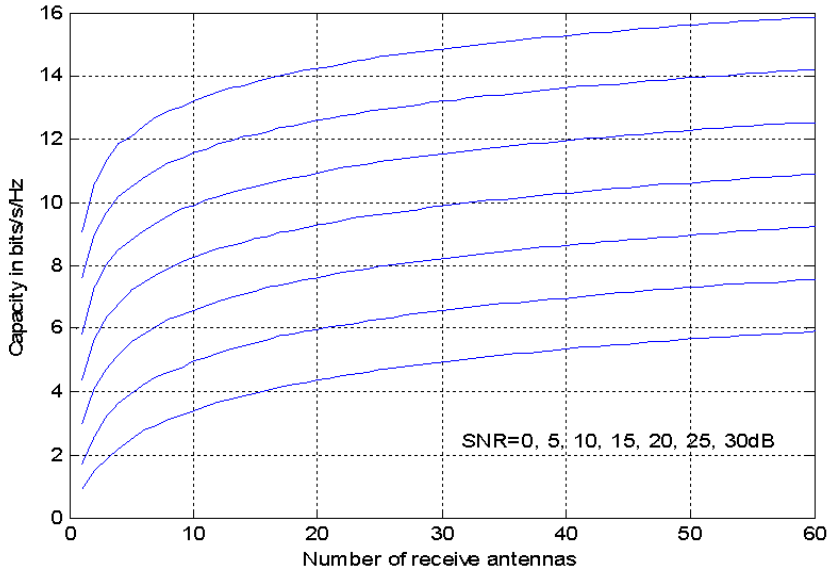

Figure 1.4. Capacity of receive diversity.

to be quite promising for high data rate transmission. As a result, receive diversity has been traditional method of enhancing the capacity and currently applied in practice. However, receive diversity still cannot meet the demand of high data rate transmission for 3G/4G.

The situation with combined transmit-receive diversity (MIMO) is much more complicated. In order to take all possible diversity paths into account, the system model in matrix form given by (1.5) is thus used. Decomposing the channel matrix using the Singular Value Decomposition (SVD), we obtain

$$\boldsymbol{H}_t = \boldsymbol{U}\boldsymbol{D}\boldsymbol{V}^H \tag{1.14}$$

where $\boldsymbol{U}$ is an $n_r \times n_r$ unitary matrix, $\boldsymbol{V}$ is an $n_t \times n_t$ unitary matrix, and $\boldsymbol{D}$ is a diagonal matrix of dimension $n_r \times n_t$ whose elements are the singular values of the original matrix in descending order.

Substituting equation (1.14) into equation (1.5) yields

$$\boldsymbol{r}_t = \boldsymbol{U}\boldsymbol{D}\boldsymbol{V}^H \boldsymbol{c}_t + \boldsymbol{n}_t \tag{1.15}$$

Multiplying both side of equation (1.15) by $\boldsymbol{U}^H$ we get

$$\boldsymbol{r}_t{}' = \boldsymbol{D}\boldsymbol{c}_t{}' + \boldsymbol{n}_t{}' \tag{1.16}$$

where

$$\boldsymbol{r}_t{}' = \boldsymbol{U}^H \boldsymbol{r}_t \tag{1.17}$$

$$\boldsymbol{c}_t{}' = \boldsymbol{V}^H \boldsymbol{c}_t \tag{1.18}$$

$$\boldsymbol{n}_t{}' = \boldsymbol{U}^H \boldsymbol{n}_t \tag{1.19}$$

The number of nonzero diagonal elements of matrix $\boldsymbol{D}$ is equal to the rank of $\boldsymbol{H}$. Let r be the rank of $\boldsymbol{H}$, $\sqrt{\lambda_i}$ the i-th singular values of $\boldsymbol{H}$. Then, the i-th entry of $\boldsymbol{r}_t{}'$ is given by

$$r_i(t)' = \sqrt{\lambda_i} c_i(t)' + n_i(t)', \quad i = 1, \ldots, r \tag{1.20}$$

Due to the unitary property of $\boldsymbol{U}$ matrix, $n_i(t)'$ is an independent Gaussian random variable with zero mean and variance of $N_0/2$ per dimension. Thus equation (1.20) can be considered as a standard model of single input single output wireless communication system with input $c_i(t)'$, output $r_i(t)'$, and channel coefficient $\sqrt{\lambda_i}$. The physical interpretation of (1.20) is therefore that the MIMO channel is equivalent to r parallel independent sub-channel with channel gain of $\sqrt{\lambda_i}$. This is the secret behind how MIMO is able to create so much good performance.

The total transmitted power on signal $\boldsymbol{c}_t'$ is given by

$$P' = \boldsymbol{c}_t'^H \boldsymbol{c}_t' = \boldsymbol{c}_t^H \boldsymbol{c}_t \tag{1.21}$$

This equation states that signal $\boldsymbol{c}_t'$ carries the same transmitted power as the signal $\boldsymbol{c}_t$. Assuming that the transmitted power on each sub-channel has an uniform distribution of all P. Thus, the capacity of sub-channel can be expressed as

$$C_i = \log_2 \left(1 + \lambda_i \frac{\rho}{n_t}\right), \quad i = 1, \cdots, r \tag{1.22}$$

Summing up these equation for $i = 1, \cdots, r$, one obtains the capacity of MIMO

$$C = \sum_{i=1}^{r} \log_2 \left(1 + \lambda_i \frac{\rho}{n_t}\right) = \log_2 \prod_{i=1}^{r} \left(1 + \lambda_i \frac{\rho}{n_t}\right) \tag{1.23}$$

The λ_i can be easily proved to be the eigenvalue of $\boldsymbol{H}\boldsymbol{H}^H$. From the definition of eigenvalue, we know

$$\prod_{i=1}^{r} (\lambda - \lambda_i) = \det \left(\lambda I_{n_r} - \boldsymbol{H}\boldsymbol{H}^H\right) \tag{1.24}$$

Let $\lambda = -\frac{n_t}{\rho}$, equation (1.24) can be manipulated to the form

$$\prod_{i=1}^{r} \left(1 + \lambda_i \frac{\rho}{n_t}\right) = \det \left(I_{n_r} + \frac{\rho}{n_t} \boldsymbol{H}\boldsymbol{H}^H\right) \tag{1.25}$$

Combining (1.23) and (1.25), we can obtain the capacity of MIMO

$$C = \log_2 \det \left(I_{n_r} + \frac{\rho}{n_t} \boldsymbol{H}\boldsymbol{H}^H\right) \tag{1.26}$$

Fig. 1.5 plots the MIMO capacity for $n_t = n_r$. Fig. 1.5 shows there is a linear increase in the capacity as a function of the number of antennas. This monotonic relationship offers an enormous gain in capacity, as shown in Table 1.1

In above derivation, the channel coefficients are time-varying random variables. Thus the capacity given in (1.11) (1.12) (1.26) is actually the instantaneous capacity.

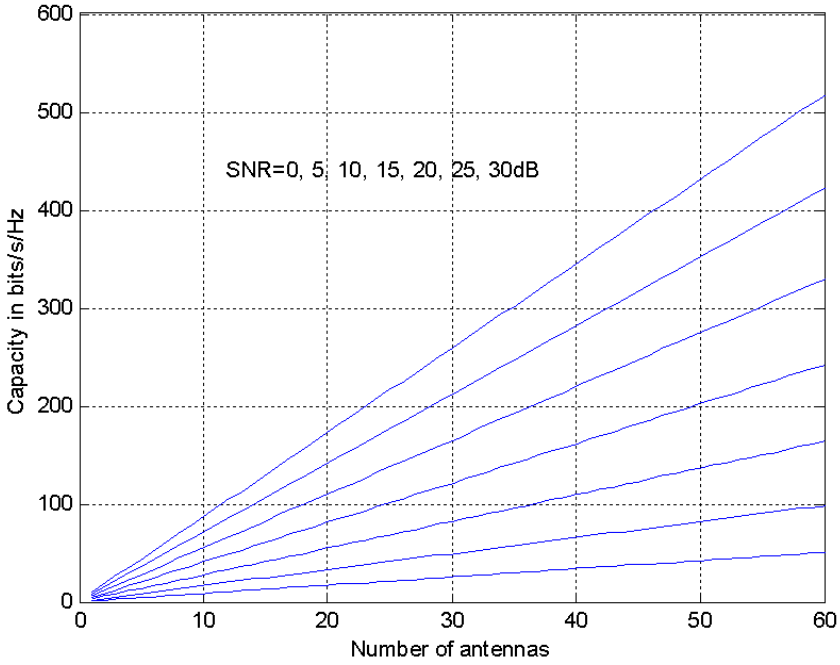

Figure 1.5. Capacity of MIMO for $n_t = n_r$.

Capacity plotted in Fig. 1.3, 1.4, and 1.5 are the average capacity obtained by averaging the instantaneous capacity over the channel realization of $\boldsymbol{H}$. The capacity above is actually the capacity of a fast fading channel. For the slow fading channel, the channel matrix has a Rayleigh distribution but constant within the duration of a frame. In this scenario, there is a nonzero probability that the Shannon capacity might be zero for particular realization of $\boldsymbol{H}$ [7]. Therefore, the capacity is measured by the capacity

Table 1.1. Numerical results of the capacity of space diversity, SNR=30 dB

System	Configuration	Capacity (bps/Hz)
MISO	4Tx1Rx	9.78
SIMO	1Tx4Rx	11.77
MIMO	2Tx2Rx	34.92

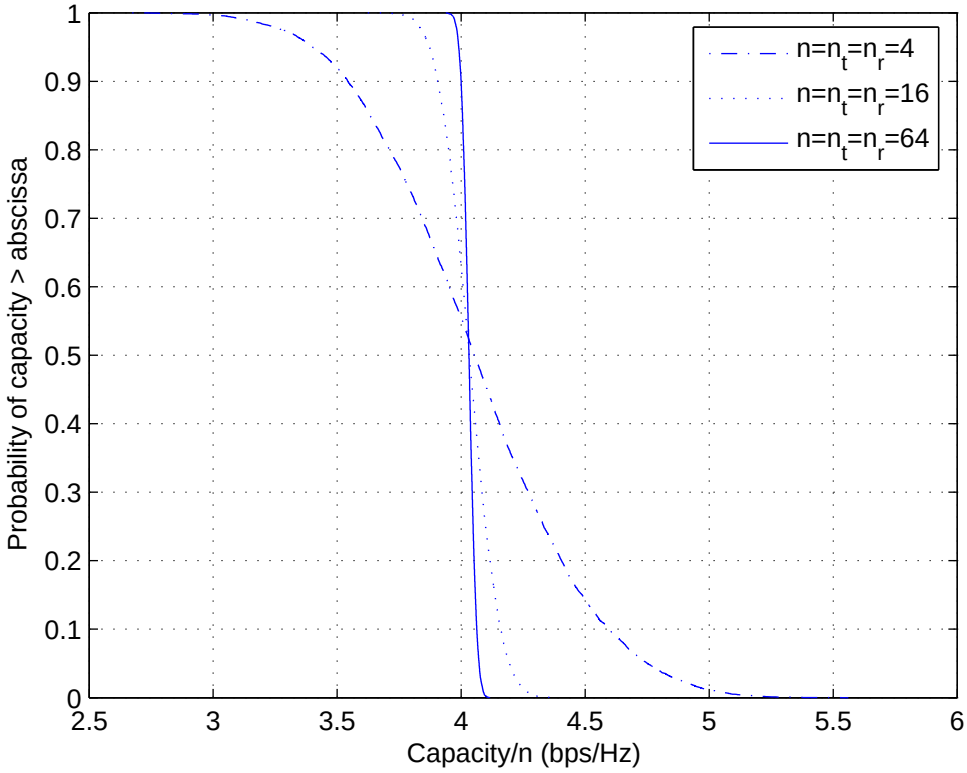

Figure 1.6. Capacity of MIMO for $n_t = n_r$.

cumulative distribution function (ccdf) in slow fading channels. The ccdf describes the probability that a specific capacity can be provided by system. Fig. 1.6 shows the ccdf of MIMO capacity. The figure indicates that capacity approaches an asymptote and becomes independent of the number of antennas as the increase of the number of antenna elements. This result is consistent with the result in fast fading channel as shown in Fig. 1.5.

1.4 Space-Time Codes

While MIMO discussed above significantly improves capacity performance, further gain can be obtained by applying channel coding in system. Channel coding has been traditionally adopted for wireless communications. For example, convolution codes have

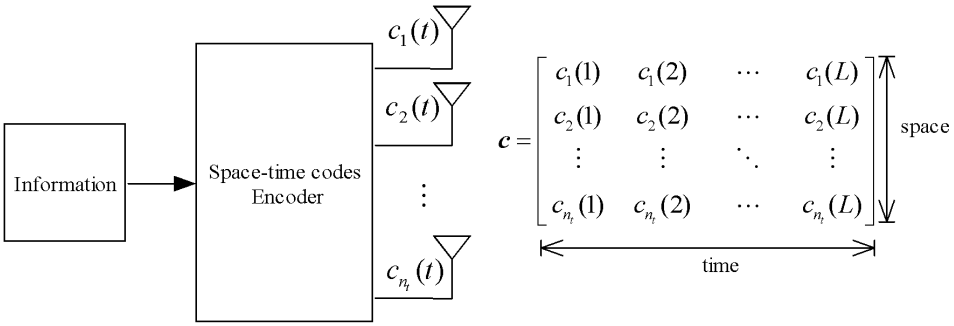

Figure 1.7. Space-time codes.

been applied in GSM to provide additional link margin and turbo codes have been proposed as a key technology in 3G. Starting with Shannon's information theory, channel coding has been developed toward the goal of approaching Shannon limit on channel capacity. However, diversity and channel coding are usually used separately or independently in a wireless system. Recently, the joint design of MIMO and channel coding has been receiving increasing attentions in wireless research community. The most conspicuous result of the activity of combining antenna diversity with channel coding is that diversity gain can be achieved, as well as coding gain. This method of operation has been referred to as the "space-time codes" [5].

The concept of space-time codes is illustrated in Fig. 1.7. Space-time codes map information symbol into an encoded symbol vector at each time slot. The vector consists of n_t M-PSK symbol. These multiple symbols are transmitted simultaneously at each time slot through multiple antennas. Thus, the transmitted symbols are inherently correlated in space. Because of the memory of the space-time codes, all encoded symbol vector are also correlated in time. This is the reason of naming them as "space-time codes".

Throughout the years there have been various efforts to achieve significant increased capacity using space-time codes. For this reason, space-time codes have emerged

as attractive means for new next generation wireless networks (3G/4G). Bell Laborites Layered Space-Time (BLAST) system is the first MIMO system for high data rate transmission [8]. In BLAST, a high data rate stream is divided into multiple lower data rate sub-streams. The multiple data sub-streams are simultaneously transmitted through multiple antennas using same frequency band. At receiver, each receive antenna output is made up of a linear combination of the multiple transmitted data streams. The data streams can be successfully separated using sophisticated signal processing technique relying on the assumption that the channel state information is perfectly known to the receiver. The spectral efficiency increase in BLAST is roughly proportional to the number of transmit antennas. BLAST had been successfully demonstrated. Its performance of spectral efficiencies was found to be about 20-40 bps/Hz, which is believed to be unprecedented wireless spectral efficiencies.

A simple but elaborate technique that provides a good illustration of the key concepts of space-time codes has been developed by Alamouti [9]. The prototype system of Alamouti's scheme was designed with two transmit antennas. Alamouti code operates on a block of input symbols. Each block consists of two symbols. The block is converted into an orthogonal matrix [1]. The orthogonal matrix is created to reduce the decoding complexity in addition to allowing full diversity gain. Thus Alamouti code does not provide coding gain. Based on the principle of Alamouti code, orthogonal space-time codes for more than two antennas have been developed and are referred to as Space-Time Block Codes (STBC) [12][11].

Based on Trellis Coded Modulation (TCM), space-time trellis codes had been proposed [5] to provide high performance. Space-time trellis codes can be considered as TCM

[1]In many mathematical texts, including [10], orthogonality is defined only for square matrices. In our case, we define a matrix to be orthogonality if its rows are mutually orthogonal, no matter if it is square. In [11], the non-square matrix with row orthogonality is called generalized orthogonal matrix

with multiple outputs. Space-time trellis codes are more attractive due to its coding gain advantage. In trellis-based codes, a better performance can be obtained by increasing the number of trellis states. However, the performance of trellis-based code are limited by the inevitable saturation of performance and the extremely high complexity of decoder realization with the increased number of states.

One way to achieve better performance is to use the turbo concept codes. Possibly one of the biggest advances in coding technology was the introduction of turbo codes, proposed by Berrou in 1993 [13]. The turbo codes successfully concatenate two recursive convolutional codes in parallel and decode iteratively, which make the codes powerful and allow achieving near Shannon capacity. Schemes that apply the principle of turbo codes into space-time codes had been referred to as space-time turbo codes.

Another way is by concatenating an outer code with inner space-time block codes. These codes make use of the orthogonal property of space-time block codes to improve the coding gain of outer codes. The outer codes may be a convolutional code, TCM, or space-time trellis codes. A well known such code is super orthogonal space-time trellis codes [14], whose outer codes is a space-time trellis codes with super-trellis structure.

1.5 Objectives

The objectives of this dissertation are to improve performance of space-time codes. Specifically, the aims are to increase diversity gain and coding gain for space-time codes. This dissertation proposes improved schemes in several applications, including space-time trellis codes, space-time turbo codes, and orthogonal space-time trellis codes. The performance of the proposed techniques had been theoretically analyzed. Detailed simulations are used to show that the implementations described in this dissertation can achieve the improved performance.

CHAPTER 2

PERFORMANCE ANALYSIS AND DESIGN CRITERIA

2.1 Introduction

In developing the concepts of space-time codes, Tarokh [5] had developed design criteria based on the upper bound of PEP. Other improved design criteria were later developed by [15][16][17]. Although subsequent works have demonstrated that limitations remain in Tarokh's criteria, they are still viewed as valuable for preliminary understanding of space-time codes because they provide good principles in designing codes. In this chapter, the performances of space-time codes are analyzed by deriving the upper bound of PEP. Design criteria based on the PEP are also introduced. The improved design criteria will be introduced later in next chapter.

The analysis for the upper bound of PEP has been studied previously [5]. In this chapter, we will review the analysis in a simplified form following the analysis given in [5]. For the first time, we also had derived the exact PEP of space-time codes. The derivation of the exact PEP given in this chapter is new and simple, which is totally different from previous derivation.

2.2 Pair-wise error probability (PEP)

Performances of space-time codes are characterized by diversity gain and coding gain. For the performance analysis, a codeword matrix is defined, allowing us to estimate the diversity gain and the coding gain. In space-time codes, the information symbols are segmented into a frame of length L. The encoded outputs associated with the frame are organized into a matrix, and is called a codeword matrix. A codeword is represented by

an $n_t \times L$ matrix whose entry is $c_i(t)$ where i is the row index with range $1 \leq i \leq n_t$ and t is the column index with range $1 \leq t \leq L$

$$\boldsymbol{c} = \begin{bmatrix} c_1(1) & c_1(2) & \cdots & c_1(L) \\ c_2(1) & c_2(2) & \cdots & c_2(L) \\ \vdots & \vdots & \ddots & \vdots \\ c_{n_t}(1) & c_{n_t}(2) & \cdots & c_{n_t}(L) \end{bmatrix} \tag{2.1}$$

The entries in each column correspond to the output signal on the trellis transition. At the decoder, the Maximum Likelihood (ML) algorithm with the assumption that the channel coefficients are perfectly known was used to estimate the transmitted codeword. Let $\boldsymbol{e}$ be an estimate of transmitted codeword at the decoder. In ML decoding, ML algorithm searches over all possible transmitted codewords and choose the most likely codeword with the highest probability $P(\boldsymbol{r}/\boldsymbol{e})$ as decoded output, where $\boldsymbol{r}$ is the receive signal given in (1.1) expressed in form of matrix

$$\boldsymbol{r} = \begin{bmatrix} r_1(1) & r_1(2) & \cdots & r_1(L) \\ r_2(1) & r_2(2) & \cdots & r_2(L) \\ \vdots & \vdots & \ddots & \vdots \\ r_{n_r}(1) & r_{n_r}(2) & \cdots & r_{n_r}(L) \end{bmatrix} \tag{2.2}$$

.

Ignoring the common terms in $P(\boldsymbol{r}/\boldsymbol{e})$, $P(\boldsymbol{r}/\boldsymbol{e})$ is typically expressed by the accumulated branch metric along the survivor path

$$AM(\boldsymbol{e}) = \sum_{t=1}^{L} \sum_{j=1}^{n_r} \left| r_j(t) - \sum_{i=1}^{n_t} h_{j,i}(t) e_i(t) \right|^2 \tag{2.3}$$

The final decision on output codeword is made, choosing the codeword with the highest $P(\boldsymbol{r}/\boldsymbol{e})$ or the lowest accumulated branch metric

$$\boldsymbol{e} = \arg \max_{\boldsymbol{e} \in \boldsymbol{D}} [P(\boldsymbol{r}/\boldsymbol{e})] = \arg \min_{\boldsymbol{e} \in \boldsymbol{D}} [AM(\boldsymbol{e})] \tag{2.4}$$

where $\boldsymbol{D}$ is the set of codewords

PEP is the probability that decoder erroneously selects codeword $\boldsymbol{e}$ as the transmitted codeword, while the codeword $\boldsymbol{c}$ is in fact transmitted. This will happen if

$$AM(\boldsymbol{c}) > AM(\boldsymbol{e}) \tag{2.5}$$

Thus, the PEP conditioned on $\boldsymbol{H}$ is given by

$$P(\boldsymbol{c} \rightarrow \boldsymbol{e}/\boldsymbol{H}) = P\left(AM(\boldsymbol{c}) > AM(\boldsymbol{e})\right) \tag{2.6}$$

Averaging $P(\boldsymbol{c} \rightarrow \boldsymbol{e}/\boldsymbol{H})$ over the probability density function of $\boldsymbol{H}$, yields the PEP as follows

$$P(\boldsymbol{c} \rightarrow \boldsymbol{e}) = \int P(\boldsymbol{c} \rightarrow \boldsymbol{e}/\boldsymbol{H}) P(\boldsymbol{H}) d\boldsymbol{H} \tag{2.7}$$

where $P(\boldsymbol{H})$ is the probability density function of $\boldsymbol{H}$

2.3 PEP for slow fading channel

In slow fading channels, the channel coefficients are constant over the duration of a frame. Thus the time dependence in channel coefficient in (1.5) can be omitted. The system model can be rewritten as

$$\boldsymbol{r} = \boldsymbol{H}\boldsymbol{c} + \boldsymbol{n} \tag{2.8}$$

where

$$\boldsymbol{n} = \begin{bmatrix} n_1(1) & n_1(2) & \cdots & n_1(L) \\ n_2(1) & n_2(2) & \cdots & n_2(L) \\ \vdots & \vdots & \ddots & \vdots \\ n_{n_r}(1) & n_{n_r}(2) & \cdots & n_{n_r}(L) \end{bmatrix} \tag{2.9}$$

Taking into account equation (2.8), equation (2.3) can be rewritten as

$$\begin{aligned} AM(\boldsymbol{e}) &= Tr\left[(\boldsymbol{r}-\boldsymbol{He})(\boldsymbol{r}-\boldsymbol{He})^H\right] \\ &= Tr\left[\boldsymbol{rr}^H - \boldsymbol{Her}^H - \boldsymbol{re}^H\boldsymbol{H}^H + \boldsymbol{Hee}^H\boldsymbol{H}^H\right] \end{aligned} \tag{2.10}$$

where $Tr[\cdot]$ is trace operator of square matrix.

The term $\boldsymbol{rr}^H$ is the common term for all codeword. It should, therefore, be omitted. Substituting equation (2.10) into equation (2.5), we get

$$Tr\left[-\boldsymbol{Hcr}^H - \boldsymbol{rc}^H\boldsymbol{H}^H + \boldsymbol{Hcc}^H\boldsymbol{H}^H\right] > Tr\left[-\boldsymbol{Her}^H - \boldsymbol{re}^H\boldsymbol{H}^H + \boldsymbol{Hee}^H\boldsymbol{H}^H\right] \tag{2.11}$$

which, after rearranging, is equivalent to

$$Tr\left[\boldsymbol{H}(\boldsymbol{e}-\boldsymbol{c})\boldsymbol{r}^H + \boldsymbol{r}\left(\boldsymbol{e}^H - \boldsymbol{c}^H\right)\boldsymbol{H}^H\right] > Tr\left[\boldsymbol{H}\left(\boldsymbol{ee}^H - \boldsymbol{cc}^H\right)\boldsymbol{H}^H\right] \tag{2.12}$$

Substituting (2.8) into (2.12) and making rearrangement of it yields

$$Tr\left\{2Re\left[\boldsymbol{H}(\boldsymbol{e}-\boldsymbol{c})\boldsymbol{n}^H\right]\right\} > Tr\left[\boldsymbol{H}(\boldsymbol{c}-\boldsymbol{e})(\boldsymbol{c}-\boldsymbol{e})^H\boldsymbol{H}^H\right] \tag{2.13}$$

Let

$$\boldsymbol{D}_{ce} = \boldsymbol{c} - \boldsymbol{e} \tag{2.14}$$

is a codeword difference matrix, and

$$\boldsymbol{A} = \boldsymbol{D}_{ce}\boldsymbol{D}_{ce}^H \tag{2.15}$$

is often called a codeword distance matrix, which is a square matrix of dimension n_t. The rank, determinant and trace of $\boldsymbol{A}$ are important features of space-time trellis codes. Performances of space-time codes are highly dependent on these parameters.

The right hand side of (2.13) thus becomes

$$\delta = Tr\left[\boldsymbol{H}\boldsymbol{A}\boldsymbol{H}^H\right] \tag{2.16}$$

which is defined as modified squared Euclidean distance between codeword $\boldsymbol{c}$ and $\boldsymbol{e}$.

The right hand side of (2.13) is a constant, and the left hand side of (2.13) is a Gaussian random variable with zero mean. Therefore, the PEP conditioned on $\boldsymbol{H}$ is then given by

$$P(\boldsymbol{c} \rightarrow \boldsymbol{e}/\boldsymbol{H}) = Q\left(\sqrt{\frac{E_s}{2N_0}\delta}\right) \tag{2.17}$$

Consider the inequality

$$Q(x) \leq \frac{1}{2}e^{-x^2/2} \tag{2.18}$$

The PEP conditioned on $\boldsymbol{H}$ is then upper bounded by

$$P(\boldsymbol{c} \rightarrow \boldsymbol{e}/\boldsymbol{H}) \leq \frac{1}{2}\exp\left(-\delta\frac{E_s}{4N_0}\right) \tag{2.19}$$

Utilizing the singular value decomposition, we have

$$\boldsymbol{A} = USV^H \tag{2.20}$$

where U and V are unitary orthogonal matrices and S is a diagonal matrix with real, non-negative eigenvalue elements λ_i in descending order

$$S = \begin{bmatrix} \lambda_1 & 0 & \cdots & 0 \\ 0 & \lambda_2 & \cdots & 0 \\ \vdots & \vdots & \ddots & \vdots \\ 0 & 0 & \cdots & \lambda_{n_t} \end{bmatrix} \tag{2.21}$$

Consider a Hermitian matrix $\boldsymbol{A}$,

$$\boldsymbol{A} = \boldsymbol{A}^H \tag{2.22}$$

Then

$$\boldsymbol{U} = \boldsymbol{V} \tag{2.23}$$

gives

$$\begin{aligned} \delta &= Tr\left(\boldsymbol{HUSU}^H\boldsymbol{H}^H\right) \\ &= \sum_{i=1}^{n_t}\sum_{j=1}^{n_r} \lambda_i \left|\beta_{j,i}\right|^2 \end{aligned} \tag{2.24}$$

where $\beta_{j,i}$ is the dot product of the j-th row vector of $\boldsymbol{H}$ and the i-th column vector of $\boldsymbol{U}$, defined as

$$\beta_{j,i} = \sum_{k=1}^{n_t} h_{j,k}u_{k,i} \tag{2.25}$$

Thus (2.19) becomes

$$P(\boldsymbol{c} \to \boldsymbol{e}/\boldsymbol{H}) \leq \frac{1}{2}\exp\left(-\sum_{j=1}^{n_r}\sum_{i=1}^{n_t}\lambda_i\left|\beta_{j,i}\right|^2\frac{E_s}{4N_0}\right) \tag{2.26}$$

Note that since $\boldsymbol{U}$ is an unitary orthogonal matrix, $\beta_{j,i}$ is an independent complex Gaussian variable. $|\beta_{j,i}|$ hence has a Rayleigh distribution

$$p\left(|\beta_{j,i}|\right) = 2\left|\beta_{j,i}\right|\exp\left(-\left|\beta_{j,i}\right|^2\right) \tag{2.27}$$

Integrating the PEP conditioned on $\boldsymbol{H}$ over random variable $|\beta_{j,i}|$ gives

$$P(\boldsymbol{c} \to \boldsymbol{e}) \leq \int_{|\beta_{n_r,n_t}|=0}^{\infty} \cdots \int_{|\beta_{1,1}|=0}^{\infty} \frac{1}{2} \exp\left(- \sum_{j=1}^{n_r} \sum_{i=1}^{n_t} \lambda_i \left|\beta_{j,i}\right|^2 \frac{E_s}{4N_0} \right) \\ p\left(|\beta_{1,1}|\right) \cdots p\left(|\beta_{n_r,n_t}|\right) d\left|\beta_{1,1}\right| \cdots d\left|\beta_{n_r,n_t}\right| \tag{2.28}$$

we finally obtain

$$P(\boldsymbol{c} \to \boldsymbol{e}) \leq \left(\prod_{i=1}^{n_t} \frac{1}{1 + \frac{E_s}{4N_0}\lambda_i} \right)^{n_r} \tag{2.29}$$

Assuming SNR is high, the PEP can be simplified as

$$P(\boldsymbol{c} \to \boldsymbol{e}) \leq \left(\prod_{i=1}^{r} \lambda_i \right)^{-n_r} \left(\frac{E_s}{4N_0} \right)^{-rn_r} \tag{2.30}$$

where r is the rank of $\boldsymbol{A}$.

2.4 PEP for fast fading channel

In fast fading channels, the system model is given by (1.5). The ML metric is therefore

$$AM(\boldsymbol{c}) = \sum_{t=1}^{L} \left\{ Tr\left[\left(\boldsymbol{r}_t - \boldsymbol{H}_t \boldsymbol{c}_t\right) \left(\boldsymbol{r}_t - \boldsymbol{H}_t \boldsymbol{c}_t\right)^H \right] \right\} \tag{2.31}$$

Consequently, equation (2.5) can be written in the form

$$\sum_{t=1}^{L} Tr\left\{ 2Re\left[\boldsymbol{H}_t \left(\boldsymbol{e}_t - \boldsymbol{c}_t\right) \boldsymbol{n}_t^H \right] \right\} > \sum_{t=1}^{L} Tr\left[\boldsymbol{H}_t \boldsymbol{A}_t \boldsymbol{H}_t^H \right] \tag{2.32}$$

where the codeword distance matrix is now defined as

$$\boldsymbol{A}_t = \left(\boldsymbol{c}_t - \boldsymbol{e}_t\right) \left(\boldsymbol{c}_t - \boldsymbol{e}_t\right)^H \tag{2.33}$$

$\boldsymbol{A}_t$ is sometime called as sub-codeword distance matrix. Since the matrix is related to the branch output, we refer to it as branch codeword distance matrix.

Since $(\boldsymbol{c}_t - \boldsymbol{e}_t)$ is a column vector, $\boldsymbol{A}_t$ is a singular matrix with rank one. In this case, the eigenvalue of $\boldsymbol{A}_t$ is equal to the squared Euclidean distance between $\boldsymbol{c}_t$ and $\boldsymbol{e}_t$

$$\lambda_1^t = \sum_{i=1}^{n_t} |c_i(t) - e_i(t)|^2 \tag{2.34}$$

Therefore, the modified squared Euclidean distance between codeword $\boldsymbol{c}$ and $\boldsymbol{e}$ is

$$\delta = \sum_{t=1}^{L} \sum_{j=1}^{n_r} \lambda_1^t \left|\beta_{j,1}^t\right|^2 \tag{2.35}$$

By continuing in the same manner for the PEP in the slow fading channel, the upper bound of PEP can be written as

$$P(\boldsymbol{c} \to \boldsymbol{e}) \leq \prod_{t=1}^{L} \left(\frac{1}{1 + \frac{E_s}{4N_0}\lambda_1^t} \right)^{n_r} = \prod_{t \in v(\boldsymbol{c},\boldsymbol{e})} \left(\frac{1}{1 + \frac{E_s}{4N_0}\lambda_1^t} \right)^{n_r} \tag{2.36}$$

where $\nu(\boldsymbol{c}, \boldsymbol{e})$ is the set of time instance $1 \leq t \leq L$ at which the squared Euclidean distance λ_1^t is not equal to zero.

By assuming SNR is high enough, equation (2.36) is reduced to

$$P(\boldsymbol{c} \to \boldsymbol{e}) \leq (d_p)^{-n_r} \left(\frac{E_s}{4N_0} \right)^{-\delta_H n_r} \tag{2.37}$$

where δ_H is the symbol Hamming distance which is defined as the number of elements in $\nu(\boldsymbol{c}, \boldsymbol{e})$, and

$$d_p = \prod_{t \in v(\boldsymbol{c},\boldsymbol{e})} \lambda_1^t \tag{2.38}$$

is defined as the product distance of codeword pair ($\boldsymbol{c}$, $\boldsymbol{e}$)

2.5 Design criteria

The upper bound of PEP on quasi-static flat fading channels and fast fading channels have been developed using Chernoff bound in [5], and were described by (2.30) and (2.37). Based on the bound, the design criteria can be derived as follows.

In (2.30) the importance of the rank of $\boldsymbol{A}$ to the PEP is that it determines the slope of the logarithm of the PEP plotted against the logarithm of SNR. This implies that the rank of $\boldsymbol{A}$ is a dominant factor in determining PEP performance. The product of nonzero eigenvalue, $\prod_{i=1}^{r} \lambda_i$, will result in PEP shift along the SNR axis. Following the definition in [5], the exponent term rn_r is called the diversity gain, and the term $\left(\prod_{i=1}^{r} \lambda_i\right)^{-n_r}$ is called the coding gain. The rank and determinant criteria has been developed by minimizing the worst PEP [5] as follows:

- The rank criterion: In order to achieve the maximum diversity, the matrix D_{ce} has to be full rank for any codewords $\boldsymbol{c}$ and $\boldsymbol{e}$. If D_{ce} has minimum rank r over the set of two-tuples of distinct codewords, then a diversity of rn_r is achieved.
- The determinant criterion: Suppose that a diversity benefit of rn_r is our target. The minimum of rth roots of the sum of determinants of all $r \times r$ principal cofactors of $A(\boldsymbol{c}, \boldsymbol{e}) = D_{ce} D_{ce}^H$ taken over all pairs of distinct codewords $\boldsymbol{e}$ and $\boldsymbol{c}$ corresponds to the coding advantage, where r is the rank of $A(\boldsymbol{c}, \boldsymbol{e})$. Special attention in the design must be paid to this quantity for any codewords $\boldsymbol{e}$ and $\boldsymbol{c}$. The design target is making this sum as large as possible. If a diversity of $n_t n_r$ is the design target, then the minimum of the determinant of $\boldsymbol{A}(\boldsymbol{c}, \boldsymbol{e})$ taken over all pairs of distinct codewords $\boldsymbol{e}$ and $\boldsymbol{c}$ must be maximized.

The upper bound of PEP for fast fading channel is described by (2.37). Similarly, minimizing the worst upper bound of PEP lead to the design criteria [5]:

- The distance criterion: In order to achieve the diversity vn_r in a rapid fading environment, for any two codewords $\boldsymbol{c}$ and $\boldsymbol{e}$ the strings $\boldsymbol{c}_t = [c_t(1)c_t(2)\cdots c_t(n_t)]$ and $\boldsymbol{e}_t = [e_t(1)e_t(2)\cdots e_t(n_t)]$ must be different at least for v values of 1 to L.
- The product criterion: Let $v(\boldsymbol{c}, \boldsymbol{e})$ denote the set of time instances $1 \leq t \leq L$ such that $[c_t(1)c_t(2)\cdots c_t(n_t)] \neq [e_t(1)e_t(2)\cdots e_t(n_t)]$ and let

$$|\boldsymbol{c}_t - \boldsymbol{e}_t|^2 = \sum_{i=1}^{n_t} |c_i(t) - e_i(t)|^2$$

Then to achieve the most coding advantage in a rapid fading environment, the minimum of the products

$$\prod_{t \in v(c,e)} |\boldsymbol{c}_t - \boldsymbol{e}_t|^2$$

taken over distinct codewords $\boldsymbol{c}$ and $\boldsymbol{e}$ must be maximized.

2.6 A derivation of exact PEP for space-time codes

2.6.1 Introduction

Performance analysis of space-time codes by deriving the upper bound of PEP has been developed in [5] and has been reviewed previously. The upper bound on PEP offers the insight in relationship between the performance and the code parameters, which has been summarized into design criteria. This forms the basis for the development of space-time codes.

Traditional theoretical analysis has paid little attention to the exact PEP, because design criteria based on upper bound can provide design guideline for the diversity gain which dominate the code performance. However, design criteria based on upper bound has no guideline for the coding gain. It has been found that codes designed according to such criteria may have same code parameters (determinant, trace, or product distance)

but have quite different coding gain in low SNR range. In order to precisely evaluate the code performance over entire SNR range, exact PEP is required. Previous derivations of exact PEP are based on residue technique combined with characteristic function [18], and moment generating function method [19]. Here we describe a straightforward method for finding exact PEP of space-time codes. In the method, the derivation is by finding the pdf of modified Euclidean distance, and the PEP conditioned on the distance is then averaged over the distance to obtain the exact PEP. In comparison to method in [18][19], our derivations are simpler and easier.

2.6.2 Exact PEP for space-time codes in slow fading channel

The derivation begins with classic equation of PEP conditioned on channel estimation, given in (2.17).

Let

$$\mu_i = \sum_{j=1}^{n_r} \lambda_i \left|\beta_{j,i}\right|^2 \tag{2.39}$$

which is a chi-square variable with $2n_r$ degrees of freedom. The Laplace transform of its pdf is given by

$$X_{\mu_i}(s) = \frac{1}{(1+s\lambda_i)^{n_r}} \tag{2.40}$$

Combining (2.39) into equation (2.24) gives

$$\delta = \sum_{i=1}^{r} \mu_i \tag{2.41}$$

Because of the statistical independence of μ_i, the Laplace transform of the pdf of δ is given by

$$X_\delta(s) = \prod_{i=1}^{r} \frac{1}{(1+s\lambda_i)^{n_r}} \tag{2.42}$$

Applying partial fraction expansion to $X_\delta(s)$ results in

$$X_\delta(s) = \sum_{i=1}^{r}\sum_{j=1}^{n_r} \frac{a_{i,j}}{(1+s\lambda_i)^{j}} \tag{2.43}$$

where

$$a_{i,j} = \frac{1}{(n_r-j)!}\frac{d^{n_r-j}}{ds^{n_r-j}}\left[(1+s\lambda_i)^{n_r} X_\delta(s)\right]\Bigg|_{s=-1/\lambda_i} \tag{2.44}$$

The terms in sum of (2.43) are the standard Laplace transform of Gamma pdf. Taking inverse Laplace transformation to (2.43) yields the pdf of δ

$$p_\delta(\delta) = \sum_{i=1}^{r}\sum_{j=1}^{n_r} \frac{a_{i,j}\delta^{j-1}}{\lambda_i^{j}\Gamma(j)} e^{-\frac{\delta}{\lambda_i}} \tag{2.45}$$

The conditional error probability of (2.17) can now be averaged over the δ distribution to obtain exact PEP

$$\begin{aligned} P(\boldsymbol{c}\to\boldsymbol{e}) &= \textstyle\int_\delta P(\boldsymbol{c}\to\boldsymbol{e}/H) p_\delta(\delta) d\delta \\ &= \sum_{i=1}^{r}\sum_{j=1}^{n_r} \textstyle\int_0^\infty Q\left(\sqrt{\frac{E_s}{2N_0}}\delta\right) \frac{a_{i,j}\delta^{j-1}}{\lambda_i^{j}\Gamma(j)} e^{-\frac{\delta}{\lambda_i}} d\delta \end{aligned} \tag{2.46}$$

By iterative use of integration parts, this integral can be evaluated in closed form as (see appendix A)

$$P(\boldsymbol{c}\to\boldsymbol{e}) = \sum_{i=1}^{r}\sum_{j=1}^{n_r} \frac{a_{i,j}}{2}\left[1 - \sqrt{\frac{\gamma\lambda_i}{1+\gamma\lambda_i}} \sum_{k=0}^{j-1} \binom{2k}{k} \frac{1}{(4+4\gamma\lambda_i)^{k}}\right] \tag{2.47}$$

where

$$\gamma = \frac{E_s}{4N_0}$$

Two examples of the application of (2.47) are illustrated as follows. First let us consider the particular case of equal eigenvalue, where $\lambda = \lambda_1 = \lambda_2 = \cdots = \lambda_r$. Then from (2.42)

$$X_\delta(s) = \frac{1}{(1+s\lambda)^{rn_r}} \tag{2.48}$$

Equation (2.48) above is obviously the Laplace transform of chi-square variable with $2rn_r$ degrees of freedom. From (2.43), it can be considered to be a term with coefficient equal to 1 and exponent equal to rn_r in sum. From (2.45) and (2.46), we have

$$P(\boldsymbol{c} \to \boldsymbol{e}) = \frac{1}{2}\left[1 - \sqrt{\frac{\gamma\lambda}{1+\gamma\lambda}} \sum_{k=0}^{rn_r-1} \binom{2k}{k} \frac{1}{(4+4\gamma\lambda)^k}\right] \tag{2.49}$$

This particular case can be applied to space-time block codes [11] and super-orthogonal space-time codes [14].

We now consider the case of the system with one receive antenna. In this case, (2.47) can be simplified as

$$P(\boldsymbol{c} \to \boldsymbol{e}) = \sum_{i=1}^{r} \frac{a_{i,1}}{2}\left(1 - \sqrt{\frac{\lambda_i\gamma}{1+\lambda_i\gamma}}\right) \tag{2.50}$$

For such a system with two transmit antennas and full diversity order, (2.44) would yield two coefficients

$$\begin{aligned} a_{1,1} &= \tfrac{\lambda_1}{\lambda_1-\lambda_2} \\ a_{2,1} &= -\tfrac{\lambda_2}{\lambda_1-\lambda_2} \end{aligned} \tag{2.51}$$

Substituting (2.51) into (2.50) gives

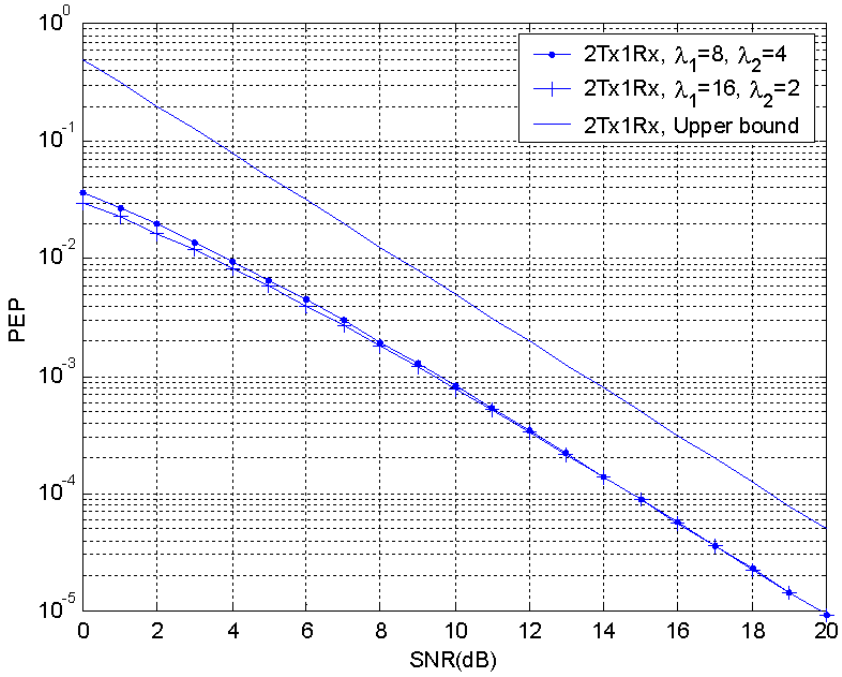

Figure 2.1. PEP of space-time codes with two transmit and one receive antennas.

$$P(\boldsymbol{c} \to \boldsymbol{e}) = \frac{1}{2}\left[1 - \frac{1}{\lambda_1 - \lambda_2}\left(\lambda_1\sqrt{\frac{\gamma\lambda_1}{1+\gamma\lambda_1}} - \lambda_2\sqrt{\frac{\gamma\lambda_2}{1+\gamma\lambda_2}}\right)\right] \tag{2.52}$$

The significance of exact PEP can be seen in Fig. 2.1, which plots the exact PEP described in (2.52) and compares it to the upper bound. The codes in the figure have different eigenvalues, but have same upper bound because the upper bound is dependent on the product of eigenvalues or determinant. However, in the low SNR range, PEP is found to be different, such that code with large trace (the sum of eigenvalues) offers superior performance. These results hint that, in the low SNR range, the upper bound may not serve as an useful forecast to the performance of space-time codes. Therefore, more accurate upper bound had been proposed in subsequent papers [15][16][17].

2.6.3 Exact PEP for space-time codes in fast fading channel

In fast fading channel, the modified squared Euclidean distance between codeword $\boldsymbol{c}$ and $\boldsymbol{e}$ is given in (2.35) as follows

$$\delta = \sum_{t=1}^{L} \sum_{j=1}^{n_r} \lambda_1^t \left| \beta_{j,1}^t \right|^2 \tag{2.53}$$

Compare the distance with that in slow fading channel, one can easily get the PEP in fast fading channel by replacing corresponding variables of (2.47) as

$$P(\boldsymbol{c} \to \boldsymbol{e}) = \sum_{t \in v(\boldsymbol{c},\boldsymbol{e})} \sum_{j=1}^{n_r} \frac{a_{t,j}}{2} \left[1 - \sqrt{\frac{\gamma \lambda_1^t}{1+\gamma \lambda_1^t}} \sum_{k=0}^{j-1} \binom{2k}{k} \frac{1}{(4+4\gamma \lambda_1^t)^k} \right] \tag{2.54}$$

CHAPTER 3

SPACE-TIME TRELLIS CODES

3.1 Introduction

By integrating spatial diversity and trellis based coding techniques, space-time trellis codes have received considerable attention, mainly because it offer coding gain as well as diversity gain, unlike space-time block codes, which only offer diversity gain.

Design issues concerning the code design criteria of space-time trellis code are discussed and the improved design criteria for space-time trellis codes are proposed in this chapter. The improved design criteria are designed to minimize frame error probability. The new codes based on proposed criteria have been successfully designed and simulated. The simulation results show that the performance of new codes based on proposed criteria can be improved compared to some existing codes.

3.2 Space-time trellis codes encoder

A Space-Time Trellis Code (STTrC), as shown in Fig. 3.1, is a multiple output trellis coded modulation.

The encoder encodes information data into M-PSK symbols. In order to guarantee full rate and avoid parallel trellis transition, the encoder has k parallel branches of register, where $k = \log_2 M$. Let i-th branch contains v_i register. Then the memory of encoder is the sum of the number of registers of each branch

$$v = \sum_{i=1}^{k} v_i \tag{3.1}$$

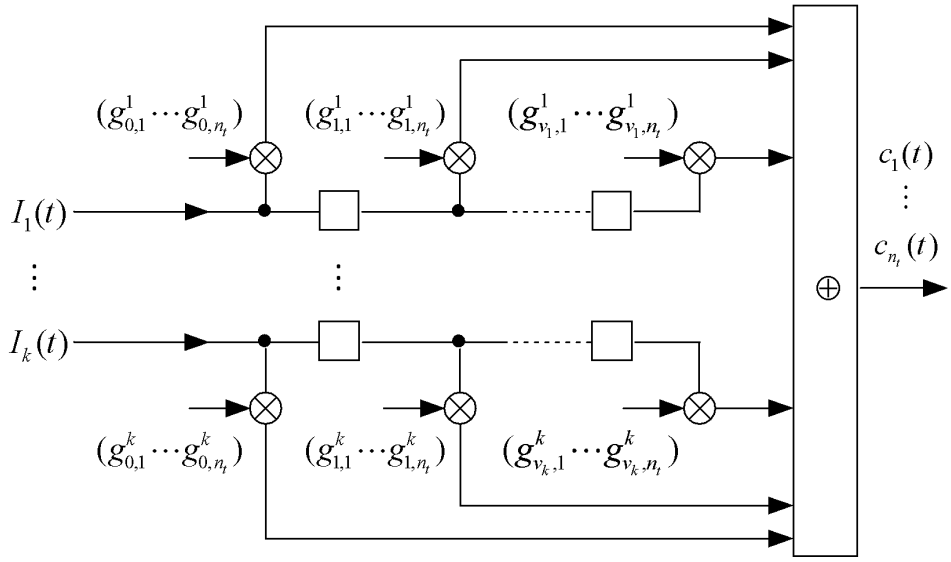

Figure 3.1. M-PSK space-time trellis code with n_t transmit antennas.

Error event length is the number of stages that the diverging state path must pass through to merge back to correct path. The diversity gain of space-time trellis cods in fast fading channel is directly dependent on the minimum error event length. Therefore, the minimum error event length is an important parameter to consider when designing a space-time trellis codes. The minimum error event length is equal to the minimum value of v_i plus one. The optimal choice of the v_i to obtain the optimal error event length for a given memory is given by

$$v_i = \lfloor \frac{v + i - 1}{k} \rfloor \tag{3.2}$$

where $\lfloor \cdot \rfloor$ denotes floor operation.

The inputs to the encoder are information symbols which are represented by k bit of information data. At each symbol epoch t, each k bit binary data, denoted by vector $\boldsymbol{I}_t = [I_1(t); \cdots ; I_k(t)]$, are directly applied to encoder in parallel and are encoded to n_t M-PSK symbols, which we present as a column vector of length n_t

$$\boldsymbol{c}_t = [c_1(t), \cdots, c_{n_t}(t)]^T \tag{3.3}$$

where the variable $c_i(t)$ is the encoded symbol in the i-th transmit antenna at time t.

The encoder is characterized by the feed forward polynomial. The output symbol and the polynomial coefficients are related by the following equation

$$c_i(t) = \sum_{j=1}^{k} \sum_{k=0}^{v_j} I_j(t-k) g_{k,i}^{j} \mod M \tag{3.4}$$

where, $g_{j,k}^{i}$ is feed forward polynomial coefficient. Its values are the integer from 0 to $M-1$.

The encoder may be characterized by a generator matrix $\boldsymbol{g}$.

$$\boldsymbol{g}_i = \begin{bmatrix} g_{0,1}^{i} & \cdots & g_{0,n_t}^{i} \\ \vdots & \ddots & \vdots \\ g_{v_i,1}^{i} & \cdots & g_{v_i,n_t}^{i} \end{bmatrix} \tag{3.5}$$

where $i = 1, 2, \cdots, k$

The generator in polynomial form is

$$\boldsymbol{G}_i(D) = \begin{bmatrix} 1 & D & \cdots & D^{v_i-1} \end{bmatrix} \boldsymbol{g}_i \tag{3.6}$$

The sequence of binary input to the i-th branch is now represented in polynomial form

$$\boldsymbol{I}_i(D) = I_i(0) + I_i(1)D + I_i(2)D^2 + I_i(3)D^3 + \cdots \tag{3.7}$$

From (3.6) and (3.7), the resulting output can be written in polynomial form

$$\begin{aligned} \boldsymbol{c}(D) &= \begin{bmatrix} c_1(D) & c_2(D) & \cdots & c_{n_t}(D) \end{bmatrix} \\ &= \sum_{i=1}^{k} \boldsymbol{I}_i(D)\boldsymbol{G}_i(D) \mod M \end{aligned} \tag{3.8}$$

The encoder can be also described by state diagram and its transfer function. Generator matrix is more convenient to the computer search of optimal codes, which is achieved by seeking optimal generator matrix to maximize the minimum distance of codeword distance matrix.

3.3 Code design criteria for space-time trellis codes in slow fading channels

3.3.1 Introduction

The early works of Tarokh [5] provided theoretical background on space-time codes. Tarokh developed the rank and determinant criteria for the quasi-static flat fading channel. The rank criterion may lead to full diversity, and makes Tarokh's criteria extremely useful for MIMO systems.

Rank and determinant design criteria have been widely viewed as the best way to code design. Many existing optimal codes had been designed based on rank and determinant criteria [20][21]. The weakness of Tarokh's criteria is that the code design criteria are based on minimizing the worst upper bound of PEP. Essentially, these criteria are also based on the assumption that the error events with minimum determinant are dominant. Although this is true for AWGN channel, this is not always the case for the quasi-static flat fading channel where there are no dominant error events [22][23]. Thus, although the rank criterion is of great importance, the determinant criterion does not provide guidelines for optimal coding gain. We will prove this by showing that the performance of the 4 state space-time trellis codes proposed by [5] is superior to that of some existing codes proposed in [20][21] for two transmit antennas and one receive antenna.

Since the introduction of the design criteria, the improved criteria had been proposed in subsequent works [15][16][17] to enhance the coding gain performance. However, these approaches are still based on PEP. In practice, the performance of space-time codes is evaluated in terms of FER. Thus, for successful code design it is important to develop design criteria based on FER over fading channel. In [23], [24], [25], and [26], the performance of space-time codes is predicted by union bound on FER, which is the function of the PEP and the Distance Spectrum (DS). A DS is a enumeration that contains the multiplicity of certain metrics of error events, which allows us to analyze the contribution of all error events to the performance. Thus, the union bound analysis is an attractive method of evaluating MIMO system performance in fading channel.

In this thesis, we described an improved design criteria based on the FER performance. The idea is to minimize the union bound on FER, leading to the improved design criteria. The similar techniques had been employed in [27]. Our method is similar to that in [27], except that we utilized the PEP proposed by Yuan [15] to upper bound the FER and the distance spectrum is calculated using alternate method. The PEP proposed by Yuan is more accurate expression for PEP. It takes into account the dependence of diversity gain on PEP. Yuan suggested that the rank and determinant criteria hold only for small diversity gain and the performance could be improved by introducing a trace criterion for large diversity gain. The trace criterion is the main improvement in rank and determinant criteria among the various improved criteria. In the union bound analysis, the coding gain mainly depends on the distance spectrum, instead of solely on distance. The difficulty associated with the distance spectrum search is the extremely high complexity of the search which limit the accurate measurement of coding gain.

3.3.2 Improved code design criteria

Several modifications to the rank and determinant criteria had been proposed in [15][16][17]. When considering the region of diversity gain, Tarokh's criteria were found to be less accurate. Thus, an important improvement over the basic rank and determinant criteria was to take into account the dependence of diversity gain on PEP [15]. In [15], Yuan suggested that the PEP is in fact diversity gain dependent. For $rn_r < 4$, the PEP can be given by (2.30). For $rn_r \geq 4$, the PEP is given by

$$P(\boldsymbol{c} \rightarrow \boldsymbol{e}) \leq \frac{1}{4} \exp\left(-n_r \frac{E_s}{4N_0} \sum_{i=1}^{r} \lambda_i\right) \tag{3.9}$$

The diversity gain boundary condition on PEP is chosen to be 4. This value is chosen to ensure that fading channels converge to Gaussian channels. Based on (3.9), the trace criterion was introduced in [15].

The rank, determinant, and trace criteria had been developed to minimize the worst PEP. These criteria reveal that good code construction requires two properties: full diversity gains and best code gain, and have been extensively used to describe the performance of space-time codes. Although the rank criterion will lead to best diversity gain, there are no guidelines for the code gain design. This is because that there are no dominant error events in quasi-static channels [22][23]. An alternative approach to performance analysis of space-time codes is to use the union bound technique, which allows us to analyze the contribution of all error events to the performance. Several performance analysis schemes based on the union bound analysis have been developed and applied in [23][26]. Generally, the union bound on FER is calculated from the PEP via a sum of PEP, given by

$$P_{FER} = \sum_{\boldsymbol{c} \in \boldsymbol{D}} \sum_{\substack{\boldsymbol{e} \in \boldsymbol{D} \\ \boldsymbol{e} \neq \boldsymbol{c}}} P(\boldsymbol{c}) P(\boldsymbol{c} \rightarrow \boldsymbol{e}) \tag{3.10}$$

where $\boldsymbol{D}$ is the set of transmitted codewords and $P(\boldsymbol{c})$ is the probability of transmitted codeword $\boldsymbol{c}$.

We first study the case of small diversity gain. Considering the rank is the dominant factor in determining the performances of space-time codes, we can assume in this research that the codes under consideration always have a full rank of n_t. This assumption is reasonable because it is easy to achieve full rank for the small diversity gain where the matrix size of $\boldsymbol{A}$ is only up to 3×3. With this assumption, the product of nonzero eigenvalues of $\boldsymbol{A}$ is equal to the determinant of $\boldsymbol{A}$. This leads to the following simplification of (2.30)

$$P(d) \leq d^{-n_r} \left(\frac{E_s}{4N_0} \right)^{-n_t n_r} \tag{3.11}$$

where d is the determinant of $\boldsymbol{A}$ and $P(d)$ is the PEP of the codeword error pair ($\boldsymbol{c}$, $\boldsymbol{e}$) with determinant d.

By combining the terms with same distance, equation (3.10) can be reduced to the weighted sum of PEP

$$P_{FER} = \sum_{d} N(d) P(d) \tag{3.12}$$

where $N(d)$ is the distance spectrum of space-time trellis codes for small diversity gain, which is defined as the average number of error events with determinant d.

Thus, for the small diversity gain, the FER, given by substituting (3.11) into (3.12), is

$$P_{FER} \leq \sum_{d} N(d) d^{-n_r} \left(\frac{E_s}{4N_0} \right)^{-n_t n_r} \tag{3.13}$$

From (3.13), clearly, we can see that the diversity gain plays the same role of determining the slope of FER as in PEP. This result means that the rank criterion can be directly applicable to FER. Similar in concept to PEP, the coding gain is defined as

$$\eta = \sum_{d} N(d) d^{-n_r} \tag{3.14}$$

Based on (3.13) and (3.14), code design criteria for the small diversity gain are designed to yield a minimum FER as following:

- Rank criterion [5]: in order to achieve the maximal diversity gain $n_t n_r$, the codeword distance matrix $\boldsymbol{A}$ has to be full rank for any codeword pairs $(\boldsymbol{c},\boldsymbol{e})$.
- To achieve optimal coding gain, the code that could provide the minimum value of η should be chosen.

  Similarly, for the large diversity gain, the FER can be given by

$$P_{FER} \leq \frac{1}{4} \sum_{T} N(T) \exp\left(-n_r \frac{E_s}{4N_0} T \right) \tag{3.15}$$

where T is the trace of codeword distance matrix $\boldsymbol{A}$. $N(T)$ is the distance spectrum of space-time trellis codes for large diversity gain, which is defined as the average number of error events with trace T.

We see from (3.15) that the trace is the exponent of the base of natural, which is scaled by SNR. This implies that the performance of FER is dominant by minimum trace for high SNR. This makes sense because the fading channels converge to AWGN channel with the increase of the diversity gain. The trace of $\boldsymbol{A}$ is equal to the squared Euclidean distance of the code, and the minimum squared Euclidean distance is usually

called as free distance. Therefore, the design criteria for the large diversity gain are to achieve optimal free distance and its spectrum:

- Trace criterion [15]: make sure that diversity gain rn_r is larger than or equal to 4, and maximize the free distance or minimum trace of codeword distance matrix $\boldsymbol{A}$.
- Minimize the average number of error events with free distance or minimum trace $N(T_0)$, where T_0 denotes free distance or minimum trace of codeword distance matrix $\boldsymbol{A}$.

3.3.3 Distance spectrum search

In order to apply proposed design criteria to space-time codes, we need to compute the distance spectrum $N(d)$ and $N(T)$. By definition, the distance spectrum is straightforward to compute from all error events or all pairs of distinct codewords. Although the rank can be obtained through systematic design, the distance spectrum is still based on search. In this research, the distance spectrum is obtained by the exhaustive computer search.

However, the complexity of distance spectrum search for time and resource grows exponentially with the length of frame and the number of trellis states, and makes it difficult to implement. The number of codewords is very large, for example 2^{260} for a simple QPSK code with frame length of 130. The number of error events is the combination of any two distinct codewords

$$N = \binom{2^{260}}{2} = 2^{518} \tag{3.16}$$

With such a lot of error events, an exhaustive computer search over all error events is infeasible.

Geometrically uniform codes will be helpful to reduce the complexity of search. The distance spectrum search for geometrically uniform code is the simplest to implement. It

is accomplished by computing the distance to all zero path, which serves as a reference. Although geometrically uniform code can significantly reduce the number of error events in search, it still has strict requirements on the length of frame and the number of trellis states for complete distance spectrum search. Furthermore geometrically uniform codes do not yield best performance for space-time codes in fading channel.

In practice, to reduce the computation complexity in our implementation, truncated distance spectrum is typically used. In truncated distance spectrum, the distance spectrum was chosen to include only the single error events with limited length of error event. An error event is said to be a single error event if the state path of the error event diverge and merge only once. Let u be the number of states. Let σ_t^i denote the state along the codeword path i at time t, where $0 \leq \sigma_t^i \leq u-1$ and $1 \leq t \leq L$. An simple error event with length l, associated with path i and j, is defined by

$$\begin{aligned} &\sigma_t^i = \sigma_t^j, t = 1 \\ &\sigma_t^i \neq \sigma_t^j, 1 < t < l-1 \\ &\sigma_t^i = \sigma_t^j, t > l \end{aligned} \tag{3.17}$$

The truncated distance spectrum is the subset of the complete distance spectrum and constitutes only a small proportion of the complete distance spectrum. Thus the coding gain based on the truncated distance spectrum is only a rough estimation. The accuracy of the coding gain depends on the way to determine the distance spectrum. Several truncated distance spectrum have been proposed [22][26]. In [22] the all zero path is assumed to be transmitted. In such a scheme, an error event, for example, is defined as that error paths diverge and merge only at zero state. However, as mentioned, this requires that the codes are geometrically uniform codes and the geometrically uniform codes do not guarantee the best performance. In [26] the distance spectrum is limited

to the first 3 minimum distance measures. However, only three measures is a very small subset and inadequate to estimate coding gain.

In this research, we compute the distance spectrum of all single error events with limited error events length, for example, single error events with $l \leq l_{max}$ are included in the distance spectrum. The General Algorithm (GA) [28] is employed for the distance spectrum search. GA is an efficient approach to the implementation of distance spectrum search, which is the most commonly used algorithm in distance spectrum search. GA works on super-state. Super-state is a state vector that contains two state i and j, denoted by $\sum_{ij}$. Let σ_i be the state i of the trellis. A super-state transition from $\sum_{ij}$ to $\sum_{pq}$ corresponds to the transition from σ_i to σ_p and transition from σ_j to σ_q, as shown in Fig. 3.2. Thus a simple error event that diverges at state i and merges at state j can be represented by a sequence of super-state

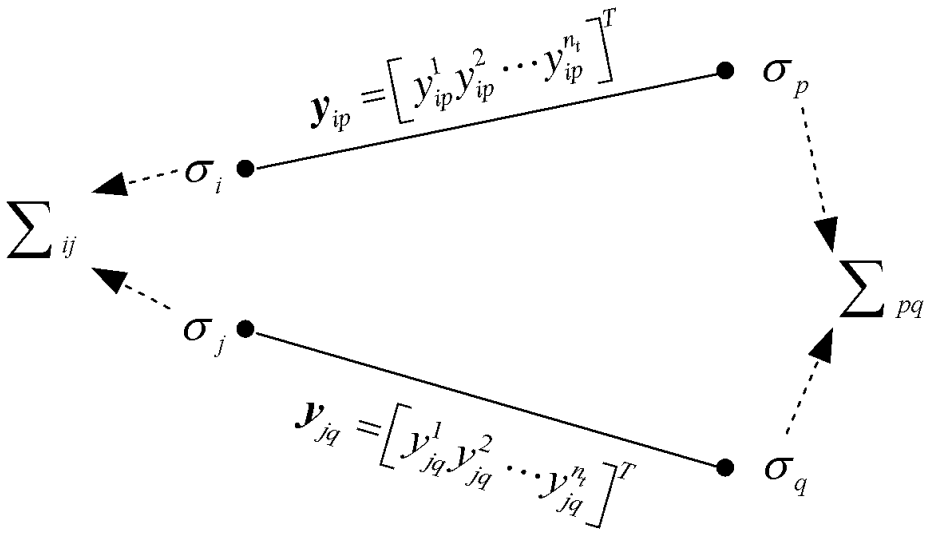

Figure 3.2. Transition of super-state: $\sum_{ij} \rightarrow \sum_{pq}$.

$$\sum_{ii} \cdots \sum_{pq} \cdots \sum_{jj}, \quad p \neq q \tag{3.18}$$

Fig. 3.2 shows that each transition has been assigned a column vector, which is the encoded output associated with the transition. The codeword distance matrix associated with the super transition form $\sum_{ij}$ to $\sum_{pq}$ is defined as

$$A\left(\sum_{ij} \rightarrow \sum_{pq}\right) = (\boldsymbol{y}_{ip} - \boldsymbol{y}_{jq})(\boldsymbol{y}_{ip} - \boldsymbol{y}_{jq})^H \tag{3.19}$$

A single error event with length k consists of k-step super-state transition. The codeword distance matrix of such error event is the sum of the codeword distance matrix of the super transition given in (3.19). For slow fading channel, the distance is either the determinant or trace of $\boldsymbol{A}$. Thus, the situation for the search of space-time codes is a little more complex than the situation described in [28]. Firstly, for the determinant search, the decision that if an error event should be included in distance spectrum is made at the step that the diverging path re-merge. This increases the complexity of search and the requirement for memory. Secondly, in addition to the distance spectrum, the rank of matrix also need to be carefully considered in determining the distance. The modified version of GA that concerns these issues is described as follows:

1. Initialization

   At the beginning of a search, a distance target is set. This value is used as a threshold to stop the algorithm. For $N(d)$ search, the value is the maximal error event length l_{max}. For $N(T)$ search, the values is the maximal trace T_{max}. The GA starts with collecting the set of codeword distance matrix for each super-state. All error events diverge at this step. Thus, the restriction at this step is that the super-state transition leaves from a common state.

Therefore, the initialization is the process of storing codeword distance matrix associated with the transition from common state to state i and j into an array. The initialization array has u elements and is expressed as

$$\begin{aligned} M_1\left(\sum ij\right) = \left(A\left(\sum 00 \rightarrow \sum ij\right), A\left(\sum 11 \rightarrow \sum ij\right),\right. \\ \left. \cdots, A\left(\sum (u-1)(u-1) \rightarrow \sum ij\right)\right) \end{aligned} \tag{3.20}$$

where $i, j \in 0, \cdots, u-1$, and $i \neq j$, the subscript of M is the step index l which is set to 1 at this step.

If the transition from a common state to state i and j does not exist, the corresponding matrix element is empty or replaced by zero.

2. Main step

The codeword array is updated at this step. The step index is set to $l = l + 1$ first. Let v be the number of information bits that apply to the encoder at each time slot. Let $M = 2^v$. Thus there are M^2 precursor super-state for each super-state. The update is performed by

$$\begin{aligned} M_{l+1}\left(\sum ij\right) &\leftarrow M_l\left(\sum p_i(0)p_j(0)\right) + A\left(\sum p_i(0)p_j(0) \rightarrow \sum ij\right) \\ &\vdots \\ M_{l+1}\left(\sum ij\right) &\leftarrow M_l\left(\sum p_i(0)p_j(M-1)\right) + A\left(\sum p_i(0)p_j(M-1) \rightarrow \sum ij\right) \\ &\vdots \\ M_{l+1}\left(\sum ij\right) &\leftarrow M_l\left(\sum p_i(M-1)p_j(M-1)\right) + A\left(\sum p_i(M-1)p_j(M-1) \rightarrow \sum ij\right) \end{aligned} \tag{3.21}$$

where the + operator adds the codeword distance matrix to each entry in the matrix array, the symbol $\longleftarrow$ represents the operation that adds the distance obtained in the right-hand side of (3.21) into the matrix $M_l\left(\sum ij\right)$, $p_i(0) \cdots p_i(M-1)$ and $p_j(0) \cdots p_j(M-1)$ are the M precursor states of σ_i and σ_j, respectively.

The update process is illustrated in Fig. 3.3

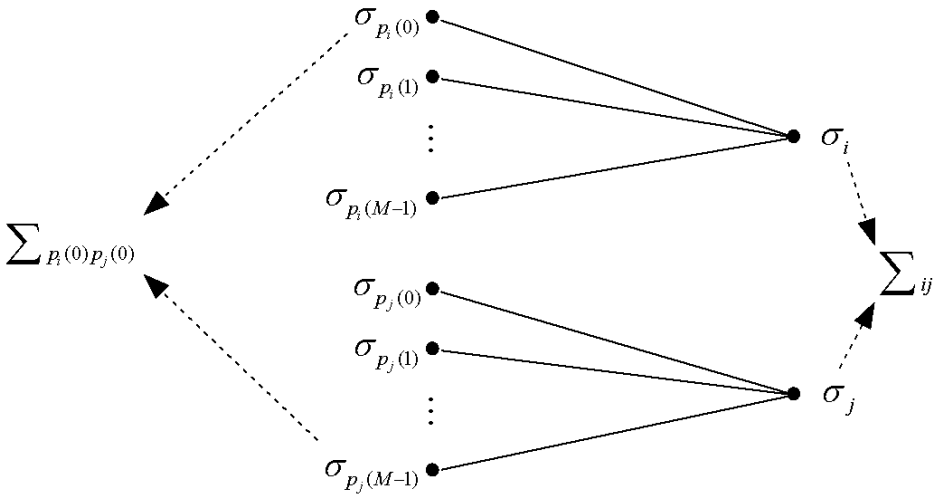

Figure 3.3. Main step.

3. Comparison

   For the trace search, eliminating the entries of $M_l\,(\sum ij)$, whose trace is larger than the preset threshold T_{max}. Then combining all the entries of $M_l\,(\sum ij)$ with same trace T. The resulting coefficients would be the multiplicity of the trace, denoted by $n_{ij}(T,l)$.

4. Check for merging path

   The existence of nonempty entry in $M_l\,(\sum ii)$ implies an error event merged at state i. Let $n(T,l)$ represent the number of error events with trace T and length l. Then

$$n(T,l) = \sum_{i=0}^{u-1} n_{ii}(T,l) \tag{3.22}$$

   For determinant search, combining all the entries in $M_l\,(\sum ii)$ with same determinant d and obtaining the multiplicity of the determinant, denoted by $n_{ij}(d,l)$. let $n(d,l)$ represent the number of error events with determinant d and length l. So

$$n(d,l) = \sum_{i=0}^{u-1} n_{ii}(d,l) \tag{3.23}$$

5. End of algorithm

   The algorithm stops if all arrays are empty for trace search, or the step index is larger than l_{max} for determinant search.

6. Distance spectrum calculation

   The distance spectrum $N(d)$ is the average number of error events having the same determinant and can be expressed as [28]

$$N(d) = \frac{1}{u} \sum_{l=2}^{l_{\max}} \frac{2 \cdot n(d,l)}{(2^v)^l} \tag{3.24}$$

   Thus (3.14) then becomes

$$\eta(l_{\max}) = \frac{1}{u} \sum_{d} \sum_{l=2}^{l_{\max}} \frac{2 \cdot n(d,l)}{(2^v)^l} d^{-n_r} \tag{3.25}$$

   Similarly, the distance spectrum $N(T_0)$ can be expressed as

$$N(T_0) = \frac{1}{u} \sum_{l} \frac{2 \cdot n(T_0,l)}{(2^v)^l} \tag{3.26}$$

The primary advantage of GA is the efficiency in time. However, GA is memory limited. As an improvement to the memory problem, a modification to GA described by Aktas [26] was also applied to the search. The modification results in a super-state reduction of a factor of 3.55.

Although the computational complexity of the truncated distance spectrum is not prohibitive, it is still extremely time consuming for the determinant spectrum $N(d)$ search. To facilitate the computation, we imposed several constraints on the search: (a) the frequencies of occurrence of signal that corresponds to the state transition are equal. (b) signal associated with state transition branches that diverge from or merge at the same state should differ by at least one symbol. The codes that violate the constraints will be excluded from the search.

In contrast to distance spectrum $N(d)$, the free distance spectrum $N(T_0)$, may be easily determined. In searching of $N(T_0)$, at each step, the error events whose trace is large than T_0 will be dropped because the trace is monotonic increase and the search is terminated when all error events are dropped.

3.3.4 Some new codes based on new criteria and distance spectrum

Based upon proposed criteria and the truncated distance spectrum, new codes have been designed through systematic searches and were presented in Tables 3.1, 3.2, and 3.3 together with some existing codes. Although the use of the truncated distance spectrum for the implementation of searches substantially achieves computational improvements, unfortunately, within this implementation the coding gain $\eta(l_{\max})$ may not agree with performance. In other words, the coding gain $\eta(l_{\max})$ only provides an estimate of performance. This is because the error event length is taken to be significantly less than frame length, and as a result, the information about the long error events are not available. In Tables 3.1 and 3.2, the new codes that are chosen depended not only on coding gain $\eta(l_{\max})$ but also on the further simulation results. In Table 3.3, the codes with the maximum value of minimum trace and minimum weight $N(T_0)$ are directly chosen from the search.

The distance spectrums of the first 3 minimum determinants are also listed in Tables 3.1 and 3.2, where d_i denote the i-th determinant and N_i denote the average number of error events with d_i. By definition of coding gain given in (3.14), it is shown that the contribution of the minimum determinant to the coding gain is insignificant. Despite possible inaccuracies in coding gain which are caused by the limited length of error events, these results justify that there is no dominant error events in space-time codes over quasi-static flat fading channel for the small diversity gain.

Table 3.1. 4 states, QPSK space-time trellis codes in slow fading channels, 1Rx

Codes	Generator matrices	r	Det	$\eta(7)$	d_1,N_1	d_2,N_2	d_3,N_3
TSC [5]	G_1=[(0 2) (2 0)] G_2=[(0 1) (1 0)]	2	4	8.099	$4, 2$	$12, 4$	$16, 1$
BBH [20]	G_1=[(2 2) (1 0)] G_2=[(0 2) (3 1)]	2	8	8.817	$8, 3$	12, 1.63	16, 0.78
CVYL [21]	G_1=[(0 2) (1 0)] G_2=[(2 2) (0 1)]	2	8	8.628	$8, 3$	12, 2.13	$20, 3$
New code	G_1=[(0 1) (2 0)] G_2=[(0 2) (1 0)]	2	4	7.818	$4, 1$	$8, 2$	$12, 1$

Table 3.2. 8 states, QPSK space-time trellis codes in slow fading channels, 1Rx

Codes	Generator matrices	r	Det	$\eta(6)$	d_1,N_1	d_2,N_2	d_3,N_3
TSC [1]	G_1=[(0 2) (2 0)] G_2=[(0 1) (1 0) (2 2)]	2	12	3.726	$12, 2$	$16, 1$	$20, 4$
BBH [5]	G_1=[(2 2) (2 0)] G_2=[(0 1) (1 0) (2 2)]	2	12	3.405	$12, 3$	$16, 1$	$20, 1.5$
CVYL [6]	G_1=[(0 2) (2 0)] G_2=[(2 1) (1 2) (0 2)]	2	16	3.224	$16, 1$	$20, 5$	28, 3.13
New code	G_1=[(0 2) (2 1)] G_2=[(2 0) (1 3) (0 2)]	2	16	3.156	$16, 1$	20, 3.5	28, 0.66

Table 3.3. 8 states, QPSK space-time trellis codes in slow fading channels, 2Rx

Codes	Generator matrices	Rank	Trace	$N(T_0)$
CVYL [6]	G_1=[(2 2) (2 1)] G_2=[(2 0) (1 2) (0 2)]	2	12	2
New code	G_1=[(0 2) (2 2)] G_2=[(2 1) (1 1) (0 2)]	2	12	1

3.3.5 Simulation

To verify the effectiveness of the proposed criteria, the performances of new codes list in Tables 3.1, 3.2, and 3.3 were evaluated by simulation. In the simulation, the encoder generates 130 symbols in each frame and transmits them over quasi-static flat fading channels. At the decoder, the ML algorithm was considered for the estimation of the transmitted codewords. The channel coefficients are assumed to be perfectly known at the decoder. The performances of the new codes are compared with those of the existing codes.

The performances of new codes are depicted in Figs. 3.4-3.6. Fig. 3.4 and 3.5 present the performance of 4 state and 8 state codes for the small diversity gain, respectively. Fig. 3.6 presents the performance of 8 state codes for the large diversity gain. All simulations show that the new codes perform better than existing codes. These results are in good agreement with the results of coding gain η and $N(T_0)$ shown in Tables 1, 2 and 3. The improvement in FER is about 0.3 dB, 0.2dB, and 0.4 dB at the FER of 10^{-3} for 4 states QPSK STTrC with two transmit antennas and one receive antenna, 8 states QPSK STTrC with two transmit antennas and one receive antenna, and 8 states QPSK STTrC with two transmit antennas and two receive antennas, respectively.

In Fig. 3.4, it is important to notice that the TSC code and the new code with determinant 4 have better performance than the BBH and CVYL code with determinant 8. The BBH and CVYL codes seem to be best suited to determinant criterion, indicating that the determinant criterion is not valid for FER performance under the condition of the small diversity gain. This simulation result demonstrates the limitation in the design criterion derived from PEP, for example the determinant criterion.

It can be noticed in Table 3.1-3.2 and Fig. 1-2 that a discrepancy occurs between performance and coding gain metrics. For example, in Table 3.2, the value of $\eta(6)$ of TSC is larger than that of BBH, but Fig. 2 shows that the performance of TSC is better than

that of BBH. The reasons for this inconsistency are that the error event length is taken to be significantly less than the frame length, and as a result, the information about the long error events are not available, as we described above.

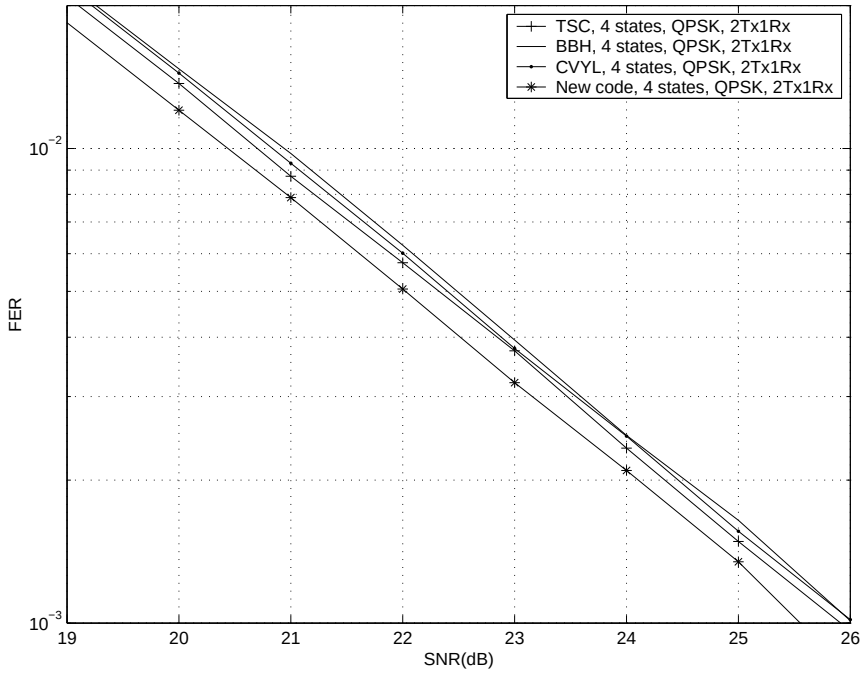

Figure 3.4. Performance of 4 states, QPSK, space-time trellis codes.

3.4 Code design criteria for space-time trellis codes in fast fading channel

3.4.1 Introduction

Designing space-time codes requires careful consideration of diversity gain and coding gain. Design criteria for space-time trellis codes in fast fading channel, namely, symbol Hamming distance criterion and product distance criterion, had been proposed in [5]. Based on these criteria, space-time trellis codes had been designed to provide maximum diversity gain with coding gain as large as desired [29].

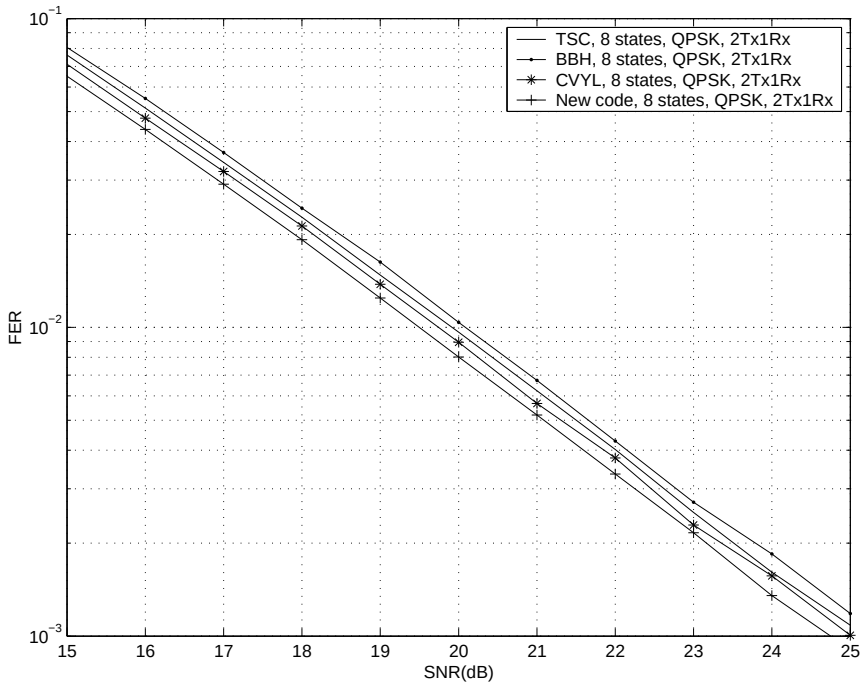

Figure 3.5. Performance of 8 states, QPSK, space-time trellis codes.

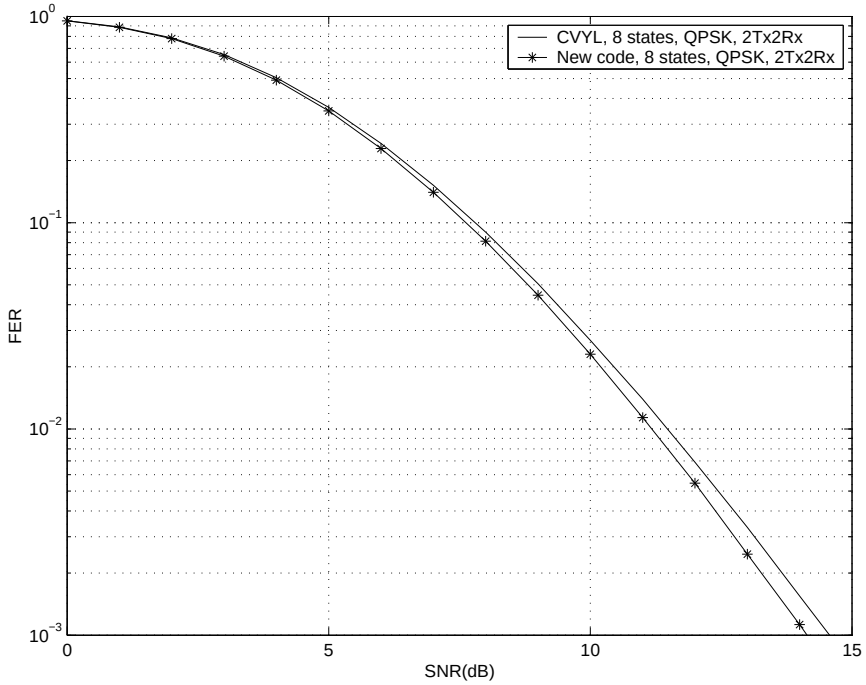

Figure 3.6. Performance of 8 states, QPSK, space-time trellis codes.

However, we also see certain problems in the criteria. In [5], Tarokh's criteria are derived to optimize the upper bound of PEP and the multiplicity of product distance are ignored. However, trellis codes with large numbers of states may result in a large multiplicity that cannot be ignored in assessing the overall coding gain [30]. Moreover, Tarokh's criteria have been developed in high SNR regions, and their analytical expressions cannot be used in low SNR regions.

Therefore, some improvements have been made to overcome these problems. Sasazaki and Ohtsuki [31] had developed an improved criteria aimed at optimizing the FER for fast fading channel. In the design, first, PEP was approximated as a function of product distance or trace, depending on the region of SNR; second, coding gain performance was further improved by using union bound analysis [23][26]. In this section, improved design criteria for space-time trellis codes in fast fading channel are introduced and utilized. The criteria are based on union bound analysis and derived from the optimal FER performance. The union bound analysis had considered the region of SNR. In the high SNR region the performance is governed primarily by symbol Hamming distance and the product criterion achieves an optimal coding gain, while in the low SNR region optimal coding gain is achieved by the trace criterion. Finally, simulation results show that the proposed criteria are effective by comparing the performances of different codes. Our design is close to that in [31], but the expression of coding gain is more accurate for high SNR and the performance behavior for moderate SNR region were discussed.

3.4.2 Design criteria

Let L denote the frame length. At each time slot t, n_t M-PSK symbols are transmitted, and are presented in form of column vector $\boldsymbol{c}_t = [c^1(t), \cdots, c^{n_t}(t)]^T$, where $1 \leq t \leq L$. A transmitted codeword is the n_t by L matrix and its i-th column corresponds to the

transmitted symbol vector at time i. The codeword matrix can be written in terms of column vector $\boldsymbol{c}_t$

$$\boldsymbol{c} = \begin{bmatrix} \boldsymbol{c}_1 & \cdots & \boldsymbol{c}_t & \cdots & \boldsymbol{c}_L \end{bmatrix} \tag{3.27}$$

In [5], the system performance is characterized by the PEP. The PEP is the probability that the decoder erroneously selects codeword $\boldsymbol{e}$ as the transmitted codeword while the codeword $\boldsymbol{c}$ is in fact transmitted, where

$$\boldsymbol{e} = \begin{bmatrix} \boldsymbol{e}_1 & \cdots & \boldsymbol{e}_t & \cdots & \boldsymbol{e}_L \end{bmatrix} \tag{3.28}$$

For the fast fading channel, the PEP is given by [5]

$$P(\boldsymbol{c} \to \boldsymbol{e}) \leq \prod_{t=1}^{L} \left(1 + d_E^t \frac{E_s}{4N_0}\right)^{-n_r} \tag{3.29}$$

where d_E^t is the squared Euclidean distance between c_t and e_t, and is given by

$$d_E^t = |\boldsymbol{c}_t - \boldsymbol{e}_t|^2 = \sum_{i=1}^{n_t} \left|c^i(t) - e^i(t)\right|^2 \tag{3.30}$$

In [5], by assuming that SNR is sufficient large, Tarokh described the PEP by the simplified expression

$$P(\boldsymbol{c} \to \boldsymbol{e}) \leq \left(\prod_{t \in \nu(c,e)} d_E^t\right)^{-n_r} \left(\frac{E_s}{4N_0}\right)^{-n_r \delta_H} \tag{3.31}$$

where $\nu(\boldsymbol{c}, \boldsymbol{e})$ is the set of time instance $1 \leq t \leq L$ at which the squared Euclidean distance d_E^t is not equal to zero. δ_H is the symbol Hamming distance which is defined as the number of elements in $\nu(\boldsymbol{c}, \boldsymbol{e})$.

In (3.31), δ_H decides the slope of PEP in logarithm domain. Analogous to the slow fading channel, the slope term $n_r \delta_H$ is often called the diversity gain. The product term

is defined as the product distance and contributes to the coding gain. Optimizing the worst PEP led to the symbol Hamming distance and product distance criteria [5].

It is well known that the symbol Hamming distance criterion is effective in realizing the best diversity gain, but the product distance criterion provides just rough guidelines on coding gain because the product distance criterion ignores the multiplicity of product distance. Moreover the criteria also does not account for the fact that the PEP may be approximated by different expression in different SNR region.

A commonly used method to analyze the performance of trellis codes is that of union bound analysis, which has the advantage of being able to exploit the benefits of distance spectrum. With this method, it is expected that the coding gain performance can be enhanced. The union bound on FER was obtained by summing the PEP weighted by distance spectrum. In the high SNR region, where SNR >>1, the PEP may be well approximated by (3.31). Thus the union bound on FER can be written as

$$\begin{aligned} P &\leq \sum_{\delta_H=\delta_{H\min}}^{L} \sum_{d_p \in D(\delta_H)} W_{\delta}^{d_p} d_p^{-n_r} \left(\frac{E_s}{4N_0}\right)^{-n_r\delta_H} \\ &= \sum_{\delta_H=\delta_{H\min}}^{L} I_{\delta_H}^{n_r} \left(\frac{E_s}{4N_0}\right)^{-n_r\delta_H} \end{aligned} \tag{3.32}$$

and

$$I_{\delta_H}^{n_r} = \sum_{d_p \in D(\delta_H)} W_{\delta_H}^{d_p} d_p^{-n_r} \tag{3.33}$$

where d_p is the product distance, $D(\delta_H)$ denote the set of product distance caused by error events with symbol Hamming distance δ_H. Each product distance d_p in $D(\delta_H)$ has a weight associated with it. The weight is defined as the average number of error events with symbol Hamming distance δ_H and product distance d_p, and is denoted by $W_{\delta_H}^{d_p}$. $I_{\delta_H}^{n_r}$ can be interpreted as the coding advantage contributed by the error events with symbol Hamming distance δ_H.

It is seen that $I_{\delta_H}^{n_r}$ is $n_r\delta_H$-order coefficient of inverse SNR. At high SNR, the dominant term in (3.32) is the lowest term. Hence, equation (3.32) reduces to the approximation

$$P \leq I_{\delta_{H_{\min}}}^{n_r} \left(\frac{E_s}{4N_0}\right)^{-n_r\delta_{H_{\min}}} \tag{3.34}$$

The design objective of this study is to minimize FER. Thus the design criteria for high SNR are as follow:

- Symbol Hamming distance criterion [5]: in order to achieve the maximum diversity in a fast fading environment, the symbol Hamming distance for any two codewords $\boldsymbol{c}$ and $\boldsymbol{e}$ must be maximized.
- Product distance criterion: in order to achieve optimal coding advantage, $I_{\delta_{H_{\min}}}^{n_r}$ must be minimized.

For small SNR region, where SNR<<1, PEP has a trace dependence given by the following equation [31]

$$P(\boldsymbol{c} \rightarrow \boldsymbol{e}) \leq \left(\sum_{t=1}^{L} d_E^t \frac{E_s}{4N_0}\right)^{-n_r} \tag{3.35}$$

In (3.35), the sum term, $\sum_{t=1}^{L} d_E^t$, is the squared Euclidean distance between code pair ($\boldsymbol{c}$, $\boldsymbol{e}$). Since this distance is equal to the trace of codeword distance matrix, the criterion based on squared Euclidean distance is also called as trace criterion. Using a similar analysis, FER can be written as

$$P \leq \sum_{d_e \in D} W_{d_e} d_e^{-n_r} \left(\frac{E_s}{4N_0}\right)^{-n_r} = I_E^{n_r} \left(\frac{E_s}{4N_0}\right)^{-n_r} \tag{3.36}$$

and

$$I_E^{n_r} = \sum_{d_e \in D} W_{d_e} d_e^{-n_r} \tag{3.37}$$

where d_e is the squared Euclidean distance or trace, D is the set of trace, W_{d_e} is the average member of error events with d_e, $I_E^{n_r}$ is recognized as the coding gain.

The coding gain is measured in terms of trace, which is equal to the weighted sum of $d_e^{-n_r}$. It should be noted that the sum, $I_E^{n_r}$, runs over all trace. This implies that all error events contribute equally to the FER. Thus when applying the design criteria for small SNR, it is important to have detailed information about the complete distance spectrum. Minimizing FER with respect to trace, led to the following criterion:

- Trace criterion: In order to achieve optimal coding performance, I_E^m should be minimized.

For the moderate SNR region, the approximation expression (3.35) and (3.31) are no longer valid and it is difficult to obtain a good approximation of PEP that has an explicit trace or product distance dependence. Equation (3.32) provides useful information about the properties of PEP in this region. From (3.32), we can conclude that the dominant contribution from the lowest-order coefficients to FER for high SNR become less significant for moderate SNR, whereas the contributions from high-order coefficients are comparable to that from the lowest-order coefficients.

3.4.3 Some new codes based on new criteria and distance spectrum

Based on proposed criteria, some new codes are obtained through computer search of distance spectrum over all candidate codes and listed in Table 3.4 together with FVY codes, where FVY codes are based on Tarokh's criteria. The method applied to the distance spectrum search is simple, but its computer implementation is time consuming and requires a large memory capacity. The computation time and required memory increase exponentially with the number of states and the length of frame. With these limitations,

the exhaustive search over all error events is infeasible. For the sake of computational tractability, the practical method is to calculate the truncated distance spectrum. To do that, in this dissertation, error events have restricted to those with the first two minimum symbol Hamming distance for the trace search. As mentioned above, design criterion for low SNR requires complete distance spectrum. Thus, the calculation of coding gain involving truncated distance spectrum of trace becomes less accurate. As a result, finding the codes that satisfy trace criterion is an iterative computational/simulation procedure that obtains near optimal codes. For high SNR, coding advantages are determined over error events with the minimum symbol Hamming distance. Thus the optimal results for $I_{\delta_H}^{n_r}$ were obtained from the best product distance spectrum.

All new codes in Table 3.4 possess the same diversity gain as the FVY codes. Thus, differences in performance between the new and FVY codes will be defined by the differences in coding gain. The new 32 states code 'a' achieves optimal coding gain for high SNR, whereas new 32 states code 'b' achieves optimal coding gain for low SNR. The rest of the new codes are optimal for both high and low SNR.

3.4.4 Simulation

In this section, we evaluated the performance of new codes over fast fading channel by simulation. In simulation, we considered a wireless system with two transmit antennas, QPSK symbol constellation, and 130 symbols per frame. The performance of the new codes was then compared with that of FVY.

Fig. 3.7 shows the performance of 8 states STTrC. The performance improvement compared with FVY is slight for one and two receive antennas. This is explained by the fact that both codes have the same coding advantage for large values of SNR. The difference in FER performance between new and FVY codes become apparent as the

Table 3.4. QPSK STTrC with two transmit antennas

code	state	generator	δ_H, d_p	$I^1_{\delta_{H\,min}}$	$I^{n_r}_E$
FVY [29]	8	G1=[(2,2)(1,2)] G2=[(0,2)(1,3)(2,0)]	2, 48	2.08e-2	I^8_E=1.05e-8
New	8	G1=[(1,2)(2,2)] G2=[(2,0)(2,1)(0,2)]	2, 48	2.08e-2	I^8_E=6.92e-9
FVY [29]	16	G1=[(0,2)(0,1)(2,2)] G2=[(2,0)(1,2)(0,2)]	3, 64	3.39e-2	I^4_E=2.04e-4
New	16	G1=[(0,2)(2,2)(0,2)] G2=[(2,1)(1,1)(2,3)]	3, 128	2.17e-2	I^4_E=1.63e-4
FVY [29]	32	G1=[(1,3)(1,2)(2,1)] G2=[(0,1)(2,0)(3,0)(1,2)]	3, 96	9.40e-3	I^4_E=1.67e-4
New (a)	32	G1=[(1,2)(2,1)(2,2)] G2=[(2,0)(2,2)(0,2)(0,2)]	3, 288	3.47e-3	I^4_E=1.60e-4
New (b)	32	G1=[(0,2)(2,1)(2,2)] G2=[(2,2)(1,2)(1,0)(0,2)]	3, 192	5.21e-3	I^4_E=6.74e-5

number of receive antennas increase. The improvement at FER of 10^{-3} is about 0.2 dB for eight receive antenna.

Fig. 3.8 shows the performance of 16 states STTrC. It was shown that new codes have superior performance. These results agree with the numerical data in Table 3.4. The improvement at FER of 10^{-3} is about 0.6 dB, 0.5 dB, and 0.4 dB for one receive antenna, two receive antennas, and four receive antennas, respectively.

Fig. 3.9 shows the performance of 32 states STTrC. It is interesting to note that these codes present very different properties. From the results presented in Table 3.4, the new code 'a' shows that good performance is to be expected for one receive antenna. However, Fig. 3.9 indicates that the new code 'b' yields the better performance. This may be due to the fact that since the new codes are designed for high and low SNR applications, they suffer performance uncertainty in moderate SNR. This uncertainty

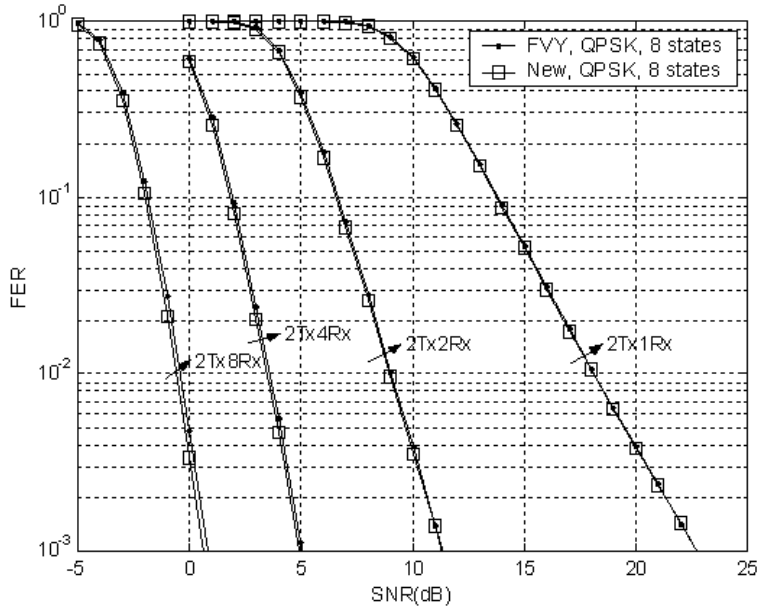

Figure 3.7. Performance of 8 states, QPSK, space-time trellis codes.

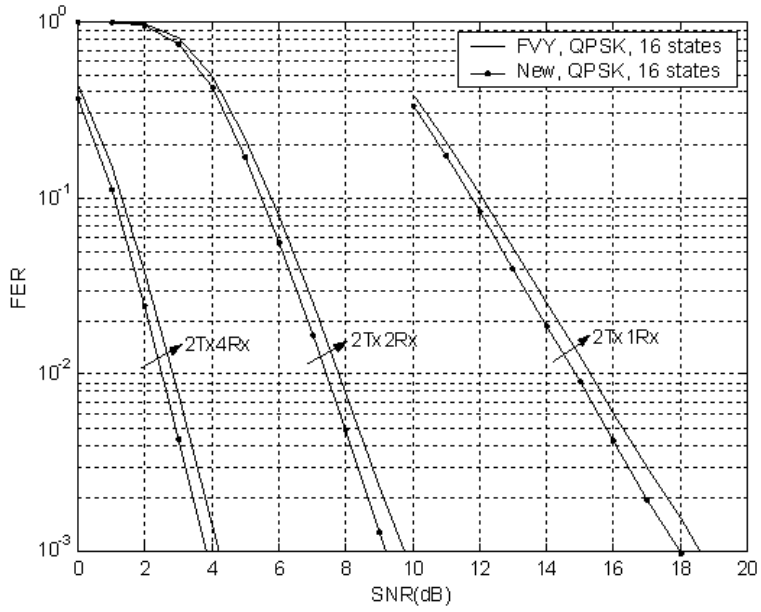

Figure 3.8. Performance of 16 states, QPSK, space-time trellis codes.

is due primarily to the omitted contribution from high-order coefficient for high SNR, which can be significant for moderate SNR. A further calculations show that I_4^1=1.95e-2, 5.12e-2, and 5.20e-2 for new code 'b', new code 'a', and FVY, respectively. These results explain the phenomenon of Fig. 3.9 to some extent. The improvement of new code 'b' against FVY in FER performance is about 0.9 dB and 0.7 dB for one receive antenna and two receive antennas, respectively.

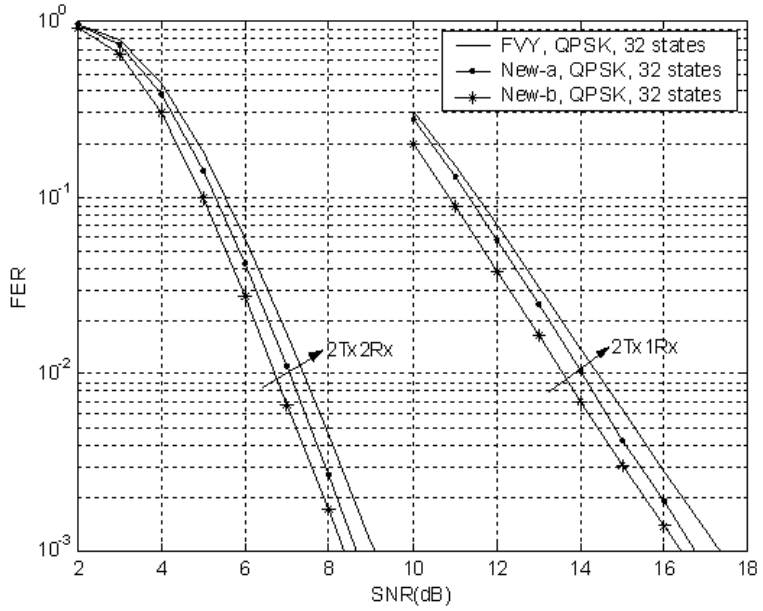

Figure 3.9. Performance of 32 states, QPSK, space-time trellis codes.

3.5 Conclusions

In this chapter, the improved design criteria based on union bound analysis for space-time trellis codes in both slow and fast fading channel have been presented. The design are performed by employing union bound analysis and by considering performance dependence on diversity gain and region of SNR. The proposed criteria were successfully

applied to space-time trellis codes. The new codes had been designed based on the new coding gain metrics and distance spectrum. The simulation results show that the new codes result in improvement in performance of FER. The improvements are about 0.2-0.9 dB at FER of 10^{-3} ,which are big number in terms of method applied.

CHAPTER 4

ORTHOGONAL SPACE-TIME TRELLIS CODES

4.1 Introduction

Space-time codes provide an effective means and method of enormously increasing system capacity for wireless communications. Tarokh, et al., first described the performance characteristics of space-time codes in terms of diversity gain and coding gain [5]. As the diversity gain determines the asymptotic slope of PEP in logarithm domain, it is the most important factor in the design of space-time codes. The design of first space-time trellis codes has focused therefore more on implementing full diversity order, but non-optimal coding gain [5]. The various improved codes have been developed to enhance the coding gain performance in subsequent works. The improvement may be implemented by finding more powerful codes that yield the minimum PEP in terms of Tarokh's criteria through exhaustive computer search [20], developing improved design criteria based on more accurate mathematical expression of PEP [15][16], and performing union bound and distance spectrum analysis [23][26]. However, as the development of space-time codes with the state of art techniques, these methods may now only provide marginal improvement.

The improvement can be increased further by introducing the orthogonal design of space-time block codes into space-time trellis codes. In slow fading channel, the coding gain depends on the minimum determinant of full rank codeword distance matrix [5]. The codeword distance matrix is a Hermitian matrix. Thus, the optimal determinant will be obtained if the codeword distance matrix is also a diagonal matrix with equal eigenvalues. Based on this principle, concatenated space-time block coding with trellis

coded modulation had been proposed [32][33]. The scheme, shown in Fig. 4.1, concatenates an outer trellis coded modulation with an inner space-time block code. Essentially, this code is still a space-time block code with extra coding gain provided by outer code.

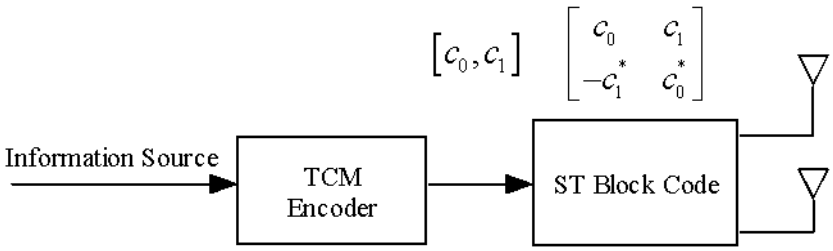

Figure 4.1. Concatenated space-time block coding with trellis coded modulation.

Super Orthogonal Space-Time Trellis Codes (SOSTTrC) have been developed in [14]. Super orthogonal space-time trellis codes are essentially the space-time trellis codes with super-trellis structure, which is illustrated in Fig. 4.2. The approach orthogonalizes the output on super-trellis transition by using Alamouti orthogonal matrix [9]. The codeword distance matrix of Alamouti code is a Hermitian diagonal matrix in which the diagonal elements are non-zero equal positive real elements. Due to its additive property, the resulting codeword distance matrix of SOSTTrC will also be a Hermitian diagonal matrix with equal eigenvalues. This full rank diagonal matrix with equal eigenvalues will result in marked improvement in the determinant of codeword distance matrix, and therefore the coding gain in slow fading channel. The essential difference between SOSTTrC and concatenated space-time block coding with trellis coded modulation is that SOSTTrC enhance the coding gain of space-time trellis codes by orthogonalizing the output of space-time trellis codes. Therefore, SOSTTrC is more attractive. Similar ideas have been proposed in [34][35]. These approaches in [14][34][35] can be applied only to two

transmit antennas. In a later paper [36], super-quasi-orthogonal space-time trellis codes for four transmit antennas were developed.

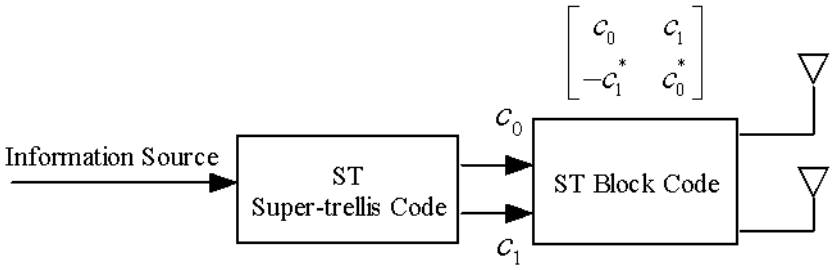

Figure 4.2. Super orthogonal space-time trellis codes.

SOSTTrC have been known to be an very effective technique for improving coding gain performance in slow fading channels. However, this code is not ideally suited for fast fading channels, because it may give rise to the diversity loss in fast fading channels [34]. In SOSTTrC, the super-trellis transition is induced by two information symbols. This super-trellis operation ensures the full rate codes, but inevitably results in parallel trellis transition. On fast fading channel, diversity gain depends on Minimum Symbol Hamming Distance (MSHD). The symbol Hamming distance measures the number of symbol positions where they differ between two codewords. Thus, the codes that exhibit parallel trellis transitions have the MSHD at most one. Although the practical MSHD is 2 because of the use of Alamouti matrix as the encoded output, however, compared to its counterpart with the same number of states but the MSHD of larger than 2 in STTrC, SOSTTrC would incur diversity loss in fast fading channels. Especially for the systems that have a large number of transmit antenna and/or a high order constellation modulation, it is very difficult to prevent parallel trellis transition from happening. Some examples are shown in the Table 4.1 below.

Table 4.1. A comparison in MSHD between QPSK STTrC and QPSK SOSTTrC

State	Codes	MSHD	Order loss?
4	STTrC	2	
4	SOSTTrC	2	No
8	STTrC	2	
8	SOSTTrC	2	No
16	STTrC	3	
16	SOSTTrC	2	Yes
32	STTrC	3	
32	SOSTTrC	2	Yes
64	STTrC	4	
64	SOSTTrC	2	Yes

Since the diversity gain of space-time codes corresponds to the asymptotic slope of the PEP, any diversity loss can translate into significant performance degradation. Thus, diversity loss is an important issue to be taken into account in space-time codes. We have, therefore, developed the Orthogonal Space-Time Trellis Codes (OSTTrC) in this dissertation, which are aimed at improving diversity gain in fast fading channels. The approach is also based on the orthogonal design of space-time block codes. But different from SOSTTrC, the parallel transition is avoided in our design. Theoretical analysis and simulation results indicate that OSTTrC have an advantage over STTrC with regards to diversity gain. However, on the other hand, OSTTrC offers a disadvantage in that it is bandwidth inefficient.

4.2 Orthogonal space-time trellis codes

SOSTTrC is particularly attractive for the design of space-time codes because of its great performance in slow fading channels. However, except for the diversity gain loss in

fast fading channels, coding gain performance depends on the product distance and the orthogonal design provides no significant benefit in improving coding gain performance in fast fading channels. Therefore, there is a need for developing a better way to improve the performance in fast fading channels. Our performance analysis shows that, in fast fading channels the practical diversity gain is the product of symbol Hamming distance and the rank of the branch codeword distance matrix. This makes it possible to improve the performance of the diversity gain by increasing the rank of the branch codeword distance matrix, and meanwhile maintaining the symbol Hamming distance of STTrC. By making use of this principle, in this chapter, we intend to propose the orthogonal space-time trellis codes, which are aimed at improving diversity gain in fast fading channel. The orthogonal space-time trellis codes are particularly simple, constructing with STTrC and space-time block codes encoder as shown in Fig. 4.3, where the space-time trellis codes is the same as in [15] and the encoder of space-time block codes encode the output of STTrC into an orthogonal matrix of space-time block codes.

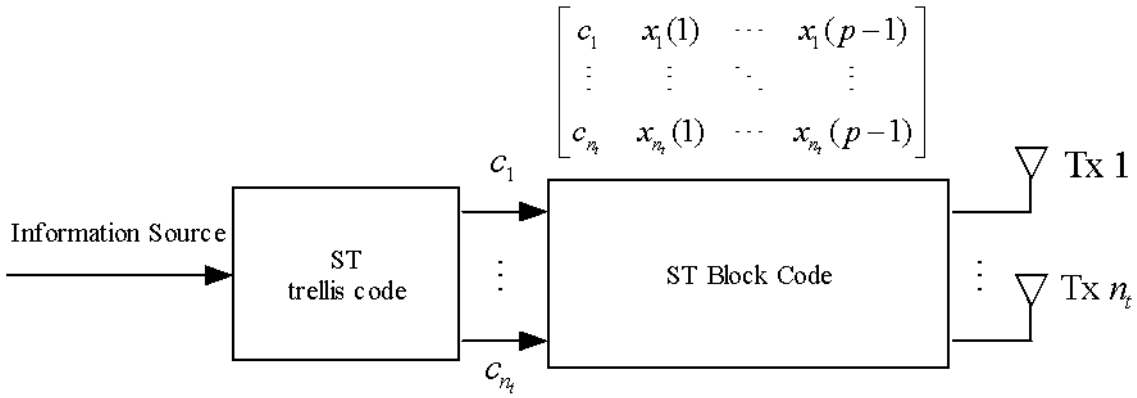

Figure 4.3. Orthogonal space-time trellis codes.

The orthogonal space-time trellis codes are generated in the following manner. At each time slot t, a parallel b bit information data are input to the STTrC encoder and

are encoded into n_t M-PSK symbols, where $b = \log_2 M$. We represent the output by a column vector of dimension n_t

$$\boldsymbol{s}_t = \begin{bmatrix} c_t^1 & c_t^2 & \cdots & c_t^{n_t} \end{bmatrix}^T \tag{4.1}$$

where T denotes transpose operation, and c_t^i is the transmitted symbol in i-th transmit antenna at time t.

This symbol vector is passed to the STBC encoder where these n_t elements are transformed into an orthogonal matrix. The resulting $n_t \times p$ orthogonal matrix takes the form:

$$\boldsymbol{c}_t = \begin{bmatrix} c_t^1 & x_t^1(1) & \cdots & x_t^1(p-1) \\ \vdots & \vdots & \ddots & \vdots \\ c_t^{n_t} & x_t^{n_t}(1) & \cdots & x_t^{n_t}(p-1) \end{bmatrix} \tag{4.2}$$

where $p = n_t$ for $n_t = 2, 4, 8$, and $p > n_t$ for $n_t = 3, 5, 6, 7, 9 \cdots$.

The column vectors in equation (4.2)

$$\boldsymbol{x}_t(i) = \begin{bmatrix} x_t^1(i) & x_t^2(i) & \cdots & x_t^{n_t}(i) \end{bmatrix}^T, \quad i \in 1, \cdots, p-1 \tag{4.3}$$

are M-PSK symbol vector. Its elements are the linear combination of c_t^i and $(c_t^i)^*$ where the superscript $*$ represents the conjugate operation, and are chosen so that the following equation is true

$$\boldsymbol{c}_t \boldsymbol{c}_t^H = \left(\left|c_t^1\right|^2 + \left|c_t^2\right|^2 + \cdots + \left|c_t^{n_t}\right|^2 \right) I_{n_t} \tag{4.4}$$

where I_{n_t} is the $n_t \times n_t$ identity matrix.

The equation above is the sufficient condition for the orthogonal design in STBC. The methods for generating such orthogonal matrix are described in [11]. From (4.4)

it is noted that the rows of $\boldsymbol{c}_t$ matrix are mutually orthogonal. For $n_t = 2, 4, 8,$ $\boldsymbol{c}_t$ is a orthogonal matrix. For $n_t = 3, 5, 6, 7, 9 \cdots,$ $\boldsymbol{c}_t$ is a matrix with orthogonal rows. In [11], the non-square matrices are called generalized orthogonal matrix. In this dissertation, $\boldsymbol{c}_t$ is in general terms referred to as the orthogonal matrix. The orthogonal matrix was originally designed to offer full diversity order, but no coding gain with low complexity in decoding hardware implementation for STBC. However, when applying the technique of orthogonal design to SOSTTrC, the state-of-the-art improvement in coding gain over STTrC can be yielded. This is due to the factor that the orthogonal matrix has two important advantages that bring the excellent performance in slow fading channels. First, it achieves guaranteed full diversity order. Secondly, the unique orthogonality property in it leads its codeword distance matrix to be a diagonal matrix with equal eigenvalues. The performance analysis of OSTTrC, which is discussed in more detail later in next section, shows that, for the purpose of improving diversity gain, the encoded output matrix is not necessary to be an orthogonal matrix. A matrix that yields codeword distance matrix that has at least a rank of two is sufficient to assure the diversity gain improvement. The primary reason that we consider the orthogonal matrix in this work is to fully exploit its two advantages to achieve optimal performance on both diversity gain and coding gain. A well-known example of such orthogonal matrix is the Alamouti matrix of form

$$\boldsymbol{c}_t = \begin{bmatrix} c_t^1 & -(c_t^2)^* \\ c_t^2 & (c_t^1)^* \end{bmatrix} \tag{4.5}$$

In OSTTrC, the orthogonalization is performed for each information symbol. Thus, the approach avoids parallel transition and maintains the symbol Hamming distance features of STTrC. However, there is a penalty to be paid by this approach: the data rate loss. In OSTTrC, a time slot consists of b information bits and is further divided into p sub-time slots. The orthogonal matrix is transmitted column by column within

time slot t, such that the i-th row is transmitted from i-th antenna, and each column is transmitted in corresponding sub-time slot. This indicates that number of transmit symbol in one information symbol duration is p at each transmit antenna, so that the code rate is $1/p$. Therefore, the scheme may be less suited for the bandwidth limited applications.

4.3 Performance analysis and design criteria

Performances of space-time codes have been analyzed by formulating upper bound on the PEP [5]. PEP refers to the probability that the decoded codeword at receiver is different from transmitted codeword. Let L be the length of frame, $\boldsymbol{c}$ be transmitted codeword and $\boldsymbol{e}$ be erroneously decoded codeword. Let c_t and e_t denote the encoded output matrix of size $n_t \times p$ at time t in codeword $\boldsymbol{c}$ and $\boldsymbol{e}$, respectively. We define codeword $\boldsymbol{c}$ and $\boldsymbol{e}$ such that $\boldsymbol{c}$ and $\boldsymbol{e}$ are matrix formed by concatenating c_t and e_t, respectively,

$$\boldsymbol{c} = [c_1 c_2 \cdots c_t \cdots c_L] \tag{4.6}$$

$$\boldsymbol{e} = [e_1 e_2 \cdots e_t \cdots e_L] \tag{4.7}$$

Let

$$\boldsymbol{B}_t = c_t - e_t \tag{4.8}$$

be a difference matrix between c_t and e_t. Since this matrix is associated with the branch output, we refer it as branch difference matrix. A branch codeword distance matrix between c_t and e_t is defined as the Hermitian square of the difference matrix of size $n_t \times n_t$

$$\boldsymbol{A}_t = \boldsymbol{B}_t \boldsymbol{B}_t^H \tag{4.9}$$

PEP of space-time codes has been developed significantly, originally considering only the branch output is a symbol vector. When the branch output is a matrix as in OSTTrC, the upper bound of PEP in fast Rayleigh fading channels is given by

$$P(\boldsymbol{c} \to \boldsymbol{e}) \leq \prod_{t=1}^{L} \prod_{i=1}^{r} \left(1 + \lambda_t^i \frac{E_s}{4N_0}\right)^{-n_r} \tag{4.10}$$

where λ_t^i is the i-th eigenvalue of $\boldsymbol{A}_t$ in descending order and r is the rank of $\boldsymbol{A}_t$

In the following derivation, SNR is assumed to be sufficient large. Hence, PEP expression in (4.10) can be approximated by

$$P(\boldsymbol{c} \to \boldsymbol{e}) \leq \prod_{t=1}^{L} \prod_{i=1}^{r} \left(\lambda_t^i\right)^{-n_r} \left(\frac{E_s}{4N_0}\right)^{-rn_r} \tag{4.11}$$

which is equivalent to

$$P(\boldsymbol{c} \to \boldsymbol{e}) \leq \left(\frac{E_s}{4N_0}\right)^{-\delta_H r n_r} \prod_{t \in v(\boldsymbol{c},\boldsymbol{e})} \left(\prod_{i=1}^{r} \lambda_t^i\right)^{-n_r} \tag{4.12}$$

where $v(\boldsymbol{c}, \boldsymbol{e})$ is the set of time instance $1 \leq t \leq L$ at which the $\boldsymbol{A}_t$ is not a null matrix, δ_H is the number of elements in $v(\boldsymbol{c}, \boldsymbol{e})$ which is recognized as the symbol Hamming distance between codeword pair $(\boldsymbol{c}, \boldsymbol{e})$.

This expression describes the diversity gain as a product of the symbol Hamming distance and the rank of $\boldsymbol{A}_t$, according to the definition of diversity gain. In STTrC, $\boldsymbol{B}_t$ is a column vector, thus r=1. In this case, only symbol Hamming distance contributes to the diversity gain. This leads to well-known symbol Hamming and product distance criteria for STTrC [5]. In OSTTrC, the symbol Hamming distance maintains the exact symbol Hamming distance of STTrC. Therefore, if r takes a value larger than one, the performance of diversity gain can be improved linearly with the rank r of $\boldsymbol{A}_t$.

By examining the inequality (4.12), one can see that the product term of eigenvalues determines the coding gain. Recognizing that the product term of eigenvalues is equal to the determinant of matrix $\boldsymbol{A}_t$ if matrix $\boldsymbol{A}_t$ has full rank, the design criteria to yield minimum PEP for OSTTrC are as follows:

- Symbol Hamming distance criterion: the minimum symbol Hamming distance of STTrC must be maximized.
- Rank criterion: branch codeword distance matrix $\boldsymbol{A}_t$, where $t \in v(\boldsymbol{c}, \boldsymbol{e})$, must have a full rank of n_t. Using this criterion together with above symbol Hamming distance criterion will offer optimal diversity gain.
- Determinant criterion: in order to provide optimal coding gain, the minimum determinant of $\boldsymbol{A}_t$ must be maximized.

The orthogonal matrix defined in (4.4) is very attractive in terms of above criteria. As mentioned, the orthogonal matrix provides guaranteed full rank for $\boldsymbol{A}_t$. It also offers unique feature for $\boldsymbol{A}_t$. It can easily be proven that $\boldsymbol{A}_t$ can be expressed as [11]

$$\boldsymbol{A}_t = \left(\left| c_t^1 - e_t^1 \right|^2 + \left| c_t^2 - e_t^2 \right|^2 + \cdots + |c_t^{n_t} - e_t^{n_t}|^2 \right) I_{n_t} \tag{4.13}$$

Equation (4.13) states that $\boldsymbol{A}_t$ is a full rank diagonal matrix, in which the diagonal elements are identical and equal to the Euclidean distance of encoded outputs of STTrC. Thus, ideally the orthogonal matrix should be chosen to make the codes robust on both diversity and coding gain. In this case, from (4.13), it can be seen that the eigenvalues will be

$$\lambda_t^i = \left| c_t^1 - e_t^1 \right|^2 + \left| c_t^2 - e_t^2 \right|^2 + \cdots + |c_t^{n_t} - e_t^{n_t}|^2 \tag{4.14}$$

for $i = 1, 2, \cdots, n_t$.

Applying the property given in (4.14) to (4.12) yields

$$P(\boldsymbol{c} \to \boldsymbol{e}) \leq d_p^{-n_t n_r} \left(\frac{E_s}{4N_0} \right)^{-\delta_H n_t n_r} \tag{4.15}$$

where

$$d_p = \prod_{t \in v(\boldsymbol{c},\boldsymbol{e})} \left(\left| c_t^1 - e_t^1 \right|^2 + \left| c_t^2 - e_t^2 \right|^2 + \cdots + \left| c_t^{n_t} - e_t^{n_t} \right|^2 \right) \tag{4.16}$$

is the product distance of STTrC.

The important properties of OSTTrC that can be observed from (4.15) are as follows. First, the diversity gain is n_t times that of STTrC. Secondly, the exponent term of the product distance gives $10 \log_{10} n_t$ dB advantage of coding gain over STTrC. In general, the orthogonal matrix is a square matrix of size n_t only for $n_t = 2$. Considering the effect of bandwidth inefficiency on decoding, the performance improvement in OSTTrC is due solely to the diversity gain, with loss of coding gain performance for $n_t > 2$ and without loss of coding gain performance for $n_t = 2$. As a consequence of these properties, symbol Hamming and product distance criteria developed for STTrC can be directly applied to OSTTrC.

4.4 Simulation

The performances of OSTTrC have been theoretically analyzed. In this section, the performances are evaluated through simulation. In simulation, we consider a MIMO system with two transmit antennas and one receive antenna. The orthogonal matrix is the Alamouti matrix given in (4.5). Thus, the code rate of OSTTrC is ½. A frame consists of 130 QPSK information symbols. To compare the results of this study with previous results, OSTTrC are formed from existing STTrC. In fast fading channels, OSTTrC is based on FVY code proposed in [29]. In slow fading channels, OSTTrC is based on CVYL code proposed in [21].

Fig. 4.4 shows the performance comparison between OSTTrC and STTrC in fast fading channels for different states, two transmit antennas, one receive antenna, and QPSK codes. The integer numbers refer, from right to left, to 4, 8, 16 state. As expected, in all cases the OSTTC show diversity gain increase of a factor of two. The FER is plotted against SNR. For a fair comparison, considering the code rate loss, the practical improvement in performance is 3 dB less than the observed improvement. The performance improvements at the FER of 10^{-3} are about 9.9 dB, 8.5 dB, 5.9 dB for 4, 8, 16 states code, respectively.

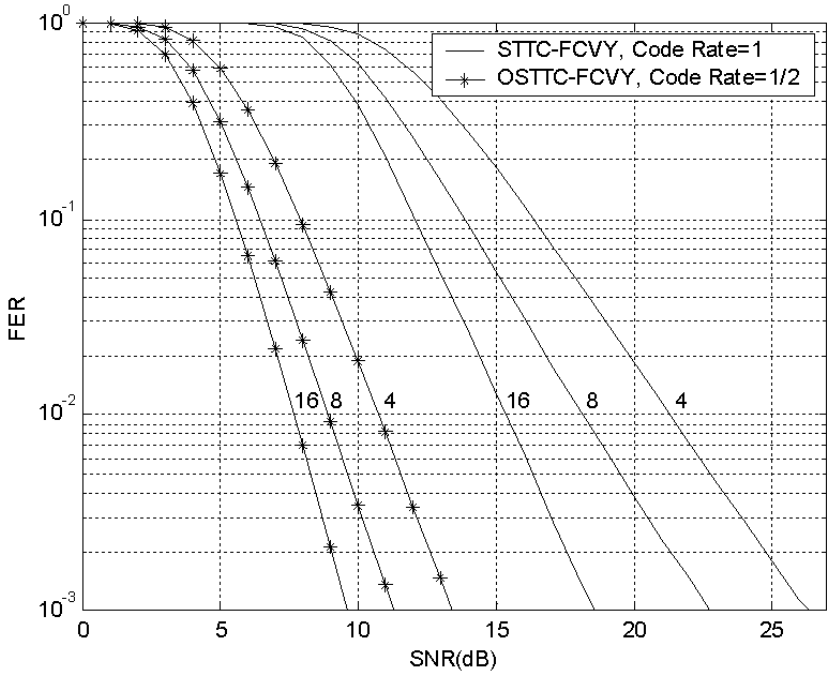

Figure 4.4. Performance of OSTTrC and STTrC in fast fading channels.

In Fig. 4.5, we show the performance comparison between 8 states OSTTrC and STTrC in slow fading channels for two transmit antennas, one receive antenna, and QPSK codes. We can see that OSTTrC also make significant improvement in slow fading

channel, which is the benefit of coding gain improvement. But there is no diversity gain improvement. This can be illustrated by the fact that the slope of the new code is parallel to the slope of the space-time trellis codes. Considering the code rate loss, the performance improvement at the FER of 10^{-3} is about 2.6 dB.

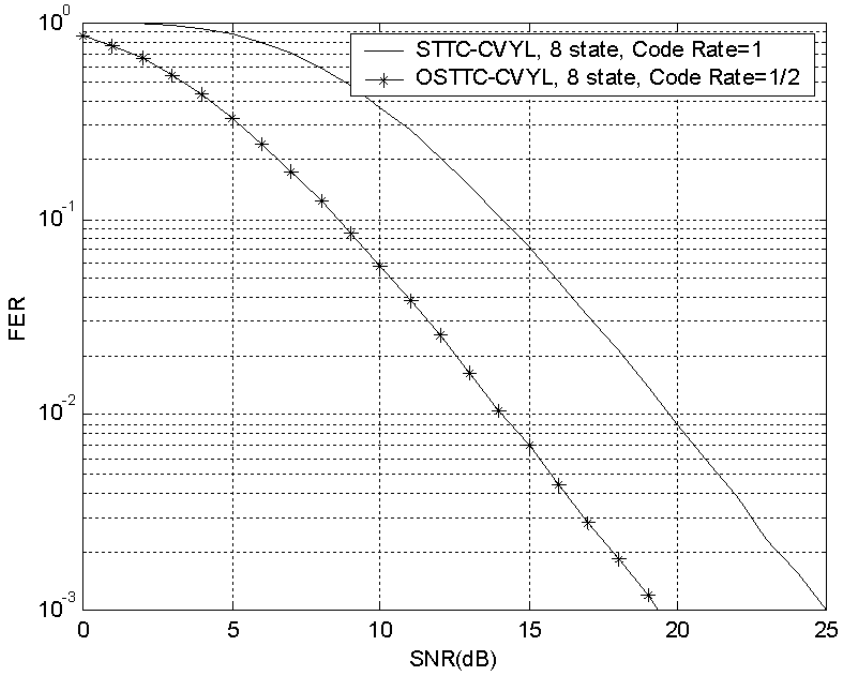

Figure 4.5. Performance of OSTTrC and STTrC in slow fading channels.

4.5 Conclusion

Performances of space-time codes are measured by the diversity gain and coding gain, and depend strongly on diversity gain. This chapter presents the orthogonal space-time trellis codes for fast fading channel, which improve diversity gain performance. This is accomplished by transforming the vector output of space-time trellis codes into an orthogonal matrix, while still maintaining the minimum symbol Hamming distance

of space-time trellis codes. The orthogonal design of STBC can contribute to both diversity gain and coding gain improvement, but only diversity gain improvement can be achieved compared to STTrC. With this code, diversity gain can increase by a factor that is equal to the number of transmit antennas in fast fading channels, which is a significant improvement over STTrC. Performances of proposed codes have been studied analytically and the design criteria have been suggested. Finally, an example is presented to demonstrate the codes. In this example, the orthogonal matrix is the Alamouti matrix. The simulation results show considerable performance improvement benefited from the improved diversity gain. A more than 5 dB improvement can be achieved in fast fading channel. The major drawback of the codes is the bandwidth inefficiency.

CHAPTER 5

FULL RATE SPACE-TIME TURBO CODES

5.1 Introduction

It has been shown that space-time trellis codes can achieve significant improvements in performance on fading channel with moderate complexity. However, the performance of trellis-based codes is limited by inevitable saturation of performance with increased number of trellis states. In addition, the complexity of decoder also becomes particularly complicated with increased number of trellis states. Turbo principle may offer potential for further significant improvements in performance. Turbo codes are well known for its ability to reach near Shannon limit performance, which has been successfully demonstrated by Berrou [13]. Since the introduction of turbo codes, the turbo principles have been widely applied to significantly improve performance in many applications, for example, turbo equalization and turbo multiuser detection. Space-Time Turbo Codes (STTuC) for MIMO systems have been recently studied by [37][38][39][40][41]. In [37] [38], space-time turbo codes are constructed based on turbo codes. In [37], the outputs of turbo codes are assigned to multiple antennas. In [38], the outputs of the component code are mapped to QPSK symbols first, and then delivered to two antennas. However, these codes are poorly suited to a large number of transmit antennas (for example, more than two antennas) and high order bandwidth efficient modulation (for example, 8-PSK). In [39][40][41], space-time turbo codes are constructed of parallel concatenated space-time trellis codes. The outputs of first and second component code are alternately punctured to provide bandwidth efficient codes. The advantage of this approach is that it is bandwidth efficient with any number of transmit antennas.

In [5], the performance of space-time codes over slow fading channel is evaluated by the upper bound of PEP, which is the function of two metrics: the rank and determinant of codeword distance matrix. Minimizing the worst PEP yields the rank and determinant design criteria that provide a basis for the code design of space-time codes. Since the PEP decays exponentially with the rank, the performance of space-time codes over slow fading channel is dominated by the error events with minimum rank of codeword distance matrix. Therefore, the rank criterion is crucial for space-time codes. In above approaches [39][40][41], the puncture operation was applied to ensure the bandwidth efficient codes. However, the punctured trellis codes may lead to a rank deficient problem [37][39][41]. The rank deficient problem is an important issue to be taken into account in space-time codes because of the reasons we mentioned above. This had been studied by [37][41]. In [37], the simulation results show that the performance degradation caused by puncturing can be remedied by the rotated construction of outputs of second component encoder. In [41], a systematic method to reduce the impact of rank-deficient on performance has been proposed. In this method, each component encoder is systematic and the outputs of second component encoder are rotated during multiplexing. This structure increases the number of candidates that satisfy the significant full rank criterion. This work has demonstrated the significant improvement on performance. Unfortunately, this approach suffers from the limitation of high design complexity due to the complicated design of the component encoder and is suitable only for simple codes with a small number of transmit antennas and low order constellation modulation.

In contrast to [41], a space-time turbo code proposed in [40] is a simple structure, suitable for the design of codes with a large number of transmit antennas. The codes are based on the space-time trellis code modulation proposed by [21]. It has the advantages of low design complexity, and can create very complicated codes, for example, 16 states, 8PSK and four antennas STTuC [42]. However, since there was no consideration given

to the rank deficient problem, the codes are dedicated to the system with high diversity gain and are not optimal for the system with small diversity gain.

In this chapter, we presented a new space-time turbo codes that exploit the advantages of [40] and [41]. In our design, the approach to reduce the impact of the rank-deficient problem on the performance shown in [41] has been followed and adapted. It means that the component code is a systematic code. The parity encoder is as same as in [40]. Thus the disadvantage associated with the design complexity has been overcome. Design criteria and performance of our new codes are also studied. In particular, we have studied the effect of rank deficient on the FER performance for small and large diversity gain. For the small diversity gain, our codes offer equivalent performance to the codes in [41]. For the large diversity gain, rank deficient has little effect on performance, and the codes in [40] provide comparable performance to our codes. A fairly simple design criterion for our new codes had been proposed. The criterion provides a especially low complexity, but very effective solution to complex codes. We provide examples in the end of the chapter to illustrate the performance of our codes.

The design in this study only deal with slow fading channel. For fast fading channel, rank deficient issue has no effect on the performance of STTuC. Very powerful STTuC for fast fading channel have been proposed in [40][42].

5.2 Space-time turbo codes

In the original paper of Berrou [13], a typical turbo code consists of two parallel concatenated recursive systematic convolutional encoders, an interleaver, and a puncture or multiplexer. STTuC is of similar construction as shown in Fig. 5.1. It consists of two parallel concatenated recursive space-time trellis code encoders connected by an odd-even symbol-wise interleaver. A puncture may be used to ensure bandwidth efficient codes.

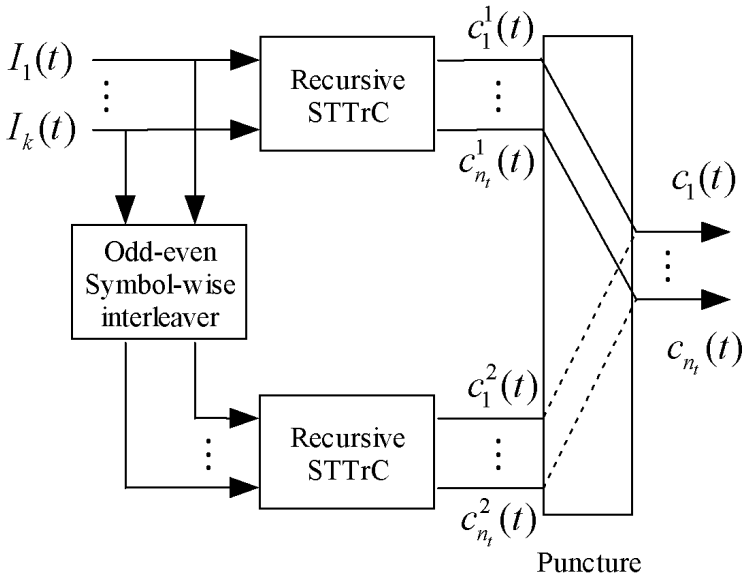

Figure 5.1. Space-time turbo codes.

In order to have the full rate, puncture operation is always performed in STTuC. In this operation, the encoded symbols at the upper encoder, which correspond to the information symbols at odd time slot, are selected to transmit. To avoid some information symbols are transmitted twice, and some information symbols are never transmitted, the lower encoder should only transmits the encoded symbols which correspond to the information symbols at even time slot [40]. For this purpose, in [40], a deinterleaver, which performs the inverse operation of interleaver, is placed at the output of the lower encoder. When the deinterleaver is applied to the encoder, it is necessary to introduce an interleaver identical to the encoder interleaver in the lower decoder. However, the use of interleaver without specific design would introduce a long sequence of zero in the received signal of the lower decoder. This may deteriorate performance. Furthermore, it has a negative effect on the performance for the delay sensitive applications. These problems can be solved by considering the use of an odd-even interleaver, which maps odd positions to odd positions and even positions to even positions. When considering the odd-even

interleaver, the deinterleaver may be removed as shown in Fig. 5.1. The removal of the deinterleaver from the lower encoder will benefit the delay sensitive applications.

In turbo codes, the performance is deeply influenced by the interleaver, which is responsible for the random-like property in turbo codes. Performance comparisons of symbol-wise and bit-wise interleaver have been studied by [43][44][41][42]. The simulations in [41][42] have demonstrated that the bit-wise interleaver achieves the same performance as the symbol-wise interleaver on slow fading channel, but the bit-wise interleaver can perform better than the symbol-wise interleaver over fast fading channel. The purpose of this research is to compare the performance of our codes with some existing codes. Therefore, the symbol-wise interleaver is employed as the simplification for decoder.

The inputs to the encoder are the information symbols which are represented by k bits of information data, where $k = \log_2 M$. At each symbol epoch t, each k bits binary data $I_t = [I_1(t), \cdots, I_k(t)]$ are directly applied to upper encoder in parallel and are encoded to n_t M-PSK symbols $\boldsymbol{c}_t^1 = [c_1^1(t), \cdots, c_{n_t}^1(t)]^T$, where $\boldsymbol{c}_t^1$ is a column vector of length n_t and the variable $c_i^1(t)$ is the encoded symbol of the upper encoder in the i-th antenna at time t. In the lower encoder, the input data are first passed through the interleaver and then passed through the lower encoder. The output of the lower encoder are similarly denoted as $\boldsymbol{c}_t^2 = [c_1^2(t), \cdots, c_{n_t}^2(t)]^T$. The symbol vector $\boldsymbol{c}_t^i$, where i=1, 2, is alternately delivered to the transmit antennas.

As has been stated, the obstacle to the STTuC is the rank deficient problem. The approach taken to overcome this problem was to rotate the output of the lower encoder. In this way, the output of the lower encoder can be written as

$$\boldsymbol{c}_t^2 = [c_{n_t}^2(t), \cdots, c_1^2(t)]^T \tag{5.1}$$

The effect of this altering is to assure that the corner of the codeword distance matrix on the main diagonal has none-zero entries [41]. The number of rank deficient matrix would be greatly reduced by using this arrangement on the output of lower encoder.

The information symbols are segmented into fixed-size frames. The encoded output which correspond to a frame are arranged into a matrix, which is referred to codeword matrix. Let L denote the frame length, which is also the interleaver length. A codeword matrix is the n_t by L matrix whose j-th column vector corresponds to the transmitted symbols at time j. Thus, the codeword matrix of the i-th encoder can be written in terms of column vector c_t^i

$$\boldsymbol{c}^i = \begin{bmatrix} c_1^i & c_2^i & \cdots & c_j^i & \ldots & c_L^i \end{bmatrix} \tag{5.2}$$

where i=1 for upper encoder and i=2 for lower encoder.

After puncturing, the punctured symbols are replaced by zero. Thus the transmitted codeword of the upper encoder is given by

$$\boldsymbol{c}^1 = \begin{bmatrix} c_1^1 & 0 & c_3^1 & 0 & c_5^1 & \cdots \end{bmatrix} \tag{5.3}$$

Similarly, the codeword of the lower encoder can be presented as

$$\boldsymbol{c}^2 = \begin{bmatrix} 0 & c_2^2 & 0 & c_4^2 & 0 & \cdots \end{bmatrix} \tag{5.4}$$

The resulting codeword of STTuC is thus given by

$$\boldsymbol{c} = \boldsymbol{c}^1 + \boldsymbol{c}^2 = \begin{bmatrix} c_1 & c_2 & \cdots & c_L \end{bmatrix} \tag{5.5}$$

where $c_i = c_i^1$ at odd time intervals, and $c_i = c_i^2$ at even time intervals.

5.3 Constituent encoder design

When applying the space-time codes technique in slow fading channel, full diversity advantage would be achieved if codeword distance matrix has full rank [5]. However, in punctured trellis codes, the full rank requirement is no longer satisfied [37][39][41], leading to low diversity gain. A solution to the rank deficient problem due to the puncture operation had been developed in [41]. The puncture operation does not allow codes to be designed to be full rank. Instead, in [41] codes are designed to reduce the number of rank deficient matrix. The approach taken in designing the codes was to create a systematic characteristic and the output of lower encoder were rotated during multiplexing. Simulation results [41] have indicated that a significant performance improvement can be achieved.

One problem encountered with this approach is in the design complexity of the component codes. The recursive characteristic that is responsible for the sparse distance spectrum is critical in turbo coding techniques. In [41], the feedback connection of one branch of register is also connected to other branches of register. These mutual connections between branches complicate the code design, as it will result in a large number of candidates of codes. For example, for $n_t = 2$, 8 states and QPSK codes, there are 2^{38} candidates. With this many candidates, an exhaustive computer search would be infeasible. In order to minimize the computation time and achieve the design goal, in [41] the codes are restricted to the case of $n_t = 2$, 8 states and QPSK with further constraints on feedback connection. This low antenna array with constraints may produce a small candidate set as low as 1024. However, if the mutual connection involves more than two and transmit antennas are more than two, it is not easy to find such a small candidate set.

In contrast to [41], a simpler space-time turbo code, which consists of parallel concatenated space-time trellis code modulation proposed in [21], has been developed by

[40]. The advantages of the code are relevant in feedback connections. Since there are no mutual connections between the branches, it has the clear advantage of low design complexity. However, because the approach does not account for the rank deficient problem, it was not able to produce an optimal performance for the punctured trellis codes.

Impressed by the considerable improvement in performance in [41] and in order to design more complicated codes for a system with small diversity gain, we proposed a new space-time turbo code that exploited the advantages of [40] and [41]. In our design, the approach to reduce the impact of the rank deficient on the performance shown in [41] has been followed and adapted. It means that the component encoder is a systematic encoder. The parity encoder is the same as in [40], and thus the disadvantage associated with the design complexity has been overcome. Compared with its counterparts in [40][41], this approach results in a low design complexity. For example, for $n_t = 2$, 8 state and QPSK code, the candidates of codes are only 1024. The new recursive systematic space-time trellis code encoder for M-PSK is shown in Fig. 5.2.

The encoder has k parallel branches of register where $k = \log_2 M$. At each time slot t, k bit information are applied to each branch in parallel. Let i-th branch contains v_i register. Then the memory of encoder is the sum of the number of register of each branch

$$v = \sum_{i=1}^{k} v_i \tag{5.6}$$

The encoder is characterized by the feed forward and feedback polynomial. The parity symbol output and the polynomial coefficients are related by the following equation

$$c_i(t) = \sum_{j=1}^{k} \sum_{k=0}^{v_j} x^j(t-k) g_{k,i}^j \mod M \tag{5.7}$$

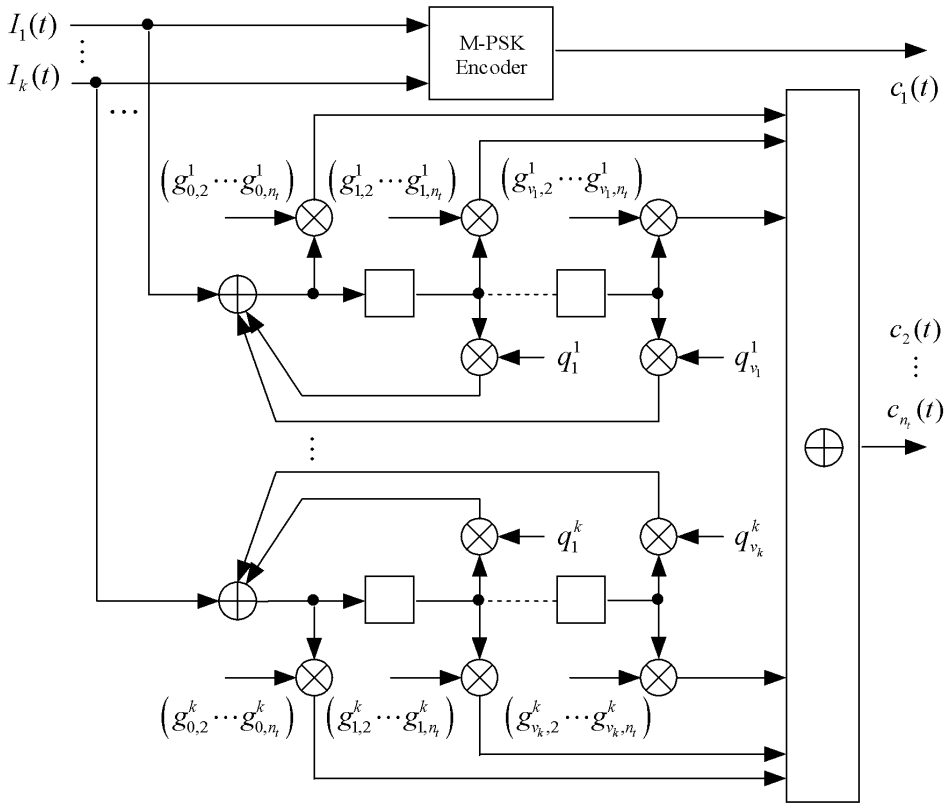

Figure 5.2. M-PSK Recursive systematic STTrC encoder.

where, $2 \leq i \leq n_t$, $c_i(t)$ is the parity symbol, and $g^j_{k,i}$ is feed forward polynomial coefficient. The value of $g^j_{k,i}$ is the integer from 0 to $M-1$. $x^j(t)$ can be calculated from the following equation

$$x^j(t) = I_j(t) + \sum_{k=1}^{v_j} x^j(t-k)q^j_k \mod 2 \tag{5.8}$$

where q^j_k is binary feedback polynomial coefficient.

5.4 Decoding algorithm

Decoding for turbo codes is an iterative decoding process based on the Maximum A Posteriori (MAP) algorithm. The MAP algorithm is optimized decoding algorithm for

minimizing symbol error rate. Because of the high computational complexity, however, the MAP algorithm is rarely used in hardware implementation. With the invention of turbo coding, the MAP algorithm has become attractive to turbo-based codes because it provides the A Posteriori information symbol Probability (APP), which is required for iterative decoding. The APP is defined as the probability of correctly decoding symbols conditioned on the received sequence, and is expressed as:

$$P(u_t = k/\boldsymbol{r}), \quad k \in \boldsymbol{I} \tag{5.9}$$

where, u_t is the information symbol at time t, k is M-PSK symbol, $\boldsymbol{I}$ is the *M-PSK* symbol set denoted by $\{0, 1, \cdots, M-1\}$, and $\boldsymbol{r}$ is the received sequence.

In trellis-based codes, a codeword corresponds to a state path at which the transition of state depends on the information symbols. In other word, if the transition is known, then the information symbol corresponding to the transition will be known. Hence, the equation (5.9) is directly related to the state transition and may be rewritten as

$$P(u_t = k/\boldsymbol{r}) = \sum_{(i,j)\in U_t=k} P(s_t = i, s_{t+1} = j/\boldsymbol{r}) \tag{5.10}$$

where, s_t is the present trellis state, s_{t+1} is the next trellis state, $(i,\ j)$ is the transition set corresponding to $u_t = k$.

By employing Bayes' rule, the APP can be expressed as:

$$\sum_{(i,j)\in u_t=k} P(s_t = i, s_{t+1} = j/\boldsymbol{r}) = \sum_{(i,j)\in u_t=k} \frac{P(s_t = i, s_{t+1} = j, \boldsymbol{r})}{P(\boldsymbol{r})} \tag{5.11}$$

In the above equation, the denominator, $P_r(r)$, is constant and common to all APP, and can be omitted in log-likelihood ratio. Therefore, the APP calculation is equivalent to estimating the probability of $P(s_r = i, s_{r+1} = j, \boldsymbol{r})$.

The received sequence, $\boldsymbol{r}$, is denoted by $\{r_1, r_2, \cdots, r_L\}$, where L is the frame length. Dividing the received sequence into three parts: two subsequences $\{r_1, r_2, \cdots, r_{t-1}\}$ and $\{r_{t+1}, r_{t+2}, \cdots, r_L\}$, and the current received signal r_t, then $P_r(s_t = i, s_{t+1} = j, \boldsymbol{r})$ can be written as by using Bayes' rule (see appendix B):

$$P(s_t = i, s_{t+1} = j, \boldsymbol{r}) = \alpha_{t-1}(i)\gamma_t(j, i)\beta_t(j) \tag{5.12}$$

where,

$$\alpha_{t-1}(i) = P(s_t = i, \{r_1, \cdots, r_{t-1}\})$$

$$\beta_t(j) = P(\{r_{t+1}, \cdots, r_L\}/s_{t+1} = j)$$

$$\gamma_t(j, i) = P(s_{t+1} = j, r_t/s_t = i)$$

We can express $\alpha_t(i)$ and $\beta_r(j)$ as a recursive expression by Using Bayes' rule and $\sum_b P(a, b) = P(a)$. That is

$$\begin{aligned}
\alpha_t(j) &= P_r(s_{t+1} = j, \{r_1, \cdots, r_t\}) \\
&= \sum_{states\ i} P_r(s_t = i, s_{t+1} = j, \{r_1, \cdots, r_t\}) \\
&= \sum_{states\ i} P_r(s_t = i, \{r_1, \cdots, r_{t-1}\}) P_r(s_{t+1} = j, r_t/s_t = i, \{r_1, \cdots, r_{t-1}\}) \\
&= \sum_{states\ i} P_r(s_t = i, \{r_1, \cdots, r_{t-1}\}) P_r(s_{t+1} = j, r_t/s_t = i) \\
&= \sum_{states\ i} \alpha_{t-1}(i)\gamma_t(i, j)
\end{aligned} \tag{5.13}$$

and

$$\begin{aligned}\beta_t(j) &= P_r(\{r_{t+1}, \cdots, r_L\}/s_{t+1} = j) \\ &= \sum_{states\ i} P_r(s_{t+2} = i, \{r_{t+1}, \cdots, r_L\}/s_{t+1} = j) \\ &= \sum_{states\ i} P_r(s_{t+2} = i, \{r_{t+2}, \cdots, r_L\}, r_{t+1}/s_{t+1} = j) \\ &= \sum_{states\ i} P_r(s_{t+2} = i, r_{t+1}/s_{t+1} = j) P_r(\{r_{t+2}, \cdots, r_L\}/s_{t+2} = i) \\ &= \sum_{states\ i} \beta_{t+1}(i)\gamma_{t+1}(i, j)\end{aligned} \tag{5.14}$$

$\gamma_t(j, i)$ is the branch transition probability and can be expressed as follows

$$\begin{aligned}\gamma_t(j, i) &= P_r(s_{t+1} = j, r_t/s_t = i) \\ &= \tfrac{P_r(s_t=i, s_{t+1}=j, r_t)}{P_r(s_t=i)} \\ &= \tfrac{P_r(r_t/s_t=i, s_{t+1}=j) P_r(s_t=i, s_{t+1}=j)}{P_r(r_t=i)} \\ &= P_r(r_t/s_t = i, s_{t+1} = j) P_r(s_{t+1} = j/s_t = i) \\ &= P_r(r_t/c_t) P_r(u_t)\end{aligned} \tag{5.15}$$

where, $\boldsymbol{c}_t$ is the output of encoder on the trellis transition from state i to state j, u_t is the input symbol of encoder to cause the transition from state i to state j , $P_r(u_t)$ is the a priori probability of u_t, and $P_r(r_t/c_t)$ is the conditional pdf of r_t given by

$$P_r(r_t/c_t) = \exp\left(-\frac{1}{2\sigma^2}\sum_{m=1}^{n_r}\left|r_m(t) - \sum_{n=1}^{n_t} h_{mn}(t)c_n(t)\right|^2\right) \tag{5.16}$$

The MAP may be summarized as follows:

Step 1. Initialize $\alpha_0(0) = 1$, $\alpha_0(j) = 0$ for all nonzero states ($j \neq 0$) of the encoder, and $\beta_{L+1}(0) = 1$, $\beta_{L+1}(j) = 0$ for all nonzero states ($j \neq 0$) of the encoder. Let t=1.

Step 2. Calculate $\gamma_t(j, i)$ using (5.15) and $\alpha_t(j)$ using (5.13) for all state j.

Step 3. If $t < L$, let $t = t + 1$ and go to step 2; else go to step 4.

Step 4. Calculate $\beta_t(j)$ using (5.14). Calculate $P_r(s_t = i, s_{t+1} = j, \boldsymbol{r})$ from (5.12).

Step 5. If $t > 1$, let $r = r - 1$ and go to step 4; else go to step 6.

Step 6. Terminate the algorithm and output all values $P_r(s_t = i, s_{t+1} = j, \boldsymbol{r})$.

The iterative turbo decoder makes use of APP in the form of Log-Likelihood Ratio (LLR) to exchange information between decoders. MAP was originally developed to deal with BPSK symbol. For space-time codes, the MAP estimation can be implemented with some slight modification to incorporate the multiple symbol, leading to the following updating formula:

$$L(u_t = k/\boldsymbol{r}) = \ln \frac{P(u_t = k/\boldsymbol{r})}{P(u_t = 0/\boldsymbol{r})} = \ln \frac{\sum\limits_{(i,j)\in u_t=k} \alpha_{r-1}(i)\gamma_r(j,i)\beta_r(j)}{\sum\limits_{(i,j)\in u_t=0} \alpha_{r-1}(i)\gamma_r(j,i)\beta_r(j)}, \quad k \neq 0, k \in I \tag{5.17}$$

where $L(u_t = k/\boldsymbol{r})$ is the APP in the form of LLR.

Substituting (5.15) into (5.17), $L(u_t = k/\boldsymbol{r})$ can be expressed as

$$\begin{aligned} L(u_t = k/\boldsymbol{r}) &= \ln \frac{\sum\limits_{(i,j)\in u_t=k} \alpha_{t-1}(i)P_r(r_t/c_t)\beta_t(j)}{\sum\limits_{(i,j)\in u_t=0} \alpha_{t-1}(i)P_r(r_t/c_t)\beta_t(j)} + \ln \frac{P(u_t=k)}{P(u_t=0)} \\ &= L_e(u_t) + L(u_t) \end{aligned} \tag{5.18}$$

where

$$L_e(u_t = k) = \ln \frac{\sum\limits_{(i,j)\in u_t=k} \alpha_{t-1}(i)P_r(r_t/c_t)\beta_t(j)}{\sum\limits_{(i,j)\in u_t=0} \alpha_{t-1}(i)P_r(r_t/c_t)\beta_t(j)} \tag{5.19}$$

is the extrinsic information, and

$$L(u_t = k) = \ln \frac{P(u_t = k)}{P(u_t = 0)} \tag{5.20}$$

is the LLR of the a priori probability of symbol k.

The extrinsic information represents the extra knowledge about the message being transmitted from the priori information and the received information sequence. The iterative decoding of turbo codes exchanges the extrinsic information between component

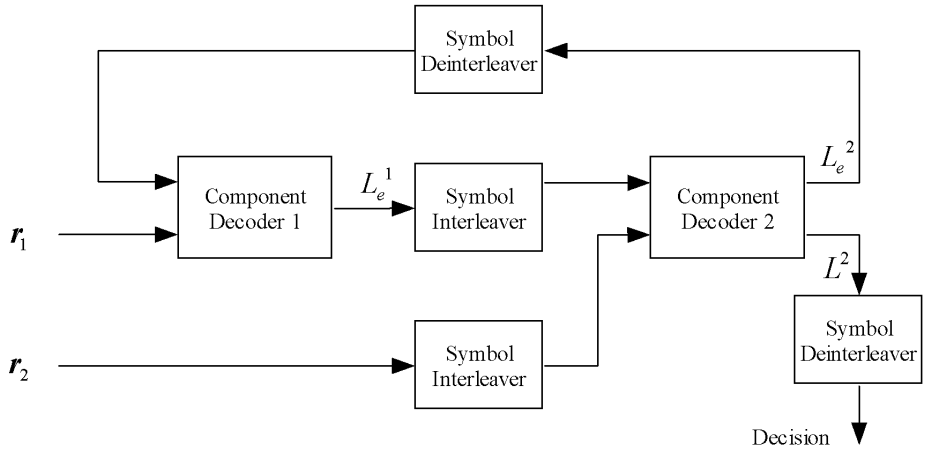

Figure 5.3. Turbo decoder: iterative decode process.

decoder. From (5.18), a priori information is needed for decoder. At the first iteration, the prior information of the first component decoder is initially set to zero. Next, all decoder use the extrinsic information of other decoder as the prior information. An illustration of the iterative decoding is shown in Fig. 5.3

The iteration process is terminated if the termination condition is reached. The final decision on output symbol is made in terms of the LLR of second decoder, such that, if all LLP is negative values, the decoded output symbol is zero; if there is at least one positive LLR, the decoder take the symbol with maximum LLR.

5.5 Code design criteria

In [5], the system performance is characterized by PEP. The PEP is the probability that decoder erroneously selects codeword $\boldsymbol{e}$ as the transmitted codeword while the codeword $\boldsymbol{c}$ is in fact transmitted. A codeword difference matrix $\boldsymbol{D}_{ce}$ is defined by subtracting codeword $\boldsymbol{e}$ from codeword $\boldsymbol{c}$

$$\boldsymbol{D}_{ce} = \boldsymbol{c} - \boldsymbol{e} \tag{5.21}$$

For the performance analysis, a codeword distance matrix is defined as

$$\boldsymbol{A} = \boldsymbol{D}_{ce}(\boldsymbol{D}_{ce})^H \tag{5.22}$$

Let $\boldsymbol{A}^i$, where i=1, 2, represents the codeword distance matrix of i-th encoder, then we can write the codeword distance matrix in the form

$$\boldsymbol{A} = \boldsymbol{A}^1 + \boldsymbol{A}^2 \tag{5.23}$$

In [5], the PEP for slow fading channel had been extensively studied, and is described by

$$P(\boldsymbol{c} \to \boldsymbol{e}) \leq \left(\prod_{i=1}^{r} \lambda_i \right)^{-n_r} \left(\frac{E_s}{4N_0} \right)^{-rn_r} \tag{5.24}$$

where r is the rank of $\boldsymbol{A}$ and λ_i is the none zero eigenvalues of $\boldsymbol{A}$.

This equation shows the importance of the rank that determines the slope of PEP in logarithm domain. To optimize the worst PEP, r turns out to be full rank and term $\prod_{i=1}^{r} \lambda_i$ turns out to be as large as desired. This lead to well-known rank and determinant criteria that had been widely applied in space-time coding design. The exponent term rn_r is known as the diversity gain.

The improvement to the rank and determinant criteria had been proposed in the subsequent works [16][17][15]. In [15], the PEP is expressed as a function of the rank and determinant, or the trace depending on the diversity gain. If the diversity gain is less than 4, (5.24) holds. If the diversity gain is larger than and equal to 4, the PEP is given by

$$P(\boldsymbol{c} \to \boldsymbol{e}) \leq \frac{1}{4} \exp\left(-n_r \frac{E_s}{4N_0} \sum_{i=1}^{r} \lambda_i \right) \tag{5.25}$$

where, the term $\sum_{i=1}^{r} \lambda_i$ is equal to the trace of $\boldsymbol{A}$.

In (5.25), the trace is scaled by SNR. Thus the degradation of PEP performance becomes significant for the small values of trace at high SNR. Therefore, the dominant component of PEP at high SNR is the error event with minimum trace. This can be explained from the fact that the fading channel converges to AWGN channel with the increased diversity gain. Maximizing the minimum trace of $\boldsymbol{A}$ would lead to another important criterion: trace criterion [15]. The trace of $\boldsymbol{A}$ is equal to the squared Euclidean distance. Thus the intent of the trace criterion is to maximize the free distance of the codes.

Based on the design criteria mentioned above, a code design method for the punctured STTuC was proposed in [41]. The design relies on the knowledge of the overall distance spectrum of the punctured STTuC and assumes that the uniform random interleaver is used in calculation of the DS. However, this assumption is particularly questionable for the DS of determinant. The requirements of using uniform random interleaver on codes mean that the overall distance should be equal to the sum of the distance of the component codes, such that

$$dis(\boldsymbol{A}) = dis(\boldsymbol{A}_1) + dis(\boldsymbol{A}_2) \tag{5.26}$$

where $dis()$ is the distance of codeword distance matrix.

Obviously, from (5.23), this requirement is not satisfied if the distance is the determinant of $\boldsymbol{A}$.

It can be seen from (5.25) that the performance is not being influenced by the rank deficient matrix. Therefore, unlike the importance of the rank for small diversity gain, the rank is not the primary concern for large diversity gain. Thus, the trace criterion is applicable to the space-time turbo codes for the large diversity gain. Therefore, the

authors [40][42] have considered applying trace criterion in the code design for large diversity gain. The design strategy is that the codes under consideration are chosen so that the component codes have the optimal trace. Although this is a simple design strategy and the trace is determined without taking into account the puncture operation, the simulations in [40][42] have indicated that the trace criterion can be considered to be reliable in the design of space-time turbo codes for large diversity gain in slow fading channel.

As mentioned, the full rank is no longer satisfied in punctured trellis codes. With this issue, the optimal rank and determinant may not give the correct performance evaluation. Therefore, the codes with optimal rank and determinant for nonpunctured trellis code may result in less than optimal performance for punctured trellis codes. Rank criterion reveals that the minimum rank is the dominant factor for PEP. It is obvious that the worst case of rank deficient is r=1. In this case, it is easy to prove that the product of none-zero eigenvalue will be equal to the trace of $\boldsymbol{A}$. Therefore, for small diversity gain, our goal is to seek the optimal trace for the coding gain in punctured trellis codes, instead of seeking the optimal determinant as usual as in nonpunctured trellis codes.

The trace criterion has been employed successfully in STTuC [40][42] for high diversity gain. However, this criterion is only a rough guideline on code design since in this criterion only the optimal trace is considered, and their multiplicity is ignored. Trellis codes with large number of states may result in a large multiplicity that cannot be ignored in assessing the overall coding gain [30]. Unlike the previous work, in this dissertation, the multiplicity of the free distance will be considered in the design as well as optimal free distance. The multiplicity can be found by computer search very accurately without introduction of significant design complexity since the trace is monotonically increased with time.

In this dissertation, based on the design strategy presented in [40][42], the trace criterion will be employed to the component code design for both small and large diversity gain. Minimizing the multiplicity of the free distance was also considered in the design. Based on the design criteria, new codes were obtained through the free distance spectrum search and listed in Table 5.1 together with some existing codes. The feed forward coefficients are obtained through computer search with respect to the trace criterion. The primitive recursive characteristic is required in order to achieve better free distance spectrum for the turbo-based codes. In this paper, the primitive polynomial is chosen to have maximum order. The free distance spectrums are also listed in Table 5.1, where T_0 denotes the free distance and N_{free} denotes the average number of the error events with T_0.

Table 5.1. QPSK space-time turbo codes in slow fading channels

Codes	State	Feed forward	Feedback	T_0 N_{free}
New STTuC	8	g_1=[0, 2] g_2=[2, 1, 1]	q_1=1+x q_2=1+x+x^2	12, 3
FCVY [40]	8	g_1=[(2 2),(2 1)] g_2=[(2 0),(1 2),(2 0)]	q_1=1+x q_2=1+x+x^2	12, 2
Tujkovic [41]	8	Qa=[10;10;01;10]	[101;110;001;100]	
New STTuC	4	g_1=[0, 2] g_2=[2, 1]	q_1=1+x q_2=1+x	10, 4
FCVY [40]	4	g_1=[(0 2),(1 2)] g_2=[(2 3),(2 0)]	q_1=1+x q_1=1+x	10, 2
New STTuC	16	g_1=[0, 2, 0] g_2=[2, 1, 2]	q_1=1+x+x^2 q_2=1+x+x^2	16, 14
FCVY [40]	16	g_1=[(1 2),(1 3),(3 2)] g_2=[(2 0),(2 2),(2 0)]	q_1=1+x+x^2 q_2=1+x+x^2	16, 14

5.6 Simulation

The performances of the new codes were evaluated using simulation. In simulation, 130 symbols are generated in each frame, the interleaver is a symbol-wise odd-even s-random interleaver, quasi-static flat fading was considered, and the channel coefficients are perfectly known at the receiver. The simulation results are shown at 10th iterations. The performances of the new codes are compared with that of existing codes. In plot, the codes proposed in [40] are labeled as FCVY, the codes proposed in [41] are labeled as Tujkovic, the codes proposed in [5] are labeled as TSC, and the codes proposed in [21] are labeled as CVYL.

A performance comparison among the 8 state codes listed in Table 5.1 are shown in Fig. 5.4 for the 2Tx1Rx system. The FER performance of our new code was essentially identical to that of Tujkovic's code. Both codes achieve a significant improvement on FER performance compared to FCVY code. It was found the improvement is more than 5 dB at the FER of 10^{-3}. The significant improvement can also be seen in Fig. 5.6 and Fig. 5.7 for 4 states and 16 states codes, respectively. The rank deficient in punctured trellis codes is demonstrated through the comparison to the TSC space-time trellis codes. Although significant performance improvement had been achieved, it was shown that the new codes are unable to produce full rank. This can be illustrated by the fact that the slope of the new codes is parallel to the slope of the TSC space-time trellis codes.

Performance considering both small diversity gain and large diversity were studied. Fig. 5.5 shows the performance comparison between proposed code and some existing codes for various space diversity configurations. From (5.25), we expect that the rank deficient has little effect on the performance for the large diversity gain. This was reflected in Fig. 5.5, from which the results indicate that the impact of rank deficient on performance becomes less severe with the increased diversity gain. As a result, the FCVY code provides comparable performance as the new codes for large diversity gain.

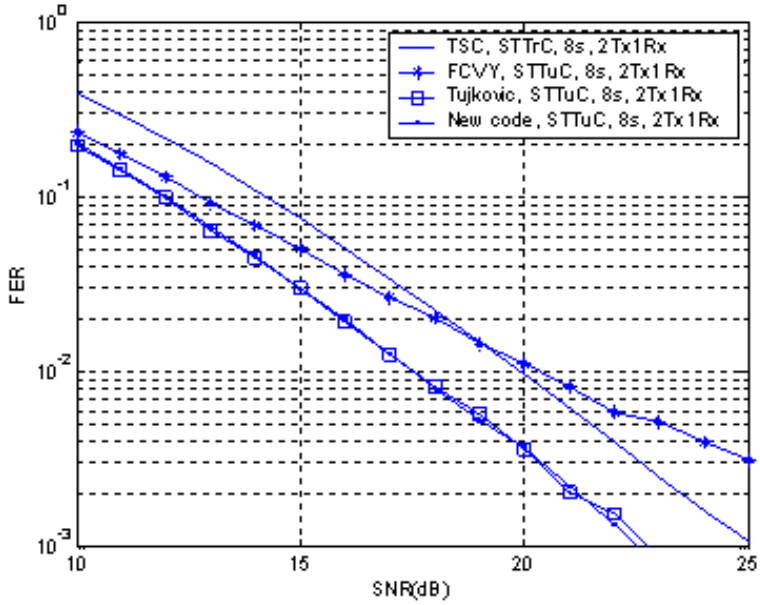

Figure 5.4. Performance of 8 states QPSK STTuC for small diversity gain.

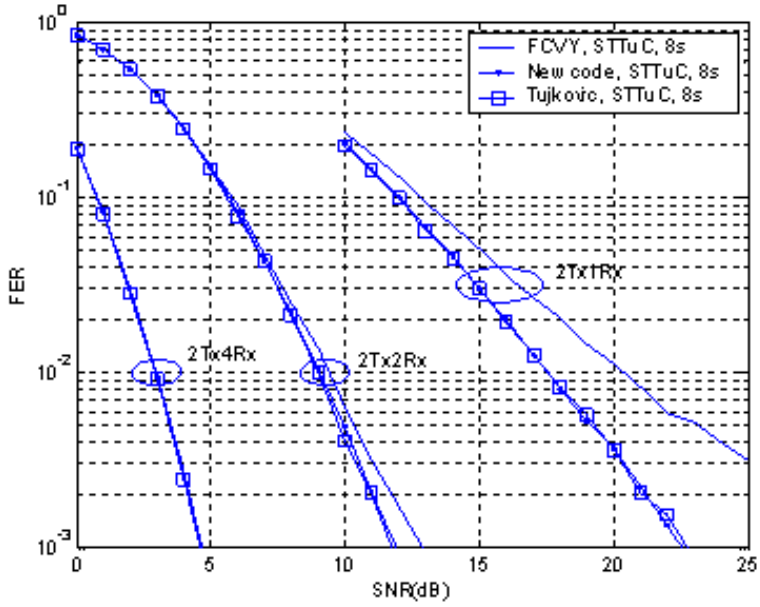

Figure 5.5. Performance of 8 states QPSK STTuC for different space diversity.

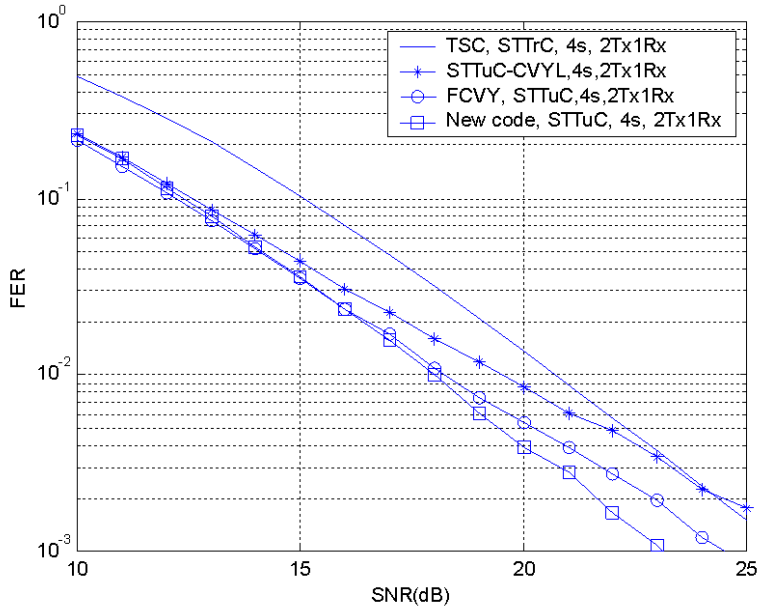

Figure 5.6. Performance of 4 states QPSK STTuC for different space diversity.

In Fig. 5.6 and Fig. 5.7, performance of codes labeled as STTuC-CVYL for various states are shown. The STTuC-CVYL are constructed based on STTrC proposed in [21] for small diversity gain using rank and determinant criteria. The component codes of FCVY are designed according to the trace criteria for large diversity gain. To the best of our knowledge, the STTrC based on the rank and determinant criteria have superior performance compared to STTrC based on trace criterion for small diversity gain. However, when applying these codes to STTuC, the performance in STTuC is inconsistent with the design criteria in STTrC as shown in Fig. 5.6 and Fig. 5.7, where performance of FCVY codes is shown to outperform that of CVYL for small diversity gain. These results indicated that trace criterion is more suitable for STTuC with small diversity gain than rank and determinant criterion, which are commonly employed for STTrC with small diversity gain.

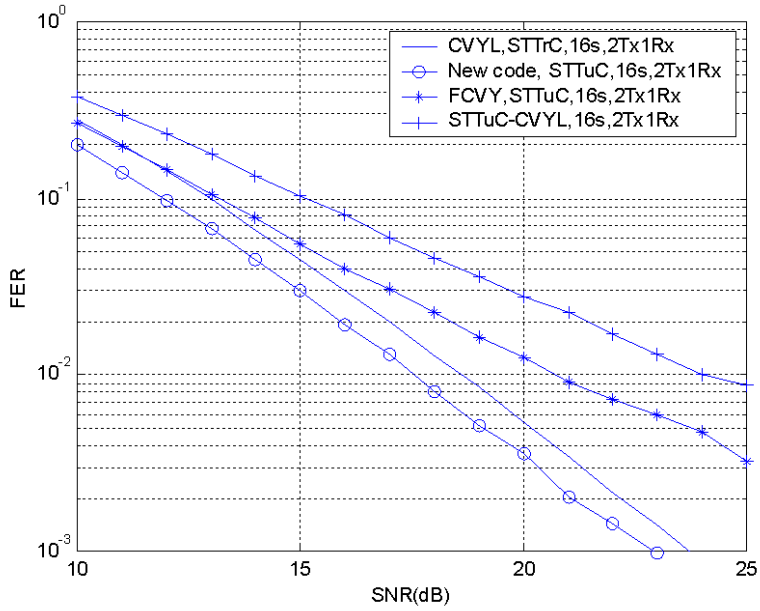

Figure 5.7. Performance of 16 states QPSK STTuC for different space diversity.

5.7 Conclusions

In this chapter, the problem of designing full rate STTuC has been addressed. The rank of codeword distance matrix is an important design parameter for the small diversity gain in space-time codes. For the large diversity gain, the performance is independent to the rank. Thus, the rank deficient problem, an inherently existing phenomenon in the punctured trellis codes, has little effect on performance. As a consequence, previous works had designed successfully STTuC for the large diversity gain. However, for the small diversity gain, the rank deficient problem must be accounted for in successful code design.

New STTuC have been presented. The proposed codes reduce the impact of rank deficient on the FER performance and has the advantage of low design complexity. Since rank of codeword distance matrix determine the diversity gain, the proposed codes actually provide improvement in diversity gain. Design criteria for the proposed codes were

introduced. In comparison to the previous works, the simulation results have shown that the proposed codes are successful in design for small diversity gain in slow fading channel. The proposed codes result in more than 5 dB improvement at FER of 10^{-3} .

CHAPTER 6

CONCLUSIONS AND FUTURE WORKS

6.1 Conclusions

In this dissertation, performance and design of space-time codes have been studied. The main objective of this dissertation has been to improve the performance of space-time codes. This dissertation covers a wide range of topics in space-time codes. It involves theoretical analysis, design, and implementation for space-time trellis codes, space-time turbo codes, and orthogonal space-time trellis codes. The main contributions of this dissertation include the following:

- A new derivation of exact PEP is given. The design criteria based on the upper bound of PEP can provide insight on performance property only for high SNR because the upper bound of PEP is loose in low SNR range. For a system with high diversity gain, the interested SNR may be in low SNR range. Thus the exact PEP is required for analyzing performance over the entire SNR range. The derivation utilizes the statistical independence properties in modified Euclidean distance to obtain the pdf of the modified Euclidean distance, and then the exact PEP can be calculated by taking the average of the PEP conditioned on the modified Euclidean distance. The exact PEP suggests that the upper bound of PEP becomes loose and inaccuracy for a certain region of SNR values. This result provides added insights into understanding space-time codes. Compared to previous derivations, our derivation is simple and comprehensible.
- Improved design criteria for space-time trellis codes in both slow and fast fading channel using union bound analysis had been proposed to provide coding gain

improvement. Criteria based on PEP are established on the basis of assumption that only dominant error event contribute to the performance. However, there are not dominant error events for space-time codes in fading channel. Union bound on FER is a function of PEP and distance spectrum and allows to analyze the contribution of all error events to performance. In our design, a more accurate PEP applied in union bound analysis leads to more accurate coding gain metrics. In order to ensure the effectiveness of using the distance spectrum as an evaluation tool in evaluating coding gain performance, a improved distance spectrum search has been proposed. With the criteria, optimal codes were searched through new coding gain performance metrics in consideration of the distance spectrum. The resulted codes were compared with so-called optimal codes and better performance were obtained. The improved design criteria can result in an improvement of 0.2-0.9 dB in FER performance at FER of 10^{-3}

- Orthogonal space-time trellis codes have been proposed. Significant improvements in coding gain performance can be achieved when space-time trellis codes are concatenated with space-time block codes, for instance, the super-orthogonal space-time trellis codes. Super-orthogonal space-time trellis codes provide significant improvement on coding gain in slow fading channel, but result in diversity gain loss in fast fading channel. The orthogonal space-time trellis codes take advantage of the benefits of the orthogonal design in space-time block codes and maintain the symbol Hamming distance in the meanwhile. The novelty to the approach is that the diversity gain are improved with a factor of the number of transmit antennas, in comparison to the super-orthogonal space-trellis codes where coding gain is improved. This fundamental difference in properties gives the hopes of achieving remarkable improvement in performance. The proposed codes provide an improvement of more than 5 dB at FER of 10^{-3}.

- New full rate space-time turbo codes for slow fading channel have been developed. Turbo-based codes are very promising to improve performance significantly. The full rank of codeword distance matrix is key characteristics to the performance of space-time codes. However, in full rate space-time turbo codes, the codeword distance matrix is a rank-deficient matrix due to the puncture operation. This limits the expected performance improvement that could result from turbo-based codes. The new space-time turbo code we proposed can reduce the impact of the rank deficient on performance with low design complexity. This is achieved by reducing the number of the rank deficient codeword distance matrix. A simple but effective design criterion has been proposed to mitigate the performance deterioration caused by rank-deficient problem. Essentially, the proposed approach improves the diversity gain of rank-deficient codes since the rank of codeword distance matrix is directly related to diversity gain. Therefore, the proposed codes could achieve considerable improvement on FER performance over quasi-static flat fading channel for the small diversity gain. The improvement is more than 5 dB at FER of 10^{-3}.

6.2 Future works

In this dissertation, a comprehensive study of space-time codes has been presented on the performance analysis and design, but some problems still deserve further investigation. First of all, our performance analysis currently employed is based on a model in which channel information are perfectly known at receiver. However, this model is not the reality that it represents. In practice, the channel estimation is never perfectly known. In high data rate transmission this estimation error can't be ignored because the length of training codeword is limited for the purpose of enhancing spectral efficiency. Thus, future work will extend the analysis to imperfect channel estimation. The analy-

sis results obtained are expected to further help investigators to understand space-time codes in different scenario.

We have shown how the use of distance spectrum can provide valuable information on the coding gain. The method of distance spectrum search used in this dissertation is not only time consuming but also memory limited. Therefore, the use of truncated distance spectrum has to be considered; so that the coding gain relies on rough estimation. We have proposed improved search method, trying to obtain spectrum as abundant as possible. However this is still far to ensure a reliable estimate on the coding gain. In order to fully benefit from distance spectrum, it would be interesting to apply other distance spectrum search method. For example, transform function may be a good candidate. The transform function is derived from the state diagram. It can provide detailed information on distance spectrum without memory limitation. Applying transform function to space-time codes might be beneficial in systematic design of space-time codes for coding gain. Moreover, this is an unexplored area in this field.

We have concentrated on identifying the performance of space-time turbo codes using MAP algorithm, which is optimized decoding algorithm used in turbo codes. However, besides performance, the complexity of decoding algorithm in turbo codes is also an important topic. Because of the high complexity in hardware implementation, MAP is not used in practical applications. Thus, decoding with reduced complexity is an important future work. One could use sub-optimal algorithm, for example, soft output Viterbi algorithm (SOVA) [45][46], MAX-log-MAP, log-MAP, and log-MAP with look-up table [47], to reduce the complexity of decoder. The choice of approach depends on the trade-off between complexity and performance.

APPENDIX A

THE INTEGRAL IN THE DERIVATION OF EXACT PEP

Consider the integral

$$\begin{aligned} I_j &= \int_0^\infty Q\left(\sqrt{\tfrac{E_s}{2N_0}}\delta\right)\tfrac{\delta^{j-1}}{\lambda^j\Gamma(j)}e^{\frac{-\delta}{\lambda}}d\delta \\ &= \tfrac{1}{\sqrt{2\pi}}\int_0^\infty\int_{\sqrt{\frac{E_s}{2N_0}}\delta}^\infty e^{-\frac{t^2}{2}}\tfrac{\delta^{j-1}}{\lambda^j\Gamma(j)}e^{\frac{-\delta}{\lambda}}dtd\delta \end{aligned} \tag{A.1}$$

Making a substitution of the form

$$\delta = \lambda\delta$$

So

$$I_j = \frac{1}{\sqrt{2\pi}\Gamma(j)}\int_0^\infty\int_{\sqrt{\frac{E_s}{2N_0}\lambda\delta}}^\infty e^{-\frac{t^2}{2}}\delta^{j-1}e^{-\delta}dtd\delta \tag{A.2}$$

Let

$$\gamma = \frac{E_b}{4N_0}$$

and

$$a = \frac{1}{\sqrt{2\pi}\Gamma(j)}$$

Integration by parts gives

$$\begin{aligned} &I_j = a\int_0^\infty\int_{\sqrt{2\gamma\lambda\delta}}^\infty e^{-\frac{t^2}{2}}\delta^{j-1}e^{-\delta}dtd\delta \\ &= -a\int_0^\infty\int_{\sqrt{2\gamma\lambda\delta}}^\infty e^{-\frac{t^2}{2}}\delta^{j-1}e^{-\delta}dt\Big|_0^\infty + \\ &a\int_0^\infty e^{-\delta}\left(-e^{-\gamma\lambda\delta}\delta^{j-1-\frac{1}{2}}\sqrt{\tfrac{\gamma\lambda}{2}} + \int_{\sqrt{2\gamma\lambda\delta}}^\infty e^{-\frac{t^2}{2}}(j-1)\delta^{j-2}dt\right)d\delta \\ &= -a\sqrt{\tfrac{\gamma\lambda}{2}}\int_0^\infty e^{-(1+\gamma\lambda)\delta}\delta^{j-1-\frac{1}{2}}d\delta + a(j-1)\int_0^\infty\int_{\sqrt{2\gamma\lambda\delta}}^\infty e^{-\frac{t^2}{2}}\delta^{j-2}e^{-\delta}dtd\delta \\ &= -a\sqrt{\tfrac{\gamma\lambda}{2}}\int_0^\infty e^{-(1+\gamma\lambda)\delta}\delta^{j-1-\frac{1}{2}}d\delta + (j-1)I_{j-1} \end{aligned} \tag{A.3}$$

The first term on the right-hand side is the gamma function. That is

$$\int_0^\infty e^{-(1+\gamma\lambda)\delta}\delta^{j-1-\frac{1}{2}}d\delta = (1+\gamma\lambda)^{-j+\frac{1}{2}}\,\Gamma\left(j-\frac{1}{2}\right) \tag{A.4}$$

From the result above, the integral then becomes

$$\begin{aligned} I_j = &-\sum_{i=0}^{j-2} a \begin{pmatrix} j-1 \\ i \end{pmatrix} i!\sqrt{\tfrac{\gamma\lambda}{2}}\,(1+\gamma\lambda)^{-j+i+\frac{1}{2}}\,\Gamma\left(j-i-\tfrac{1}{2}\right)+ \\ &a\,(j-1)!\int_0^\infty\int_{\sqrt{2\gamma\lambda\delta}}^\infty e^{-\frac{t^2}{2}}e^{-\delta}dtd\delta \end{aligned} \tag{A.5}$$

The integral in (A.5) can be solved as follows

$$\begin{aligned} &\int_0^\infty\int_{\sqrt{2\gamma\lambda\delta}}^\infty e^{-\frac{t^2}{2}}e^{-\delta}dtd\delta \\ &= -e^{-\delta}\int_{\sqrt{2\gamma\lambda\delta}}^\infty e^{-\frac{t^2}{2}}dt\Big|_0^\infty - \int_0^\infty e^{-(1+\gamma\lambda)\delta}\sqrt{2\gamma\lambda}\tfrac{1}{2}\delta^{-\frac{1}{2}}d\delta \\ &= \tfrac{\sqrt{2\pi}}{2} - \sqrt{\tfrac{\gamma\lambda}{2}}\,(1+\gamma\lambda)^{-\frac{1}{2}}\,\Gamma\left(\tfrac{1}{2}\right) \end{aligned} \tag{A.6}$$

Combing (A.6) and (A.5), we have

$$\begin{aligned} I_j &= a\,(j-1)!\tfrac{\sqrt{2\pi}}{2} - \sum_{i=0}^{j-1} a \begin{pmatrix} j-1 \\ i \end{pmatrix} i!\sqrt{\tfrac{\gamma\lambda}{2}}\,(1+\gamma\lambda)^{-j+i+\frac{1}{2}}\,\Gamma\left(j-i-\tfrac{1}{2}\right) \\ &= \tfrac{1}{2}\left[1 - \tfrac{1}{\sqrt{\pi}}\sum_{i=0}^{j-1}\tfrac{\sqrt{\gamma\lambda}}{(j-1-i)!}\,(1+\gamma\lambda)^{-j+i+\frac{1}{2}}\,\Gamma\left(j-i-\tfrac{1}{2}\right)\right] \end{aligned} \tag{A.7}$$

Replacing i with j-1-i in the sum, we have the result

$$\begin{aligned} I_j &= \tfrac{1}{2}\left[1 - \tfrac{1}{\sqrt{\pi}}\sum_{i=0}^{j-1}\tfrac{\sqrt{\gamma\lambda}}{i!}\,(1+\gamma\lambda)^{-i-\frac{1}{2}}\,\Gamma\left(i+\tfrac{1}{2}\right)\right] \\ &= \tfrac{1}{2}\left[1 - \sqrt{\tfrac{\gamma\lambda}{1+\gamma\lambda}}\sum_{i=0}^{j-1}\tfrac{(i-0.5)(i-1.5)\cdots 0.5}{i!}\,(1+\gamma\lambda)^{-i}\right] \\ &= \tfrac{1}{2}\left[1 - \sqrt{\tfrac{\gamma\lambda}{1+\gamma\lambda}}\sum_{i=0}^{j-1}\begin{pmatrix} 2i \\ i \end{pmatrix}\tfrac{1}{(4+4\gamma\lambda)^i}\right] \end{aligned} \tag{A.8}$$

APPENDIX B

EQUATION FOR THE DECODING OF TURBO CODES

The equivalent a posteriori information symbol probability is

$$\begin{aligned} &P\left(s_t = i, s_{t+1} = j, \boldsymbol{r}\right) \\ &\quad = P\left(s_t = i, s_{t+1} = j, \left\{r_1, \cdots, r_{t-1}\right\}, r_t, \left\{r_{t+1}, \cdots, r_L\right\}\right) \end{aligned} \tag{B.1}$$

Using Bayes' rule, the equation can be written as

$$\begin{aligned} &P\left(s_t = i, s_{t+1} = j, r\right) \\ &\quad = P\left(\left\{r_{t+1}, \cdots, r_L\right\} / s_t = i, s_{t+1} = j, \left\{r_1, \cdots, r_{t-1}\right\}\right) \\ &\qquad P\left(s_t = i, s_{t+1} = j, \left\{r_1, \cdots, r_{t-1}\right\}, r_t,\right) \\ &\quad = P\left(\left\{r_{t+1}, \cdots, r_L\right\} / s_t = i, s_{t+1} = j, \left\{r_1, \cdots, r_{t-1}\right\}\right) \\ &\qquad P\left(s_{t+1} = j, r_t / s_t = i, \left\{r_1, \cdots, r_{t-1}\right\}\right) P\left(s_t = i, \left\{r_1, \cdots, r_{t-1}\right\}\right) \end{aligned} \tag{B.2}$$

In the first term of (B.2), if s_{t+1} is given, the receive vector $r_{t+1}, \cdots, r_L$ will only dependent on it. Therefore, we have

$$\begin{aligned} &P\left(\left\{r_{t+1}, \cdots, r_L\right\} / s_t = i, s_{t+1} = j, \left\{r_1, \cdots, r_{t-1}\right\}\right) \\ &\quad = P\left(\left\{r_{t+1}, \cdots, r_L\right\} / s_{t+1} = j\right) \end{aligned} \tag{B.3}$$

Similarly, in the second terms of (B.2), r_t is only dependent on s_t, thus

$$P\left(s_{t+1} = j, r_t / s_t = i, \left\{r_1, \cdots, r_{t-1}\right\}\right) = P\left(s_{t+1} = j, r_t / s_t = i\right) \tag{B.4}$$

Substituting (B.3) and (B.4) into (B.2) to give the final equation

$$\begin{aligned} &P\left(s_t = i, s_{t+1} = j, r\right) \\ &\quad = P\left(s_t = i, \left\{r_1, \cdots, r_{t-1}\right\}\right) P\left(s_{t+1} = j, r_t / s_t = i\right) \\ &\qquad P\left(\left\{r_{t+1}, \cdots, r_L\right\} / s_{t+1} = j\right) \end{aligned} \tag{B.5}$$

REFERENCES

[1] T. S. Rappaport, *Wireless Communications: Principles and Practice*. Prentice Hall, 1996.

[2] http://www.qualcomm.com/press/releases/2005/050504_rfr6500.html.

[3] E. Telatar, "Capacity of multi-antenna gaussian channels," *European Transactions on Telecommunications*, vol. 10, no. 6, pp. 585–595, Nov.-Dec. 1999.

[4] G. J. Foschini and M. J. Gans, "On limits of wireless communication in a fading environment when using multiple antennas," *Wireless Personal Communication*, vol. 6, no. 3, pp. 311–335, 1998.

[5] V. Tarokh, N. Seshadri, and A. R. Calderbank, "Space-time codes for high data rate wireless communication: performance criteria and code construction," *IEEE Trans. on Inform. Theory*, vol. 44, no. 2, pp. 744–765, Mar. 1998.

[6] C. E. Shannon, "A mathematical theory of communication," *Bell Sys. Tech. J.*, vol. 27, pp. 379–423, 623–656, 1948.

[7] L. Ozarow, S. Shamai, and A. Wyner, "Information theoretic considerations for cellular mobile radio," *IEEE transactions on Vehicular Technology*, vol. 43, pp. 359–378, May 1994.

[8] G. D. Golden, G. J. Foschini, R. A. Valenzuela, and P. W. Wolniasky, "Detection algorithm and initial laboratory results using the v-blast space-time communication architecture," *Electronics Letters*, vol. 35, pp. 14–15, January 1999.

[9] S. M. Alamouti, "A simple transmit diversity technique for wireless communications," *IEEE J. Select. Areas Commun.*, vol. 16, no. 8, pp. 1451–1458, OCT. 1998.

[10] E. Kreyszig, *Advanced Engineering Mathematics*, 8th ed. Wiley, 1999.

[11] V. Tarokh, H. Jafarkhani, and A. R. Calderbank, "Space-time block codes from orthogonal designs," *IEEE Trans. Info. Theory*, vol. 45, no. 5, pp. 1456–1467, July 1999.

[12] V.Tarokh, H. Jafarkani, and A. Calderbank, "Space-time block coding for wireless communications: Performance results," *IEEE JSAC*, vol. 17, no. 3, pp. 451–460, March 1999.

[13] C. Berrou, A. Glavieux, and P. Thitimajshima, "Near shannon limit error correcting coding and decoding: turbo codes," in *Proc. of IEEE Int. Conference on Communication*, Geneva, Switzerland, May 1993, pp. 1064–1070.

[14] H. Jafarkhani and N. Seshadri, "Super-orthogonal space-time trellis codes," *IEEE Trans. Inf. Theory*, vol. 49, no. 4, pp. 937–950, Apr. 2003.

[15] J. Yuan, Z. Chen, B. Vucetic, and W. Firmanto, "Performance and design of space-time coding in fading channels," *IEEE Transactions on Communications*, vol. 51, no. 12, pp. 1991–1996, Dec. 2003.

[16] M. Tao and R. S. Cheng, "Improved design criteria and new trellis codes for space-time coded modulation in slow fading channels," *IEEE Commun. Lett.*, vol. 5, pp. 313–315, July 2001.

[17] D. M. Ionescu, "New results on space-time code design criteria," *WCNC 1999 - IEEE Wireless Communications and Networking Conference*, no. 1, Sep. 1999, pp. 684–687.

[18] M. Uysal and C. N. Georghiades, "Error performance analysis of space-time codes over rayleigh fading channels," *Journal of Communications and Networks (JCN)*, vol. 2, no. 4, pp. 351–356, December 2000.

[19] M. K. Simon, "Evaluation of average bit error probabilities for space-time coding based on a simpler exact evaluation of pair-wise error probability," *Journal of Communications and Networks*, vol. 3, no. 3, pp. 257–264, September 2001.

[20] S. Baro, G. Bauch, and A. Hansmann, "Improved codes for space-time trellis-coded modulation," *IEEE Commun. Lett.*, vol. 4, no. 1, pp. 20–22, Jan. 2000.

[21] Z. Chen, B. Vucetic, J. Yuan, and K. L. Lo, "Space-time trellis codes with two, three and four transmit antennas in quasi-static fading channels," in *Proc. of IEEE ICC'02*, New York, May 2002, pp. 1589–1595.

[22] H. Bouzekri and S. Miller, "Analytical tools for space-time codes over quasi-static fading channels," in *Proc. IEEE Globecom*, vol. 2, 2001, pp. 1118–1121.

[23] A. Stefanov and T. M. Duman, "Performance bounds for space-time trellis codes," *IEEE Transactions on Information Theory*, vol. 49, no. 9, pp. 2134–2140, Sep. 2003.

[24] C. Liao and V. K. Prabhu, "Improved code design criteria for space-time trellis codes over quasi-static flat fading channels," in *proceeding of IEEE SPAWC*, 2005, pp. 7–11.

[25] ——, "Design of space-time trellis codes in fast and flat fading channel," in *proceeding of IEEE MAPE*, vol. 2, 2005, pp. 1111–1114.

[26] D. K. Aktas and M. P. Fitz, "Computing the distance spectrum of space-time trellis codes," *WCNC 2000 - IEEE Wireless Communications and Networking Conference*, no. 1, Sep. 2000, pp. 51–55.

[27] Y. S. Jung and J. H. Lee, "New measure of coding gain for space-time trellis codes," in *Proc. ISIT 2001*, Washington, D. C., USA, June 2001, p. 198.

[28] S. Benedetto, M. Mondin, and G. Montorsi, "Performance evaluation of trellis-coded modulation schemes," *Proc. IEEE*, vol. 82, pp. 833–855, June 1994.

[29] W. Firmanto, B. Vucetic, and J. Yuan, "Space-time tcm with improved performance on fast fading channels," *IEEE Trans. Commun. Lett.*, vol. 5, no. 4, pp. 154–156, April 2001.

[30] J. Proakis, *Digital Communications*, 3rd ed. New York, NY: McGraw-Hill, 1995.

[31] Y. Sasazaki and T. Ohtsuki, "Improved design criteria and new trellis codes for space-time trellis coded modulation in fast fading channels," *Trans. of IEICE, E86-B*, no. 3, pp. 1057–1062, Mar. 2003.

[32] S. M. Alamouti, V. Tarokh, and P. Poon, "Trellis coded modulation and transmit diversity: Design criteria and performance evaluation," in *Proc. IEEE ICUPC98*, Oct. 1998, p. 703707.

[33] Y. Gong and K. B. Letaief, "Concatenated spacetime block coding with trellis coded modulation in fading channels," *IEEE TRANSACTIONS ON WIRELESS COMMUNICATIONS*, vol. 1, no. 4, pp. 580–590, OCTOBER 2002.

[34] D. M. Ionescu, K. K. Mukkavilli, Z. Yan, and J. Lillberg, "Improved 8- and 16-state space-time codes for 4psk with two transmit antennas," *IEEE Communications Letters*, vol. 5, no. 7, pp. 301–303, July 2001.

[35] S. Siwmogsatham and M. P. Fitz, "Improved high-rate space-time codes via orthogonality and set partitioning," in *Proc. of IEEE WCNC'02*, vol. 1, Mar 2002, pp. 264–270.

[36] H. Jafarkhani and N. Hassanpour, "Super-quasi-orthogonal space-time trellis codes for four transmit antennas," *IEEE Transactions on Wireless Communications*, vol. 4, no. 1, pp. 215–227, Jan. 2005.

[37] H.-J. Su and E. Geraniotis, "Space-time turbo codes with full antenna diversity," *IEEE Transactions on Communications*, no. 1, pp. 47–57, Jan. 2001.

[38] Y. Liu, M. P. Fitz, and O. Y. Takeshita, "Qpsk space-time turbo codes," *ICC 2000 - IEEE International Conference on Communications*, no. 1, pp. 292–296, June 2000.

[39] D. Cui and A. M. Haimovich, "Performance of parallel concatenated space-time codes," *IEEE Communications Letters*, vol. 5, no. 6, pp. 236–238, June 2001.

[40] W. Firmanto, Z. Chen, B. Vucetic, and J. Yuan, "Design of space-time turbo trellis coded modulation for fading channels," *GLOBECOM 2001 - IEEE Global Telecommunications Conference*, no. 1, pp. 1093–1097, Nov 2001.

[41] D. Tujkovic, "Performance analysis and constituent code design for space-time turbo coded modulation over fading channels," *Asilomar conference*, Pacific Grove, USA, Nov. 9-12 2003.

[42] Y. Hong, J. Yuan, Z. Chen, and B. Vucetic, "Space-time turbo trellis codes for two, three, and four transmit antennas," *IEEE Transactions On Vehicular Technology*, vol. 53, no. 2, pp. 318–328, MARCH 2004.

[43] C. Fragouli and R. Wesel, "Bit vs. symbol interleaving for. parallel concatenated trellis coded modulation," in *Proc. Globe Comm.*, vol. 2, 2001, pp. 931–935.

[44] B. Scanavino, G. Montorsi, and S. Benedetto, "Convergence properties of iterative decoders working at bit and symbol level," in *Proc. Globe Comm.*, vol. 2, 2001, pp. 1037–1041.

[45] J. Hagenauer and P. Hoeher, "A viterbi algorithm with soft-decision outputs and its applications," in *Proceedings of GLOBECOM'89*, vol. 3, 1989, pp. 1680–1686.

[46] C. Liao and V. K. Prabhu, "Improvement in sova based normalization scheme for turbo codes," in *proceeding of IEEE MAPE*, vol. 2, 2005, pp. 1147–1149.

[47] P. Robertson, E. Villebrum, and P. Hoeher, "A comparison of optimal and suboptimal map decoding algorithms operating in the log domain," in *Proc. Int. Conf. Communications*, Seattle, WA, June 1995, pp. 1009–1013.

BIOGRAPHICAL STATEMENT

Chen Liao was born in JiangXi, China, in 1965. He had received his B.S degree in electrical engineering from national university of defence technology, China, in July 1986. He earned his master's degree in electrical engineering from the University of Texas at Arlington (UTA) in 2001. Following his graduation with master's degree, he continued his studies as a Ph.D student at UTA.

From July 1986 to July 1999, he was with Shanghai Institute of Satellite Engineering (SISE), where he was a senior lead engineer of payload data transmission system of FY-1 satellite. He is currently working towards his Ph.D degree. His research interests are in the wireless communications with emphasis on channel coding, MIMO, space-time codes, and MIMO-OFDM.